AN ABSTRACT OF THE DISSERTATION OF

David Earl Rupp for the degree of Doctor of Philosophy in Water Resources Engineering presented on December 1, 2005.

Title: On the Use of Recession Slope Analysis and the Boussinesq Equation for Interpreting Hydrographs and Characterizing Aquifers.

Abstract approved:

Signature redacted for privacy.

John S. Selker

The method of recession analysis proposed by *Brutsaert and Nieber* [1977] remains one of the few analytical tools for estimating aquifer hydraulic parameters at the field-scale and greater. In the method, also referred to as "recession slope analysis", the receding limb of the hydrograph is examined as $-dQ/dt = f(Q)$, where Q is discharge and f is an arbitrary function. The parameters of the observed function f are related to analytical solutions to the 1-D Boussinesq equation for unconfined flow in a homogeneous, horizontal aquifer. Conveniently, these solutions can all be expressed in the general form $-dQ/dt = aQ^b$, where a is a function of the aquifer dimensions and hydraulic properties and b is a constant. The four central chapters that follow investigate aspects of the theory and implementation of recession slope analysis. The first chapter is an application of the method for calculating the field-scale saturated hydraulic conductivity k of a mildly-sloping tile-drained field. It is also shown how the method of recession slope analysis can be applied to water table recession data. Furthermore, an alternative method for calculating k from the same data is presented that does not require estimating $-dQ/dt$. This is of practical interest because of the substantial noise generated when taking time derivatives of real data. The second chapter reveals how the standard approach to calculating $-dQ/dt$ from real data can lead to artifacts in plots of $\log(-dQ/dt)$ versus $\log(Q)$ which can in turn lead to incorrect interpretations of the recession slope curves. In response, an alternative technique for estimating $-dQ/dt$ is proposed. In the third chapter, analytical solutions to the Boussinesq equation are derived for a horizontal aquifer in which the saturated hydraulic conductivity k is allowed to vary as a power law of height above bedrock.

This is of interest as many soils exhibit decreasing k with depth. In addition, the effect of the power-law k profile on the recession parameters a and b is discussed. The final chapter is a partial assessment of the Brutsaert and Nieber method for sloping aquifers, both for the homogeneous case and for when k varies as power law with height. It is found that the existing analytical solutions to the 1-D Boussinesq equation for a sloping aquifer, each based on their own simplifying assumptions, are inappropriate for a Brutsaert and Nieber-type analysis. However, an examination of numerical solutions to the non-linear Boussinesq equation revealed "empirical" relationships between aquifer parameters and recession slope curves that permit the derivation of approximate analytical solutions for the late part of the recession period when the curves converge to the form $-dQ/dt = aQ^b$.

On the Use of Recession Slope Analysis and the Boussinesq Equation for Interpreting
Hydrographs and Characterizing Aquifers

by

David Earl Rupp
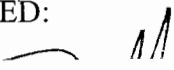
A DISSERTATION

submitted to

Oregon State University

in partial fulfillment of
the requirements for the
degree of

Doctor of Philosophy

Presented December 1, 2005
Commencement June 2006

Doctor of Philosophy dissertation of <u>David Earl Rupp</u> presented on <u>December 1, 2005</u>

APPROVED:

Signature redacted for privacy.

Major Professor, representing Water Resources Engineering

Signature redacted for privacy.

Head of the Water Resources Graduate Program

Signature redacted for privacy.

Dean of the Graduate School

I understand that my dissertation will become part of the permanent collection of Oregon State University libraries. My signature below authorizes release of my dissertation to any reader upon request.

Signature redacted for privacy.

David Earl Rupp, Author

ACKNOWLEDGEMENTS

The last half-dozen years with John Selker have been a fantastic education. John and I have embarked upon numerous and varied research paths in that time, many of which are only tangentially, if at all, represented explicitly in this dissertation. Regardless of whether the fruits, or lack thereof, of a specific investigation have made it into these pages, I would like to thank a multitude of individuals who aided me or taught me something along the way.

On the pesticide monitoring project, working with Ed Peachey was an inspiration. When in the field together, I always seemed to get twice as much done in half the time. Others to whom I owe gratitude for their assistance in the field are Kristy Warren, Josh Owens, Chris Vick, Laila Parker and Starr Metcalf. I cannot recall if Jeff Feaga ever braved the rain or carried RV batteries for me, but his sense of humor certainly lightened the load.

On the rainfall modeling project, Mina Ossiander stretched my mind by challenging me, along with Richard Keim, to think about a world of fractals.

On the Chilean hydrology project, Hamil Uribe's friendship has been essential. In the field, Theresa Blume, Fernando Soto, Don Romilio and Adam Wiskind were invaluable. In a host of ways the following people have made things happen: Samuel Ortega, Oscar Reckmann, Jorge Vergara, Octavio Lagos, and Richard Cuenca. Though he was never invited to go to Chile, Jirka Simunek was instrumental in our analysis of well data. Patricia Zambrano made going to Chile feel like coming home.

Erick Burns and Kellie Vaché have been great colleagues, and I am especially grateful to Erick for reviewing several of my manuscripts.

I thank also John Bolte and Brian Wood for their willingness to serve on my committee.

Of course, I would not have done this without the love of my family and friends.

CONTRIBUTION OF AUTHORS

Kristina Warren and Joshua Owens collected the tile-drain discharge and water table data for the study site in Chapter 2 and initiated the field-scale analysis of hydraulic conductivity based on the data. Josh Owens also collected soil samples from the site and determined saturated hydraulic conductivity and water retention properties of the samples in the laboratory.

Jan Boll and Erin Brooks provided a sounding board for several of the ideas in Chapter 5 and collected the field data used to test the theory presented.

TABLE OF CONTENTS

TABLE OF CONTENTS (Continued)

TABLE OF CONTENTS (Continued)

LIST OF FIGURES

LIST OF TABLES

On the Use of Recession Slope Analysis and the Boussinesq Equation for Interpreting Hydrographs and Characterizing Aquifers

Chapter 1 - Introduction

The analysis of the recession limb of hydrographs for forecasting drought flows and investigating the ground water flow regime in basins has over a century-long history [see reviews in *Hall*, 1968; *Tallaksen*, 1995]. The part of this history that still remains very relevant today are the attempts to link features of the recession curve to the physical properties of a basin's aquifer.

Brutsaert and Nieber [1977] made a provocative contribution when they proposed examining the *slope* of the drought flow hydrograph, or dQ/dt, against the discharge Q, such that

$$\frac{dQ}{dt} = f(Q) \tag{1}$$

where f denotes an arbitrary function, and comparing plotted data against analytical solutions for aquifer discharge. In particular, they focused on the Boussinesq equation for 1-dimensional flow in a rectangular, horizontal, homogeneous, and unconfined aquifer where lateral flow in the unsaturated zone is neglected (note the many simplifications made).

What makes this method of analysis particularly alluring is that three well-known analytical solutions to the Boussinesq equation can be expressed in the form

$$-\frac{dQ}{dt} = aQ^b \tag{2}$$

where b is a dimensionless constant and a is a function of the geometric and hydraulic properties of the "Boussinesq" aquifer. Moreover, streamflow recession data frequently exhibit the form of the power law in (2). Graphed in log-log space, (2) has the additional attractive feature of appearing as a straight line. In theory, from (2) one can estimate basin-scale effective values for the aquifer parameters, such as the saturated hydraulic conductivity k for example.

However, there are many reasons why one might question the appropriateness of using the 1-dimensional Boussinesq aquifer as a model for basin discharge. To begin, a natural basin is certainly not one-dimensional, rectangular and homogeneous. Nor is the flow likely to be truly horizontal and only in the saturated zone. Furthermore, there may be other contributions and/or losses to streamflow than from merely an unconfined groundwater source. Despite these apparent problems, the use of the 1-dimensional Boussinesq equation in the Brutsaert and Nieber fashion continues to be applied (see, for example, Chapter 5, Introduction). The series of papers that follow investigate some of the apparent limitations of the Boussinesq aquifer and some practical issues concerning the Brutsaert and Nieber approach.

In Chapter 2, the existing analytical solutions to the Boussinesq equation are compared to discharge and water table measurements taken in a tile-drained field: an intermediate setting between a laboratory where the aquifer properties are well-defined and a natural basin where aquifer properties and initial and boundary conditions are generally poorly understood. The important issue of the scaling of hydrological parameters is also addressed. Specifically, k estimated at the field scale using the Brutsaert and Nieber method is compared to small scale estimates of k of numerous soil samples tested in the laboratory.

Both Chapters 2 and 3 deal with the practical implementation of the Brutsaert and Nieber method. In Chapter 2, an alternative technique for parameter estimation is presented in order to avoid taking the time derivative of discharge data, a calculation which is often very sensitive to data noise. The specific issue in Chapter 3 is that of previously perceived patterns in plotted recession data. It is shown that these patterns are artifacts of the usual manner for estimating the slope of the hydrograph (dQ/dt),

and are not manifestations of physical phenomena. An alternative manner of calculating dQ/dt versus Q is presented that does not produce such artifacts and thus increases the power of the analysis method.

Chapters 4 and 5 address aquifer inhomogeneity by allowing k to decrease with depth, a common characteristic of soils. Analytical solutions are derived for the Boussinesq equation with a power-law k profile and the effects on the recession parameters a and b in (2) are discussed.

Chapter 5 tackles the general utility of the Brutsaert and Nieber method for estimating the hydraulic parameters of a non-horizontal aquifer. Short-comings of the existing analytical solutions to the Boussinesq equation for a sloping aquifer are first discussed. Next, by examining numerical solutions to the Boussinesq equation for a sloping aquifer, analytical relationships between properties of the recession slope curves and properties of the aquifer are sought. These relationships are tested against data from a hillslope in which k is known to decrease markedly with depth.

Chapter 2 - Analytical Methods for Estimating Saturated Hydraulic Conductivity in a Tile-Drained Field

David E. Rupp[1], Joshua M. Owens[1], Kristina L. Warren[1,2], and John S. Selker[1]

1: Department of Bioengineering; Oregon State University; Corvallis, OR

2: Presently at Camp Dresser & McKee; Bellevue, WA

Abstract

Determination of field-scale hydraulic properties is required for many hydrologic predictions. Four analytical methods for determining the saturated hydraulic conductivity k on the field scale for a field drained by a network of parallel drains are considered. These methods, all derived from the Boussinesq equation, relate: 1) time rate of change of discharge to discharge; 2) relative discharge to time; 3) time rate of change of water table height to height; and 4) relative water table height to time. Though all four methods eliminate the need to know precisely the beginning time of the recession curve, which is in practice ambiguous, Methods 2) and 4) do not require taking time derivates of observations, which introduces noise. The mean field-scale k based on several recession events on two 1 ha fields using all methods was 4 m/d. This is near the median k of 5 m/d calculated from 40 soil cores taken at various depths within the same fields, but five times less than the mean k of the soil cores (20 m/d).

1. Introduction

The use of spatially-distributed ecosystem models to address complex issues involving water quantity and quality lead naturally to a need for estimates of model parameters corresponding to the scale of the model elements. For hydraulic properties of soils this is problematic because almost all field characterization methods work at spatial scales on the order of 0.1 m^3 or less. To acquire values of the hydraulic properties at the scale of the model requires not only extensive sampling but a leap of faith regarding what is the effective value of the hydraulic property at the larger scale. A further complication is that hydrologic processes may be operating that simply are not measurable at the small scale.

Observation of outflow and water table height in drained farmland affords an opportunity to estimate saturated hydraulic conductivity, a primary hydraulic parameter present in many models, for volumes of soil on the order of 10^4 m^3: volumes more in correspondence with the scale of land-use units. With measurements of drain discharge and/or water table height in time following a significant rainfall or irrigation event, saturated hydraulic conductivity can be estimated with relative ease with transient analytical solutions given the proper conditions.

Early development of analytical solutions for a falling water table arose from the interest in determining appropriate drain spacing [Glover, as reported by *Dumm*, 1954; *Luthin*, 1959; *Luthin and Worstell*, 1959; *van Schilfgaarde*, 1963; Tapp and Moody, as reported by *Dumm*, 1964]. These equations solve for drain spacing given the drop of the water table in time at the midpoint between two parallel drains. *Luthin* [1959] and *Luthin and Worstell* [1959] began with the assumption, based on observations, that the drain discharge is a linear function of water table height at the midpoint between the two drains, whereas, the *Glover* equations, along with the improvements proposed by *Tapp and Moody*, and the equation of *van Schilfgaarde* [1963], are solutions of a draining unconfined aquifer in which the Dupuit approximation is invoked. All assume a certain shape to the initial water table profile. *Van Schilfgaarde* [1963] introduced a correction to the solution to account for the

effect of convergence, following *Hooghoudt* [1940]. These equations have been used along with field measurements of water table height and drain discharge to estimate saturated hydraulic conductivity [e.g., *Talsma and Haskew*, 1959; e.g., *Hoffman and Schwab*, 1964].

Nearly forty years before *Hooghoudt* [1940] presented his steady-state drain formula, Boussinesq examined a special case of the transient drainage of an initially saturated unconfined aquifer. Boussinesq's equation describes the water table height h in rectangular homogeneous aquifer of depth D and width B that is draining into a fully-penetrating channel (see Figure 1):

$$\frac{\partial h}{\partial t} = \frac{k}{\varphi} \frac{\partial}{\partial x} \left(h \frac{\partial h}{\partial x} \right) \tag{1}$$

where t is the time since the start of the recession, k is the saturated hydraulic conductivity, and φ is the drainable porosity. Here the Dupuit approximation is invoked and the effect of capillarity is neglected. We will refer to this system as a Dupuit-Boussinesq aquifer [e.g., *Brutsaert and Nieber*, 1977]. *Polubarinova-Kochina* [1962, pp. 507-508] presented an exact solution to (1) for $B = \infty$ and is therefore valid in early times before the no-flow boundary at $x = B$ has an appreciable effect:

$$h(x,t) = 2.365D(Y - 2Y^4 + 3Y^7 - (4/11)Y^{10} - \cdots) \tag{2}$$

where $Y = 0.4873 \eta^{1/2}$ and $\eta = (x\varphi^{1/2})/[2(kDt)^{1/2}]$. The discharge per unit length q derived from (2) is

$$q(t) = 0.332(k\varphi)^{1/2} D^{3/2} t^{-1/2} \tag{3}$$

At late times when the boundary at B is affecting the drop in water table, *Boussinesq* [1904] provided an exact solution to (1):
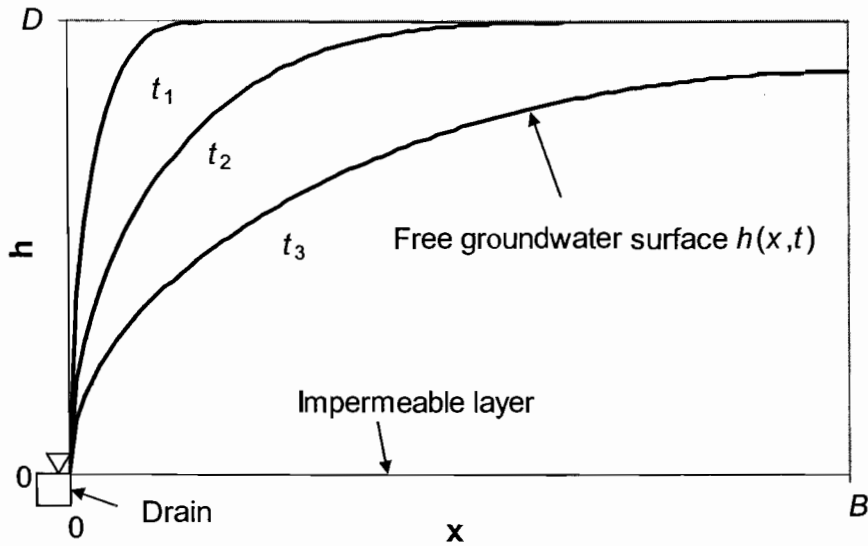
Figure 1. Schematic representation of an initially saturated unconfined rectangular aquifer draining into a fully penetrating channel. The curve at t_1, t_2, and t_3, represent the early, transitional, and late times during drawdown, respectively.

$$h(x,t) = \frac{D\phi(x/B)}{1+1.115\left(\dfrac{kD}{\varphi B^2}\right)t} \tag{4}$$

where $\phi(x/B)$ is the initial form of the free surface and is described by an inverse incomplete beta function [see *Polubarinova-Kochina*, 1962, pp. 515-517]. Note that in (4) $t = 0$ when $h(B, t) = D$ and $h(x: x<B, t) < D$. The discharge corresponding to (4) is

$$q(t) = \frac{0.862kD^2}{B\left[1+1.115\left(\dfrac{kD}{\varphi B^2}\right)t\right]^2} \tag{5}$$

The difficulty in applying equations (2) through (5) to estimate aquifer parameters from water table or discharge observations arises from the necessity to know the time of origin of the recession event. However, as noted by *Brutsaert and Nieber* [1977], when referring to continuous river flow records, "...it is practically impossible to determine in any consistent way the beginning of each recession...." This issue is no less of a problem for drain flow records despite the large difference in scale.

In response, *Brutsaert and Nieber* [1977] suggested analyzing the slope of the hydrograph as a function of discharge Q in order to eliminate the dependency on time. The rate of change of Q can be expressed as a power function of Q for both (3) and (5):

$$\frac{dQ}{dt} = -aQ^b \tag{6}$$

where $Q = 2qL$, and L is the drain length. For the early-time solution (3)

$$a_1 = \frac{1.133}{k\varphi D^3 L^2} \qquad b_1 = 3 \tag{7}$$

and for the late-time solution (5)

$$a_2 = \frac{4.804k^{1/2}L}{\varphi A^{3/2}} \qquad b_2 = 3/2 \tag{8}$$

where $A = 2LB$. This procedure has been shown to be applicable for determining baseflow separation and aquifer parameters in basins [*Troch, et al.*, 1993; *Brutsaert and Lopez*, 1998; *Szilagyi and Parlange*, 1998; *Szilagyi, et al.*, 1998]. *Parlange et al.* [2001] presented an analytical approximation to (1) which unifies the early and late-time solutions.

In this paper we present a methodology for applying (4) and (5) which eliminates the need to know the time of origin. We apply these methods, along with the procedure proposed by *Brutsaert and Nieber* [1977], to water table height and discharge measurements from a drained field to determine the saturated hydraulic conductivity k of the field. These values of k are compared to values of k determined in the laboratory from soil cores.

2. Study Area and Relevant Data

The methodology described in the following section was applied to two adjacent fields in the northern Willamette Basin, Oregon. Field 1 is approximately 1.4 ha and was planted with grass in the fall of 2001, and Field 2 is approximately 1.1 ha and was planted with grass in the fall of 2000. The soil classification in both fields is Woodburn silt loam, or fine-silty, mixed, mesic aquultic argixerolls. Woodburn silt loam is reported as having a depth of roughly 1.6 m, a clay content ranging from 10-30%, and a saturated hydraulic conductivity of between 0.4-1.2 m/day [*Otte, et al.*, 1974]. Both fields have slopes of 0-3%.

Each field has system of drains composed of one main drain fed by a set of lateral drains spaced 12.2 m apart, all of 10.16 cm (4 in) diameter perforated plastic pipe (Figure 2). There are 13 lateral drains each 79.3 m in length in Field 1 and 11 lateral drains each 68.6 m in length in Field 2. The drains were installed in 1990 at a depth of approximately 1.2 m with a slope of 0.001 m/m. Both these systems are connected to a larger drainage system underlying a total area of approximately 9.5 ha. The drain outlet empties into a small natural channel that feeds a stream approximately 150 m distant and 15 m below the fields.

Field work consisted of collecting soil samples for laboratory analysis, monitoring water table levels, measuring the discharge from the drains, and measuring rainfall intensity. Undisturbed soil cores were taken in each field to characterize the distribution of k and water retention. Two samples were collected at depths of 0.3, 0.6, 0.9 and 1.2 m at 10 locations in, or very near, the fields for a total of 80 samples (40 for k and 40 for water retention) (see Figure 2).

Water table height in Field 2 was observed in 5 piezometers located in a transect perpendicular to the lateral drains. In total, 20 piezometers spaced 1.52 m apart and inserted to a depth of 2 m were installed in the fields in August, 2001, but because of pressure logger failures and some non-responding piezometers, most were not analyzed. Pressure transducers with data loggers (In-Situ "MiniTroll", Laramie, WY) placed at the bottom of the piezometers recorded depth of water in one-hour intervals during two sampling periods in 2002: Jan. 29 – Feb. 13 and Mar. 27 – Apr. 30.

In each of Fields 1 and 2, a turbine flow meter (Seametrics TX101) measured flow in the drain and a data logger recorded discharge at 5-minute intervals. Each flow meter was installed in a 6.35 cm (2.5 in) diameter PVC pipe of approximately 1 m in length that replaced the section of drain. Using a pair of elbows connected in an S-shape to each end of the PVC pipe, the pipe rested at least one drain diameter below the drain itself, keeping the PVC pipe full at all times as required for flow measurements. The diameter constriction from to 10.16 to 6.35 cm also increased the flow velocity, which allowed for measurements of lower discharges than would otherwise have been achievable with the flow meter. The flow meter is designed to operate properly at velocities between 0.06 and 9.2 m/s (equivalent to 17 and 2500 m^3/d in the 6.35 cm diameter PVC pipe). The location of each flow meter is shown in Figure 2. The drained area measured by the flow meters in Fields 1 and 2 is approximately 1.35 and 1.00 ha, respectively. A tipping-bucket rain gauge (0.2 mm resolution) and data logger recorded rainfall at the site.
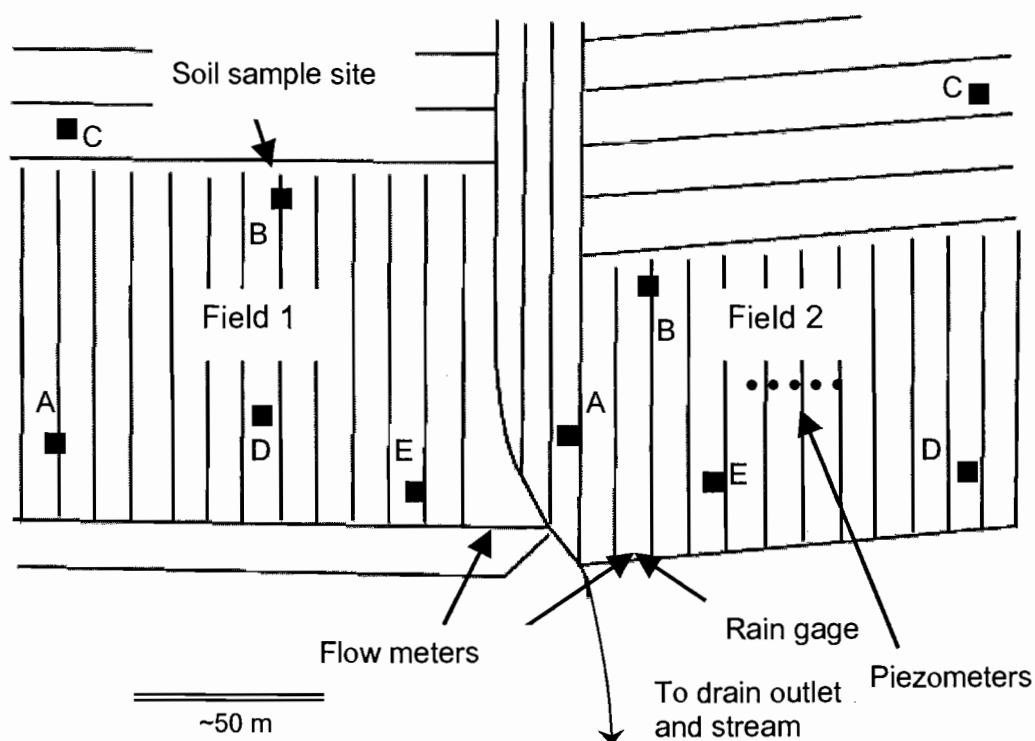
Figure 2. Drainage system in Fields 1 and 2 with instrumentation and soil sample sites. Locations are approximate.

3. Methodology

Soil cores 0.054 m in diameter and 0.060 m in height were analyzed for k in the laboratory using a constant or falling head permeameter, depending on the permeability [*Klute and Dirksen*, 1986]. Water retention measurements were made on cores 0.054 m in diameter and 0.030 m in height using a pressure bomb following the procedure described in *Klute* [1986]. For each sample, volumetric water content was measured at five to eight pressures between -3.3 kPa to -296.4 kPa.

The methods described below for calculating the field-scale saturated conductivity require values of drainable porosity φ. Estimates were made from both the core-scale and field-scale data. From the water retention analysis of the soil cores, a lower limit to φ was calculated as the loss in volumetric water content as the pressure was reduced from -3.3 kPa to -10 kPa. Given the depth of the drains (on the order of 1 m), -10 kPa was the pressure considered to be the closest to that of the soil above the water table during recession. Others have used a pressure of -5.9 kPa (-0.6 m H$_2$0) for similar conditions [e.g., *Talsma and Haskew*, 1959; *van Schilfgaarde*, 1963], but these data were not available to us. An upper limit to φ was calculated as the difference in the saturated water content and the water content at -10 kPa, under the assumption that the water content at 0 kPa is equal to the moisture loss after oven-drying a core previously saturated in a laboratory. However, this porosity is likely to be greater than the field-saturated water content, resulting in an overestimate of φ.

At the field scale, φ was estimated by comparing the volume of drain flow during the recession period with the corresponding drop in water table. Assuming that the average water table drop observed in n piezometers represents the average water table drop in the drained area A over a period $t_2 - t_1$, φ is calculated from

$$\varphi = \frac{\int_{t_1}^{t_2} Q(t)}{A \frac{1}{n} \sum_{i=1}^{n} \left[h_i(t_1 - \Delta t) - h_i(t_2 - \Delta t) \right]} \tag{9}$$

The time lag Δt is included because the time of highest water table precedes the time of peak flow. We let t_1 be the time of peak flow and t_2 be the latest time at which we believed the flow meter measurements were reliable, so in practice $t_2 - t_1$ was approximately 8 hours. Vertical movement of water past the drainage system will result in (9) underestimating φ. A second method for determining φ from water table drop and drain flow during recession is presented at the end of Section 3.4.

We calculated the saturated hydraulic conductivity of the fields using four analytical methods which relate: 1) rate of change in discharge to discharge; 2) relative discharge to time; 3) rate of change of water table height to height; and 4) relative water table height to time.

3.1. Rate of Change of Discharge vs. Discharge

The rate of change in discharge was graphed against discharge for each of the major recession events. To smooth out noise in the data, the rate of change in discharge was approximated at each observation with

$$\frac{dQ}{dt} \approx \frac{1}{n}\sum_{i=1}^{n}\frac{Q_{i+1}-Q_i}{\Delta t} \tag{10}$$

and plotted vs. the corresponding mean discharge:

$$Q \approx \frac{1}{n+1}\sum_{i=1}^{n+1}Q_i \tag{11}$$

With $n = 12$ and $\Delta t = 5$ min, each Q point represents a mean hourly discharge.

Following *Brutsaert and Nieber* [1977], we examined the curve of $\ln(-dQ/dt)$ vs. $\ln Q$ to see where if either, or neither, of the early- and late-time solutions appeared to be valid, i.e. where the slope b appeared as 3 or 1.5, respectively. Where a line of slope b could be reasonably fit to the data, the conductivity k was calculated from the intercept a using either (7) or (8) as appropriate.

3.2. Relative Discharge vs. Time

Where the late-time solution appeared to hold, another estimate of k was made from the observed discharge at $t = t_2$ divided by a reference discharge at $t = t_1$. Substituting $Q/2L$ for q in (5), taking the ratio $Q(t_2)/Q(t_1)$, and solving for k yields

$$k = \frac{\varphi B^2}{1.115D} \left[\frac{Q(t_1)^{1/2} - Q(t_2)^{1/2}}{t_2 Q(t_2)^{1/2} - t_1 Q(t_1)^{1/2}} \right] \tag{12}$$

As it is, (12) requires knowledge of D, the height of the water table above the midpoint between parallel drains at $t = 0$. However, solving (5) at $t = 0$, gives an expression for D

$$D = \left(\frac{Q(0)B}{1.724Lk} \right)^{1/2} \tag{13}$$

that can be substituted into (12) to yield a solution for $k^{1/2}$:

$$k^{1/2} = \frac{(1.724)^{1/2} L^{1/2} \varphi B^{3/2}}{1.115} \left\{ \left[\frac{Q(t_1)^{1/2} - Q(t_2)^{1/2}}{t_2 Q(t_2)^{1/2} - t_1 Q(t_1)^{1/2}} \right] \frac{1}{Q(0)^{1/2}} \right\} \tag{14}$$

By eliminating D, we have merely introduced another unknown, $Q(0)$, one that we have already mentioned is particularly difficult to estimate from field data. However, we can further eliminate $Q(0)$ algebraically. If we again take the ratio of two discharges $Q(t)/Q(0)$ while substituting (13) for D into (5), we can solve for $Q(t)$:

$$Q(t)^{1/2} = \frac{Q(0)^{1/2}}{1 + \Omega Q(0)^{1/2} t} \tag{15}$$

where, for brevity, we let $\Omega = (1.115 k^{1/2})/(1.724^{1/2} \varphi L^{1/2} B^{3/2})$. After appropriate substitution of (15) into (14), twice for $t = t_1$ and once for $t = t_2$, one eventually arrives at an equation for k independent of $Q(0)$:

$$k = \frac{1.387 L\varphi^2 B^3}{Q(t_1)} \left[\left(\frac{Q(t_1)}{Q(t_2)} \right)^{1/2} - 1 \right]^2 \frac{1}{(t_2 - t_1)^2} \tag{16}$$

The consequence of (16) is that it is not necessary to know the precise moment when $t = 0$, but only that t_1 lies somewhere after the time at which the long-term solution becomes valid. We can therefore define any late time in the recession curve as zero and use the corresponding discharge at that time as the initial discharge $Q(0)$, thus addressing the primary objection of *Brutsaert and Nieber* [1977] to using discharge vs. time data to estimate k. Testing for the validity of the late-time solution can be done, for example, by graphing k vs. time elapsed from a reference time t_1, to see where k is constant, or by using the approach of *Brutsaert and Nieber* [1977].

Another way to arrive at (16) is to integrate (6) from $Q(t_1)$ to $Q(t_2)$, then solve for k using the parameters in (8). Using the same procedure, a corresponding early-time expression for k can be derived from the parameters in (7):

$$k = \frac{2.266}{\varphi D^3 L^2} \left[\frac{Q(t_2)^2 Q(t_1)^2}{Q(t_1)^2 - Q(t_2)^2} \right] (t_2 - t_1) \tag{17}$$

3.3. Rate of Change of Water-Table Height vs. Height

For the late time solution (4), the time rate of change of water table height assumes the form of a power function:

$$\frac{dh(x,t)}{dt} = -ah(x,t)^b \tag{18}$$

where the constants a and b are

$$a_3 = \frac{1.115k}{\varphi B^2 \phi(x/B)} \qquad b_3 = 2 \tag{19}$$

To estimate k, we followed the same procedure as in Section 3.1, examining the curve of $\ln(-dh/dt)$ vs. $\ln h$ to see if and where the curve had a slope b of 2. Where a line of slope b could be reasonably fit to the data, the conductivity k was calculated from the intercept a using (19). A series expansion was employed to approximate the inverse of the incomplete beta function $\phi(x/B)$ [see equation 25.4.4, *Abramowitz and Stegun*, 1972].

Unfortunately, the early-time solution (2) does not lead to the simple form of (18), thus an equivalent early-time analysis of water table height observations cannot be conducted.

3.4. Relative Water-Table Height vs. Time

A fourth estimate of k was made, also at late times, from observations of the water table height with respect to a reference water table height at the same location x. Taking the ratio of two water table heights $h(x,t_2)/h(x,t_1)$, where $h(x,t)$ is defined by (4), and solving for k yields

$$k = \frac{\varphi B^2}{1.115 h(B,0)}\left[\frac{h(x,t_1) - h(x,t_2)}{h(x,t_2)t_2 - h(x,t_1)t_1}\right] \tag{20}$$

where D has been replaced by $h(B,0)$. In practice, it is unlikely that we will know the precise time at which $t = 0$ and hence $h(B,0)$. However, we can eliminate $h(B,0)$ from (20) with some algebraic manipulation. Again taking the ratio of two water heights $h(B,0)/h(B,t)$, we are at expression for $h(B,0)$ as

$$h(B,0) = \frac{h(B,t)}{1 - \left(\dfrac{1.115k}{\varphi B^2}\right)h(B,t)t} \tag{21}$$

Substituting (21) for $t = t_1$ into (20) and solving again for k yields

$$k = \frac{\varphi B^2}{1.115h(B,t_1)}\left[\frac{h(x,t_1)}{h(x,t_2)} - 1\right]\frac{1}{(t_2 - t_1)} \tag{22}$$

As we did with discharge in Section 3.2, we eliminated the need to know the water table height at the time of origin. Though we don't need to know our position x, we are required to have an initial measure at $t = t_1$ of the water table height at $x = B$.

We can arrive at a similar expression by integrating (20) from $h(t_1)$ to $h(t_2)$. Using the parameters in (21), the solution for k is

$$k = \frac{\varphi B^2 \phi(x/B)}{1.115h(x,t_1)}\left[\frac{h(x,t_1)}{h(x,t_2)} - 1\right]\frac{1}{(t_2 - t_1)} \tag{23}$$

By equating (22) and (23), we see that $\phi(x/B) = h(x/t)/h(B,t)$. In the case of (23), we no longer need an initial observation at the midpoint between parallel drains, but we are required to know our position x.

It is of special interest to note that k is proportional to φ in (22) and (23) but that k is proportional to φ^2 in (16). This allows us to determine φ independent of k by equating (22) or (23) with (16). Let

$$c_1 = \frac{1}{Q(t_1)(t_2 - t_1)^2}\left[\left(\frac{Q(t_1)}{Q(t_2)}\right)^{1/2} - 1\right]^2 \tag{24}$$

which from (16) is constant when the late-time solution is valid. Similarly, let

$$c_2 = \frac{1}{h(B,t_1)(t_2 - t_1)}\left[\frac{h(x,t_1)}{h(x,t_2)} - 1\right] \tag{25}$$

which from (22) is also constant. Substituting (24) into (16), substituting (25) into (22), and equating the two results yield the following expression for φ:

$$\varphi = 0.697(BL)^{-1}(c_2/c_1) \tag{26}$$

4. Results

The saturated hydraulic conductivities of the soil cores showed no clear relation with depth (Figure 3), suggesting vertical homogeneity on the field-scale. The values of k of the soil cores from the two fields ranged from 1.7×10^{-4} to 1.7×10^2 m/d, though one low value from each field stands out from the rest (Figure 3). The arithmetic means for Field 1 and 2 are 23 and 19 m/d, respectively, and the geometric means for Field 1 and 2 are 4.6 and 2.9 m/d, respectively. The medians are 6.4 m/d and 3.6 m/d for Fields 1 and 2, respectively. The lowest value from each field has only a minor effect on the arithmetic and geometric means, but a large effect on the harmonic mean. The harmonic means for Field 1 and 2 using all values are 0.003 and 0.035 m/d, respectively, while the harmonic means for Field 1 and 2 excluding the lowest value from each field are 1.94 and 0.87 m/d, respectively. The relative cumulative frequency distributions of k for each field are shown in Figure 4.

The mean drainable porosity of the soil cores based on the difference in water content at -3.3 kPa and -296.4 kPa was 0.016 and 0.017 for Fields 1 and 2, respectively. Based on the oven-dried porosity and water content at -296.4 kPa, the mean drainable porosity of the soil cores was 0.121 and 0.133 for Fields 1 and 2, respectively. Using these values as lower and upper bounds to drainable porosity leaves us with a degree of uncertainty of nearly an order of magnitude when calculating hydraulic conductivity. Moreover, the variability among cores was very high: the lower bound estimates ranged from 0.004 to 0.029 and the upper bound estimates ranged from 0.032 to 0.276 for both fields combined.
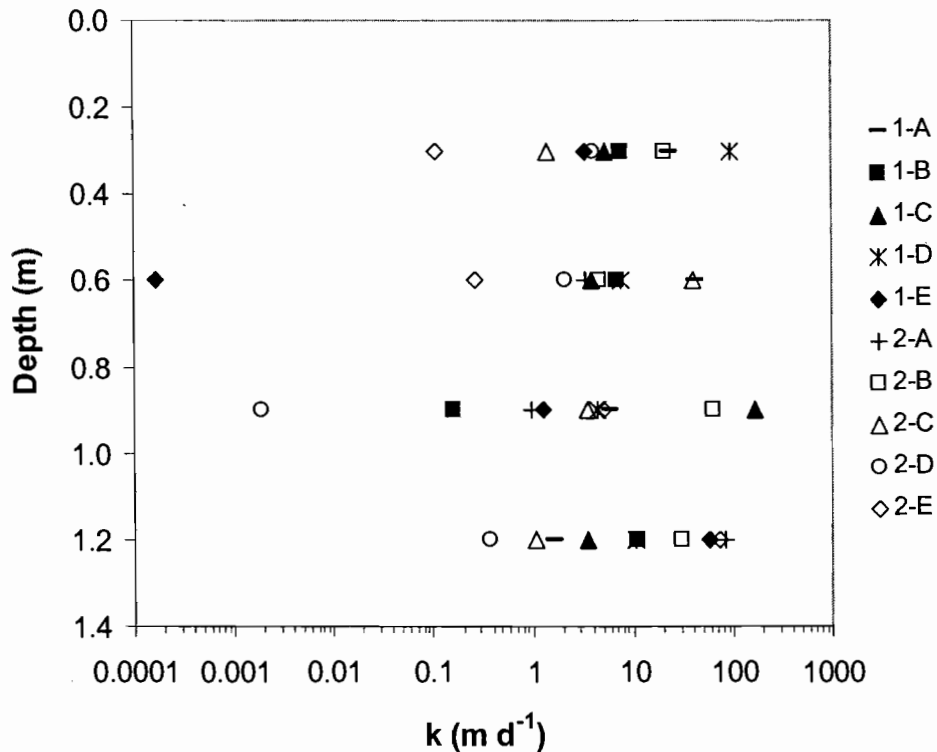
Figure 3. Saturated hydraulic conductivity of soil cores with depth. The number and letter of each soil sample label refers to the field and auger-hole, respectively.

Two rainfall events occurred that produced appreciable flow in the drain in Field 2 during the period that the water table was being monitored. These are designated as Events 5 and 6. Figure 5 shows the discharge from the drain and the water table depth measured at various piezometers during these two events. From (8), φ was calculated to be 0.015 and 0.018 from the first and second event, respectively. In this calculation we used only the first eight hours of recession data because of the unusual activity observed for both events in the flow meter when the discharge dropped to approximately 50 m^3/d (see Figure 5). In contrast, φ as determined from (26) using the first several hours of recession is 0.023 for each of the two events. The

different values resulting from the two methods may be due in part to the scarcity of piezometers, particularly near the drain where the water table drop would be least. Other studies which have calculated φ from discharge after a measured drop in water table have reported values ranging from 0.04 to 0.07 [*Talsma and Haskew*, 1959; *Hoffman and Schwab*, 1964; *El-Mowelhi and Van Schilfgaarde*, 1982]. The following results are based on $\varphi = 0.023$ for each field.
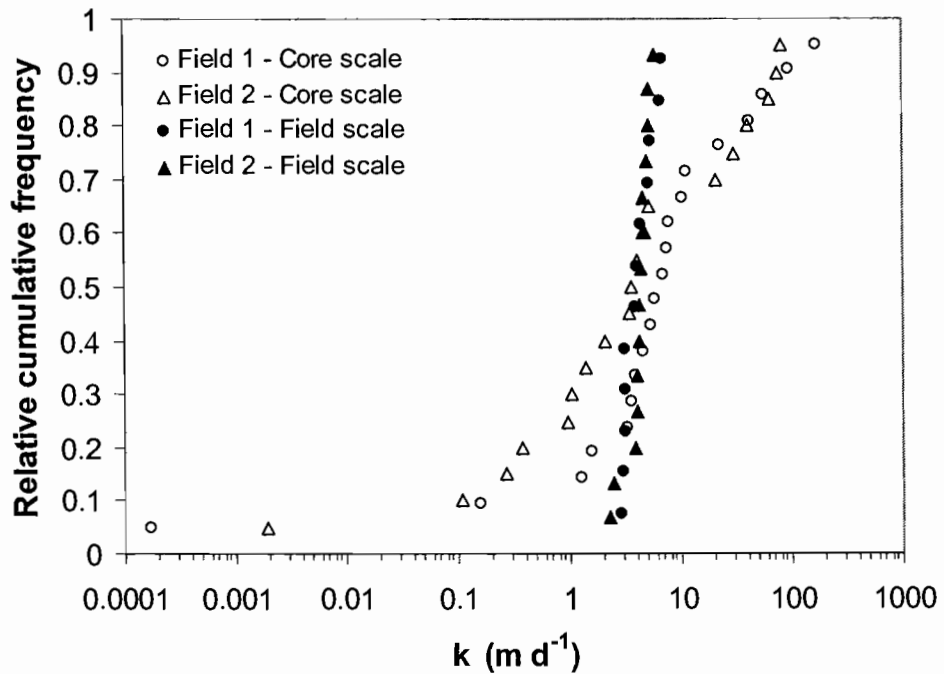
Figure 4. Relative cumulative frequency distribution of saturated hydraulic conductivity. The open circles and squares are values of k from laboratory analysis of soil cores and the closed circles and squares refer to the estimates made from drain discharge and water table height observations. Variability in soil core-scale k is due to spatial heterogeneity, while variability in field-scale k arises from different recession events and different analysis methods.
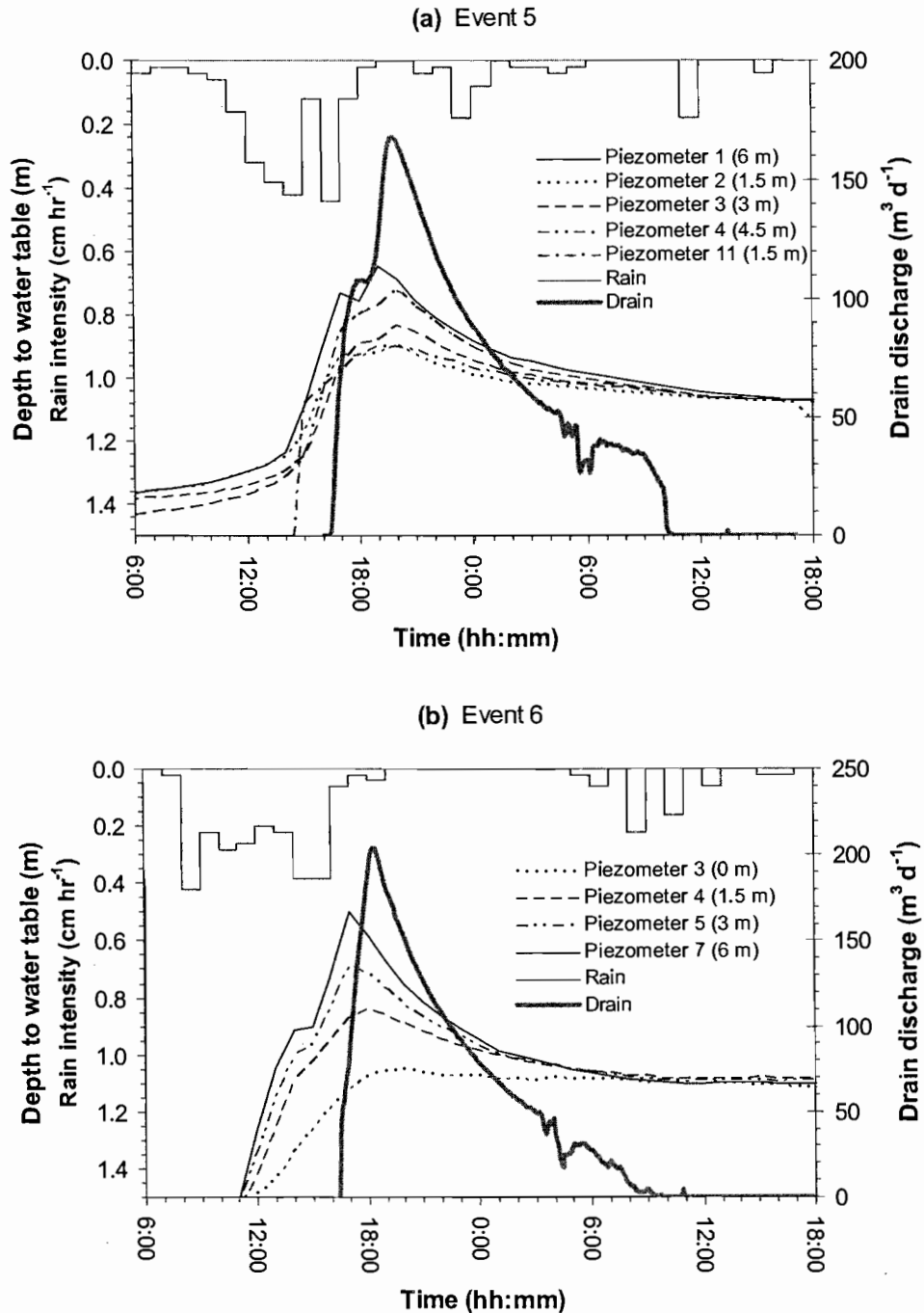
Figure 5. Water table heights from piezometer observations and the drain hydrographs in Field 2 for (a) Event 5 on Feb. 7-8, 2002 and (b) Event 6 on Mar. 11-12, 2002. Listed to the right of each piezometers number is the approximate distance from the closest drain. The numbering of the piezometers was not consistent between the two periods. Hourly rainfall intensity is at the top of each graph.

4.1. Rate of Change of Discharge vs. Discharge

Six rainfall events produced flow in Field 1 and four events produced flow in Field 2 sufficient for an analysis of k using the method described in Section 3.1. In every recession there stands out a portion of the dQ/dt vs. Q curve that appears log-log linear with a slope of 1.5, corresponding to the late-time solution (Figure 6). In contrast, there
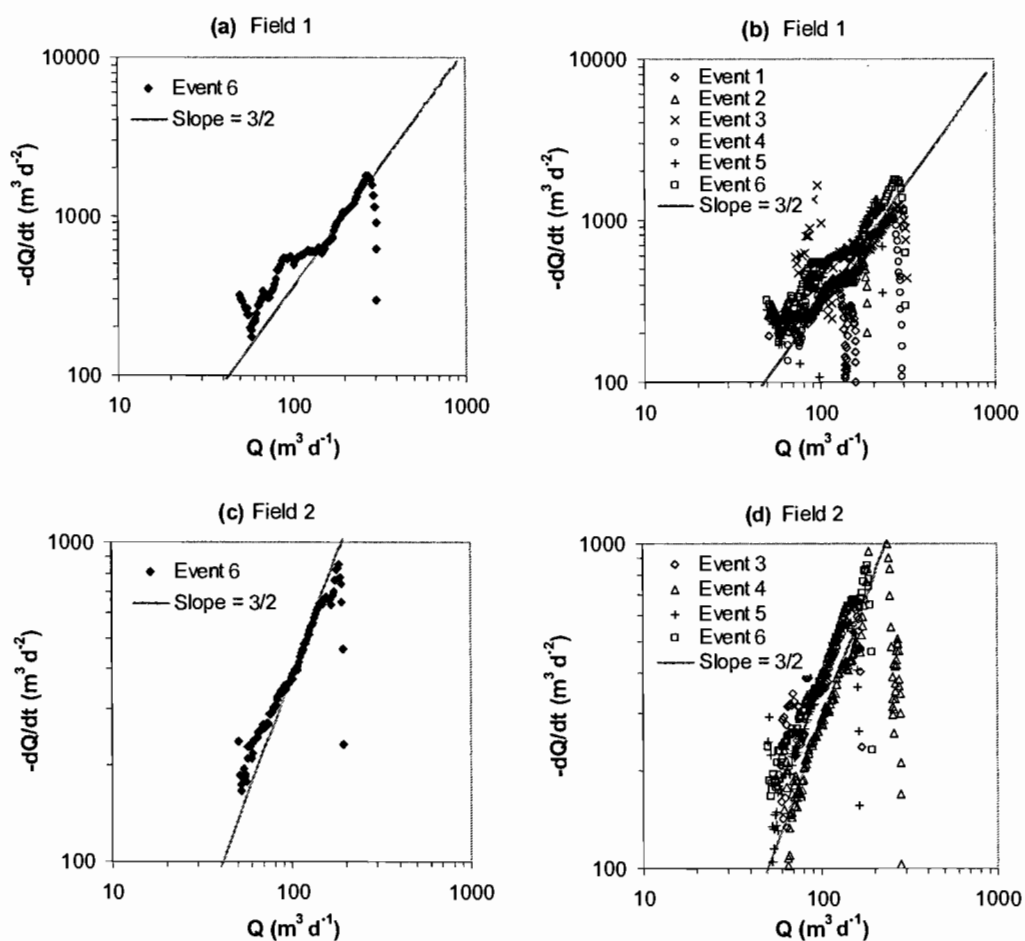
Figure 6. The observed time rate of change of discharge vs. discharge in Field 1 (a and b) and Field 2 (c and d). The figures on the left contain observations from one recession event, and the figures on the right contain observations from all major recession events. The straight solid line in each graph has a slope of 3/2.

is no clearly definable section of any recession curve that fits the early-time solution (Figure 6). The duration of recession that fits (6) with $b = 1.5$ ranges from approximately 3 hours (Field 1) to at most 7 hours (Field 2). The flow meter exhibited an unusual behavior consistently in Field 2 but inconsistently in Field 1: a sudden drop in discharge beginning near 50 m^3/d and lasting for 1-2 hours before rising again. It is for this reason that no data in Figure 6 are graphed below 50 m^3/d. Based on the log-log linear sections of the each curve, k calculated from (8) varied from 3 to 7 m/d for the six events in Field 1 and 2 to 5 m/d for the four events in Field 2 (see Table 1). (Due to the uncertainty in φ, drain depth, and other parameters such as B and L, we report only one significant figure.)

Table 1. Saturated Hydraulic Conductivity Calculated from Drain Discharge and Water Table Measurements

Field	Event	Date	k (m/d)			
			Method 3.1 dQ/dt vs. Q	Method 3.2 Q/Q_o vs. t	Method 3.3 dh/dt vs. h	Method 3.4 h/h_o vs. t
1	1	22-Nov-01	4	4		
	2	29-Nov-01	4	3		
	3	16-Dec-01	3	3		
	4	25-Jan-02	3	3		
	5	07-Feb-02	7	7		
	6	11-Mar-02	5	5		
	Mean		*4*	*4*		
2	3	16-Dec-01	4	4		
	4	25-Jan-02	2	2		
	5	07-Feb-02	5	4	4	4
	6	11-Mar-02	5	4	5	5
	7	19-Mar-02			5	6
	Mean		*4*	*4*	*5*	*5*

The method designation refers to the section numbers in the text

4.2. Relative Discharge vs. Time

For each recession curve, the reference value of discharge Q_o was selected that, through trial and error, resulted in k being the most constant for the longest period of time. In all cases during the recession period k is seen to remain relatively constant for a period ranging from as little as 1.5 hours to as long as 7 hours (Figure 7). This was often followed by an increase in k over time, which is a result of the discharge decreasing at a faster rate than predicted by (5) (Figure 7a). Light rainfall occurring during the recession on a few occasions resulted in an apparently excellent fit by maintaining a slightly elevated discharge (for example, see Figure 7c). Values of k determined from (16) ranged from 3 to 7 m/d for Field 1 and 2 to 4 m/d for Field 2. These numbers are consistent with values calculated with (8) (see Table 1).

4.3. Rate of Change of Water Table Height vs. Height

In all piezometers during Events 5 and 6, the dh/dt vs. h curve appears log-log linear with a slope of 2 between roughly $h = 0.6$ and 0.1 m, suggesting that the late-time solution is valid over this range of heights and over this time span of approximately 48 hours (see Figures 8a through d). During Event 6, the sharp drop in dh/dt at near $h = 0.15$ m is due to rain during this period maintaining a relatively constant water table height. Below $h = 0.1$ m and $dh/dt = 0.1$, noise makes analysis of the data difficult, thus the appropriateness of fitting a curve to the data in Event 7 is dubious (Figures 8e and f). Based on the log-log linear sections of the each curve, k calculated from (19) ranged from 2 to 6 m/d for the five piezometers in Event 5, and k ranged from 4 to 6 m/d for three piezometers in Event 6 (the piezometer closest to the drain was not used because it showed very little change in height). Despite the uncertainty of the data, we estimated k to range from 2 to 8 m/d for Event 7. The mean values of k per event are given in Table 1.
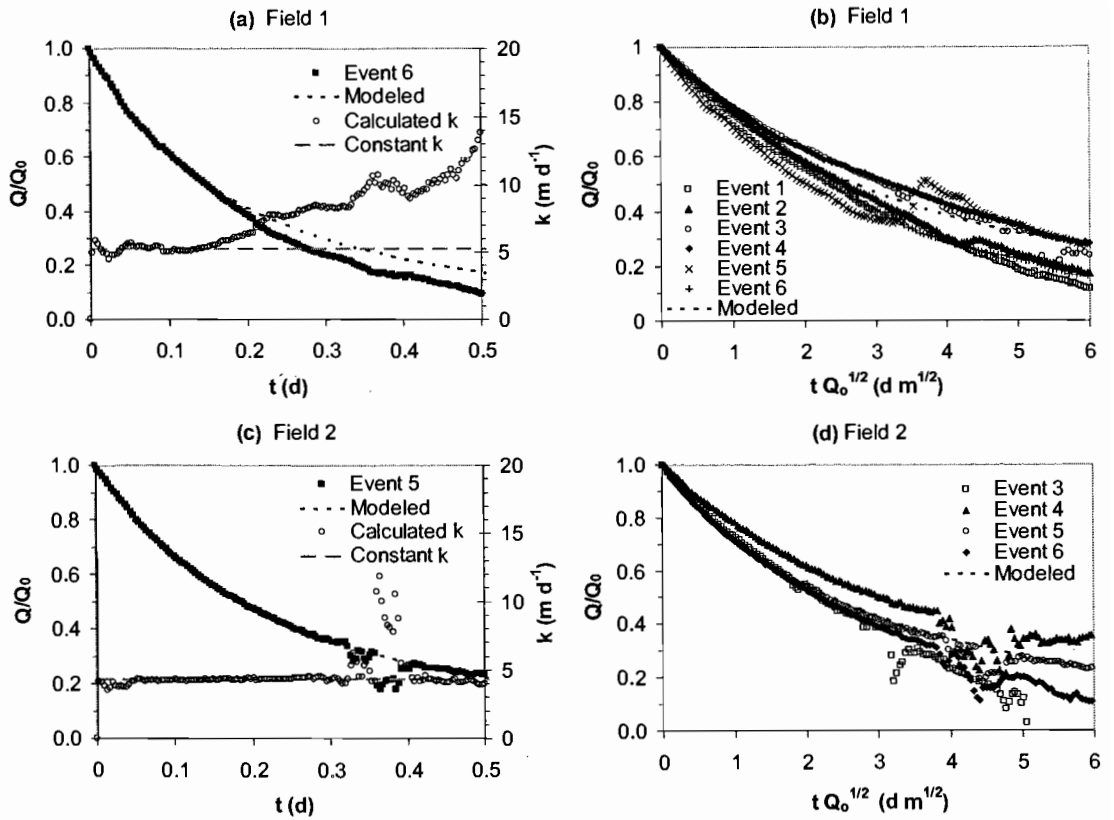
Figure 7. Relative observed (points) and modeled (dashed line) discharge vs. time in Field 1 (a and b) and Field 2 (c and d). The figures on the left show k vs. time for one piezometer calculated from (18) (open circles). The figures on the right show all major recession events with time normalized by the square root of the reference discharge.
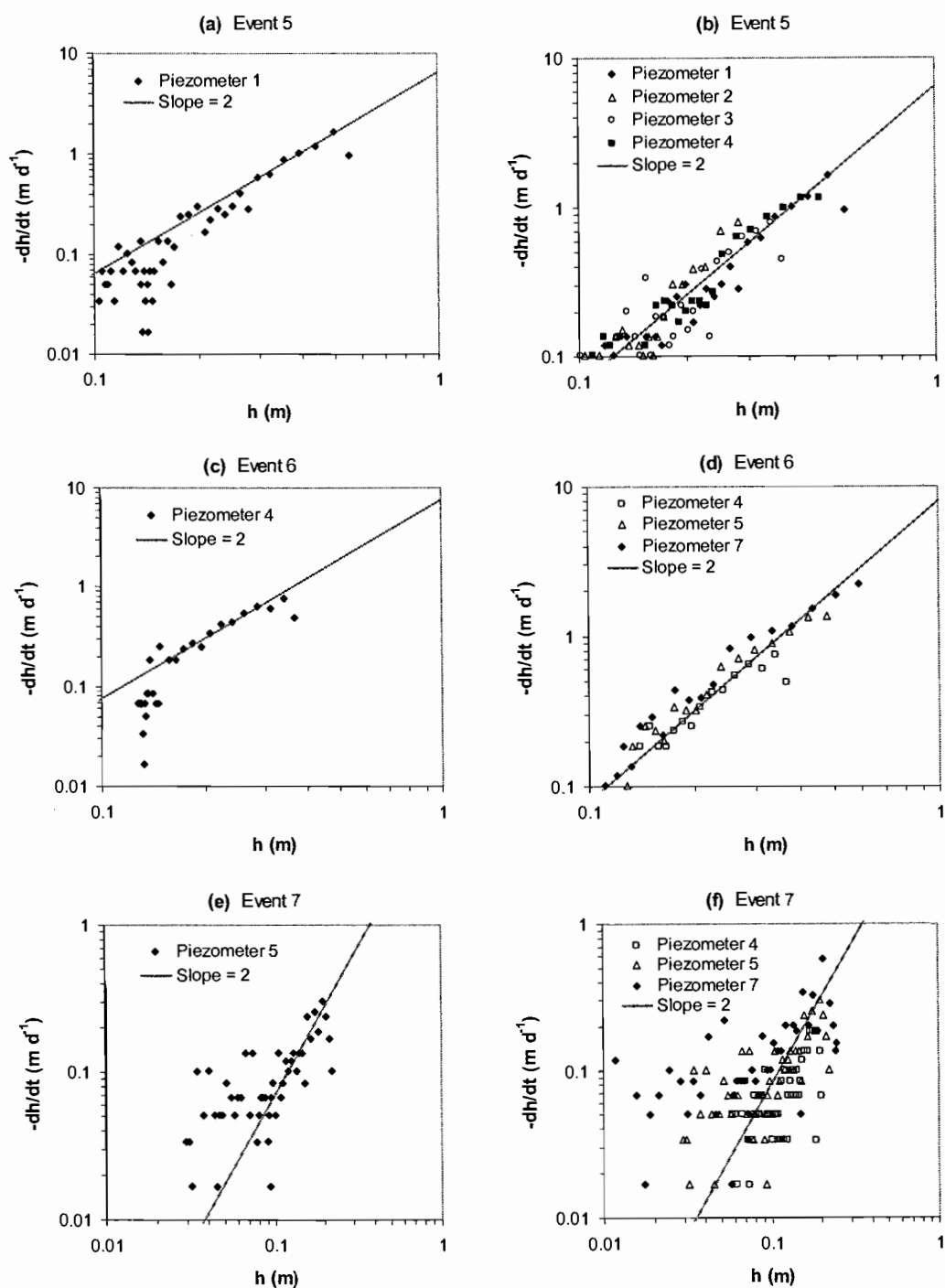
Figure 8. Time rate of change of water table height vs. water table height for recession Events 5 (a and b), 6 (c and d), and 7 (e and f). The figures on the left contain observations from one sample piezometer, and the figures on the right contain all the piezometer observations from a single water table profile.

4.4. Relative Water-Table Height vs. Time

The values of k calculated from (22) remained relatively constant for all the piezometers over the first half day of recession for Events 5 and 6, and for over a day for Event 7 (see Figures 9a, c, and e). Rain during the first twelve hours of recession during Event 5 maintained the water table height slightly higher than the predicted drawdown, whereas the water table dropped quicker than what the model predicted in Event 6 during the ten hours of recession when no rain was recorded. The relative drawdown curves observed in the different piezometers within events are similar, though the relative drop in water table with time was observed to be greater in the piezometers further from the drain tile (Figures 9b, d, and e). From the piezometers used in Event 5, where rain during the recession was a factor, k ranged from 3 to 5 m/d. In Events 6 and 7, k ranged from 4 to 7 m/d and from 4 to 9 m/d, respectively. The mean values of k per event are given in Table 1.
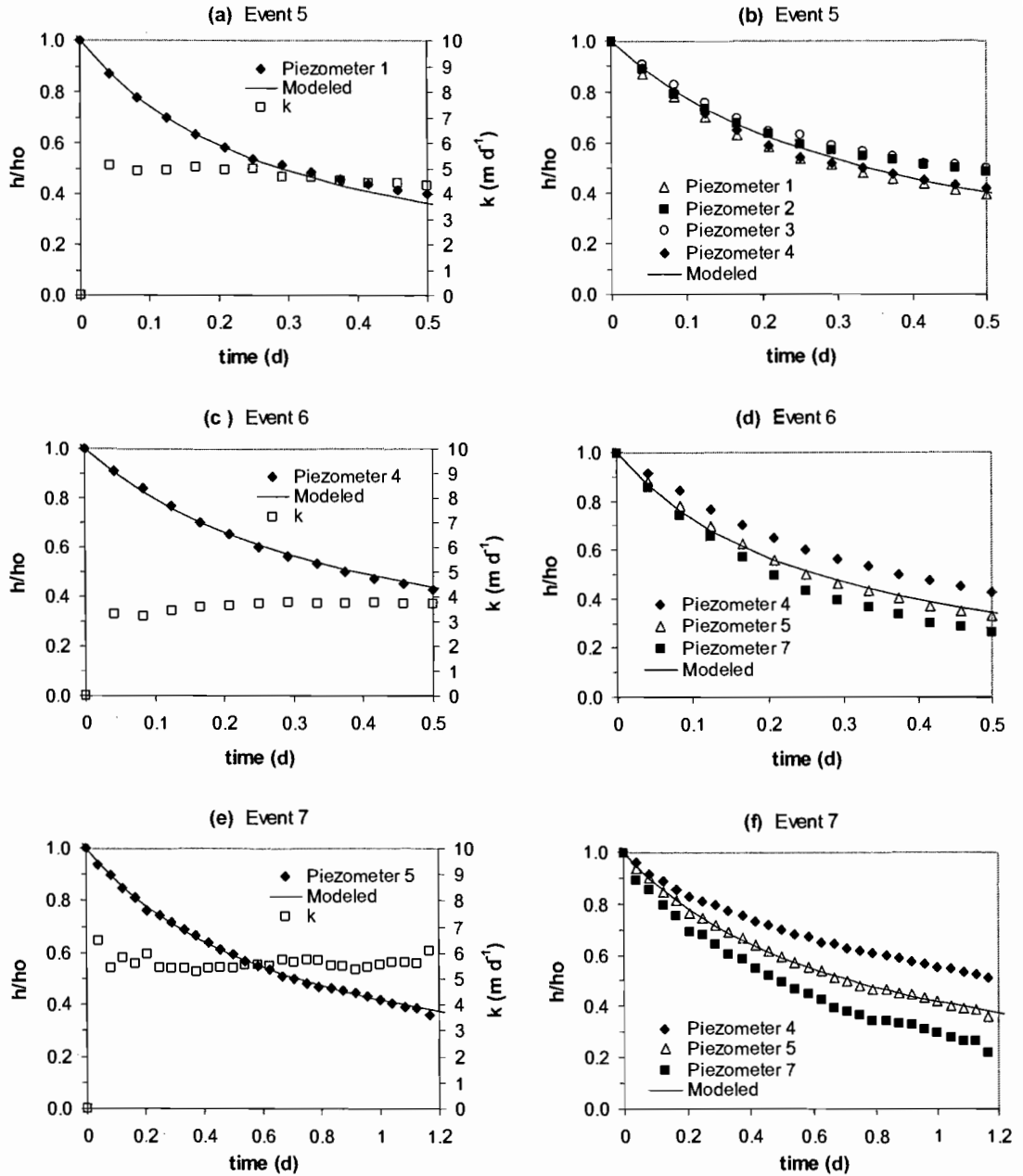
Figure 9. Relative water table height vs. time for recession Events 5 (a and b), 6 (c and d), and 7 (e and f). The figures on the left contain observations from one sample piezometer, with the calculated values of hydraulic conductivity shown as open squares. The figures on the right contain all the piezometer observations from a single water table profile.

5. Discussion and Conclusion

An analysis is presented of four analytical methods for determining the saturated hydraulic conductivity on the field scale for a field drained by a network of parallel drains. All methods are based on transient solutions of the Boussinesq equation [*Boussinesq*, 1904; *Polubarinova-Kochina*, 1962]; two make use of recession water table height and two use recession discharge. Of the two that require discharge measures, one examines the discharge-time relationship, and the second examines the relation of the time rate of change of discharge with discharge. The advantage of this latter method, according to *Brutsaert and Nieber* [1977], is that it eliminates the need to know the initial or reference time ($t = 0$), which is in practice ambiguous. However, we show that by analyzing relative water table height vs. time or relative discharge vs. time and by using substitution to remove initial water table height from the solutions, we are free to choose any time as an initial time so long as it falls within the range of times for which the solutions are valid. For the purpose of assessing the validity of certain solutions, the methodology of *Brutsaert and Nieber* [1977] is very useful. We adopt the technique of *Brutsaert and Nieber* [1977] for aquifer discharge and apply it to water table observations.

Although a field drained by parallel perforated pipes buried some distance above an impermeable layer as was investigated here does not meet all the assumptions of the Boussinesq aquifer, the analysis methods presented appear to be applicable. Encouraging, however, are the findings of *Szilagyi* [2003], who showed that, at least for a solution of the Laplace equation, k estimation was only slightly sensitive to errors made in defining the depth of the impermeable layer. It should be noted that the assumption made there was that the water table drop was much less than the initial saturated thickness, which is probably not the case here.

Notable, but not surprising, is the absence of discharge observations that fit the early-time solution of *Polubarinova-Kochina* [1962]. We can see why this is so from the time and discharge during the transition between the early- and late-time solutions. A rough estimate of the discharge at the time of transition can be made by equating (7)

in (6) with (8) in (6) [*Brutsaert and Lopez*, 1998]. This results in $Q = 1.309kD^2L/B$. This equation for discharge can be substituted into (3) or (5), which, solving for time, yields $t = 0.257B^2\varphi/kD$.

Based on the previous equations, the timing and discharge of the transition period for Event 6 in Field 2 are roughly 1 hour and 300 m^3/d, respectively. Thus the lifetime of the early-time solution is short relative to the duration of identifiable precipitation events (typically here < 10 hours). Furthermore, at discharges of this order, the drain would be operating under positive pressure and not acting as an open channel, so (3) would not be applicable. An estimate of the maximum discharge of the drain under open channel conditions can be made from Manning's equation: $Q = (1/n)A(A/P)^{2/3}S^{1/2}$, where A is the cross-sectional drain area, P is the wetted perimeter, S is the slope and n is Manning's coefficient [*Manning*, 1891]. Using a value of $n = 0.01$ for plastic [*Neale and Price*, 1964], the maximum open channel Q for the drains in Fields 1 and 2 is roughly 200 m^3/d. It can be seen in Figure 6 that it is around this value of Q when the slopes of curves become 1.5, suggesting that nearly as soon as the drain is no longer under positive pressure the aquifer begins to behave as a Dupuit-Boussinesq aquifer and that the late-time solution is valid. Further evidence for the appropriateness of the Dupuit-Boussinesq aquifer is the agreement between the piezometer observations and the theoretical water table profiles generated from (4) (see Figure 10). The fit is quite reasonable given the uncertainty in the measured depth of drain and the lateral position of the piezometers with respect to the drain.

After several hours of drainage without any further rainfall, the discharge decreases faster than predicted by the late-time discharge solution. One possible explanation is greater discharge, thus faster drainage, than predicted due to the assumption of an impermeable layer at drain depth when in actuality the impermeable layer is situated at some unknown depth below the drains. In other words, if the model permitted water to enter the drain radially from below, the aquifer would drain faster [e.g., *van Schilfgaarde*, 1963]. The result would be an overestimation of k using the methods reported in this study.
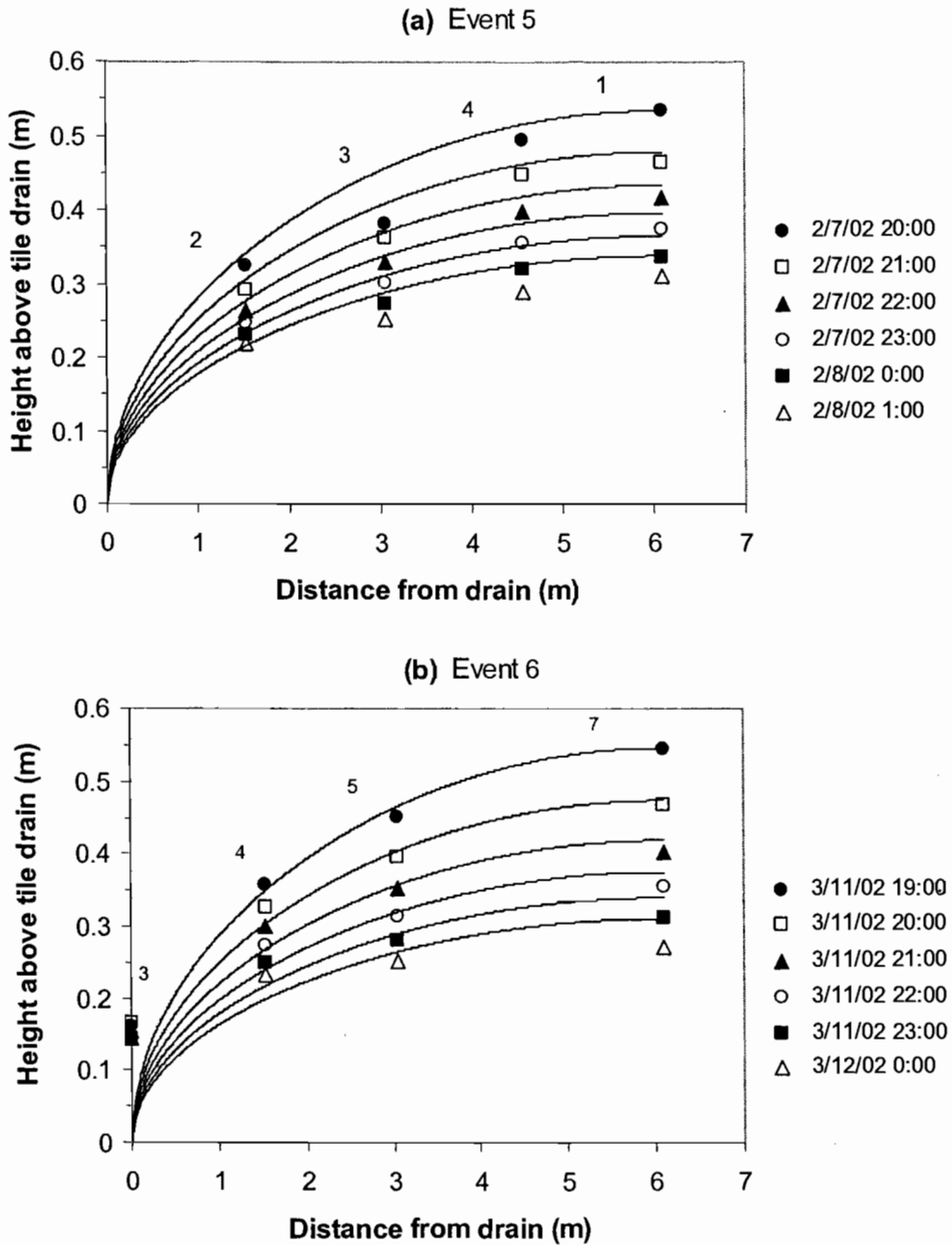
Figure 10. Observed (points) and theoretical (curves) water table heights in Field 2 for (a) Event 5 and (b) Event 6. The curves, like the points, represent 1 hour intervals. The piezometers numbers are indicated in the figures. Only the approximate position of the piezometers with respect to the drains was known. For example, piezometer 3 is shown in (b) as being exactly at the drain, but in reality it was somewhere in the proximity of the drain tile. The numbering of the piezometers was not consistent between the two events.

A second explanation is deep percolation of water moving past the drainage system. The downward movement of water becomes progressively greater in proportion to the water leaving via the drains as the water table approaches the height of the drainage system, thus becoming a greater factor with time. The rate of vertical flow could be estimated from the rate at which the water table lowered once it dropped below the drain system. However, an examination of the water table observations for Events 6 and 7 shows that such an analysis is not straightforward (see Figure 11). When the water table falls below the height of the drain, $-dh/dt$ increases and stays relatively constant at approximately 0.12 m/d. This break in the recession curve probably reflects the influence of the regional ground water table, which is known to drain to the stream 150 m away and 15 m below the lowest point in the field, and probably occurs when the local and regional water tables are in correspondence and begin lowering at the same rate. However, without further analysis of the regional flow system, it is unclear how regional pressure gradients are affecting the local water table when it is above the height of the drain system.

Another factor affecting the drainage is the changing drainable pore volume, which we assumed is constant but in theory is a function of the water table height [e.g., *van Schilfgaarde*, 1963]. The water retention data from the soil cores do show a decrease in water content of just under 0.02 m^3/m^3 from -0.34 m H_2O to -1.02 m H_2O, which is significant when compared to the assumed constant drainable porosity of 0.023. However, an increasing drainable pore volume with falling water table would have an effect counter to what the discharge observations reveal, suggesting that this is not a critical consideration here.

In summary, the four methods described above for calculating saturated hydraulic conductivity k were found to be applicable to a field containing a system of parallel drains. Calculated values of k were consistent among methods and consistent among recession events within the same field. The advantage of the methods that do not rely on taking derivates of the data is that noise is not introduced, which can complicate analysis.
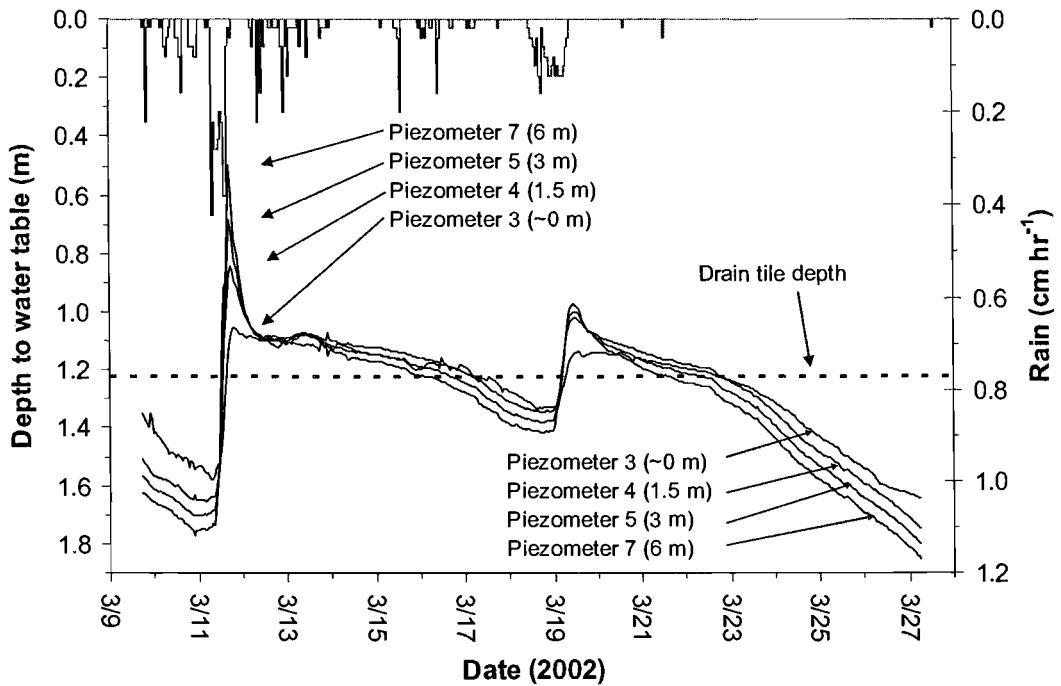
Figure 11. Observed depth to water table during an 18 day period in Field 2. The peaks on March 11 and March 19 correspond to Events 6 and 7, respectively. Listed to the right of each piezometer number is the approximate distance from the nearest drain.

These values of k estimated at the field scale (~4 m/d) were much less than the mean k of 20 m/d calculated from 40 soil cores and much closer to their median k of 5 m/d. The near complete saturation of the soil cores during the laboratory analysis versus the likely incomplete saturation of the soil in the field may explain part of this discrepancy. These results do suggest, however, that non-linear scale effects, which we would expect to result in higher conductivities at the field scale than at the core scale, do not play a significant role in the drainage of these fields during the wet winter season.

Acknowledgments

References

Abramowitz, M., and I. A. Stegun (Eds.) (1972), *Handbook of Mathematical Functions*, 1046 pp., Dover, New York.

Boussinesq, J. (1904), Recherches théoriques sur l'écoulement des nappes d'eau infiltrées dans le sol et sur débit de sources, *J, Math. Pures Appl., 5me Ser., 5*, 5-78.

Brutsaert, W., and J. P. Lopez (1998), Basin-scale geohydrologic drought flow features of riparian aquifers in the southern Great Plains, *Water Resour. Res., 34*, 233-240.

Brutsaert, W., and J. L. Nieber (1977), Regionalized drought flow hydrographs from a mature glaciated plateau, *Water Resour. Res., 13*, 637-643.

Dumm, L. D. (1954), New formula for determining depth and spacing of subsurface drains in irrigated lands, *Agric. Engng., 35*, 726-730.

Dumm, L. D. (1964), Transient-flow concept in subsurface drainage: its validity and use, *Trans. ASAE, 7*, 142-151.

El-Mowelhi, N. M., and J. Van Schilfgaarde (1982), Computation of soil hydrological constants from field drainage experiments in some soils of Egypt, *Trans. ASAE, 25*, 984-986.

Hoffman, G. J., and G. O. Schwab (1964), Tile spacing prediction based on drain outflow, *Trans. ASAE, 13*, 444-447.

Hooghoudt, S. B. (1940), Bijdragon tot de Kennis van Eenige Natuurkundige Groothen van den Grond, 7. Algemeene Beschouwing van het Probleem van de Detail Ontwatering en de Infiltratie door middle van Parallel Loopende Drains, Greppels, Slooten en Kanalen, *Verslag. Landbouwk. Onderzoek., 46*, 515-707.

Klute, A. (1986), Water Retention: Laboratory Methods, in *Methods of Soil Analysis. Part 1, second ed, Agronomy Monograph No. 9*, edited, pp. 635-662.

Klute, A., and C. Dirksen (1986), Hydraulic Conductivity and Diffusivity: Laboratory Methods, in *Methods of Soil Analysis. Part 1, second ed, Agronomy Monograph No. 9*, edited, pp. 687-734.

Luthin, J. N. (1959), The falling water table in tile drainage. II. Proposed criteria for spacing tile drains, *Trans. ASAE,* 44-45.

Luthin, J. N., and R. V. Worstell (1959), The falling water table in tile drainage. III. Factors affecting the rate of fall, *Trans. ASAE,* 45-51.

Manning (1891), On the flow of water in open channels and pipes., *Trans. Institute of Civil Engineers of Ireland.*

Neale, L. C., and R. E. Price (1964), Flow characteristics of PVC sewer pipe, *J. Sanitary Engng Div., Div. Proc. 90SA3, ASCE,* 109-129.

Otte, G. E., D. K. Setness, W. A. Anderson, F. J. Herbert, and C. A. Knezevich (1974), Soil Survey of the Yamhill Area, 138 pp, USDA, Soil Conservation Service; in Cooperation with the Oregon Agriculture Experiment Station.

Parlange, J. Y., M. B. Parlange, T. S. Steenhuis, W. L. Hogarth, D. A. Barry, L. Li, F. Stagnitti, A. Heilig, and J. Szilagyi (2001), Sudden drawdown and drainage of a horizontal aquifer, *Water Resour. Res., 37,* 2097-2101.

Polubarinova-Kochina, P. Y. (1962), *Theory of Ground Water Movement,* 613 pp., Princeton University Press, Princeton, N. J.

Szilagyi, J. (2003), Sensitivity analysis of aquifer parameter estimations based on the Laplace equation with linearized boundary conditions, *Water Resour. Res., 39,* SBH81-SBH87.

Szilagyi, J., and M. B. Parlange (1998), Baseflow separation based on analytical solutions of the Boussinesq equation, *J. Hydrol., 204,* 251-260.

Szilagyi, J., M. B. Parlange, and J. D. Albertson (1998), Recession flow analysis for aquifer parameter determination, *Water Resour. Res., 34,* 1851-1857.

Talsma, T., and H. C. Haskew (1959), Investigation of water-table response to tile drains in comparison with theory, *J. Geophys. Res., 64,* 1933-1944.

Troch, P. A., F. P. De Troch, and W. Brutsaert (1993), Effective water table depth to describe initial conditions prior to storm rainfall in humid regions, *Water Resour. Res., 29,* 427-434.

van Schilfgaarde, J. (1963), Design of tile drainage for falling water tables, *J. Irrigation Drainage Div., Proc. ASCE IR,* 1-10.

Chapter 3 - Information, Artifacts, and Noise in *dQ/dt-Q* Recession Analysis

David E. Rupp and John S. Selker

Department of Bioengineering, Oregon State University, Corvallis, OR

Abstract

The plotting of the time rate of change in discharge dQ/dt versus discharge Q has become a widely-used tool for analyzing recession data since *Brutsaert and Nieber* [1977] proposed the method. Typically the time increment Δt over which the recession slope dQ/dt is approximated is held constant. It is shown here this that leads to upper and lower envelopes in graphs of $\log(-dQ/dt)$ versus $\log(Q)$ that have been observed in previous studies but are artifacts. The use of constant time increments also limits accurate representation of the recession relationship to the portion of the hydrograph for which the chosen time increment is appropriate. Where dQ/dt varies by orders of magnitude during recession, this may exclude much of the hydrograph from analysis. In response, a new method is proposed in which Δt for each observation in time is properly scaled to the observed drop in discharge ΔQ. It is shown, with examples, how the new method can succeed in exposing the underlying relationship between dQ/dt and Q where the standard method fails.

1. Introduction

For investigating base flow, *Brutsaert and Nieber* [1977] suggested analyzing the slope of the recession curve as a function of discharge Q rather than the recession time series, thus eliminating the need of a time reference. This is advantageous because of the practical impossibility of determining the precise beginning of a base flow recession event from real stream flow data. *Brutsaert and Nieber* [1977] also provided a procedure to interpret these diagrams in terms of physically meaningful parameters. Recession slope analysis has been applied widely since for determining aquifer parameters [*Zecharias and Brutsaert*, 1988b; *Troch, et al.*, 1993; *Brutsaert and Lopez*, 1998; *Parlange, et al.*, 2001; *Mendoza, et al.*, 2003; *Rupp, et al.*, 2004; *Malvicini, et al.*, 2005] and base flow separation [*Szilagyi and Parlange*, 1998].

Operationally, the instantaneous slope of the recession curve dQ/dt is not measured directly but is approximated numerically from a drop in discharge "ΔQ" occurring over a time increment Δt. In the aforementioned studies, Δt was held constant.

The optimal choice of the time increment Δt follows from consideration of the process under investigation, the precision of the data, and the degree of noise [*Tallaksen*, 1995]. In other words, Δt must be at least large enough to detect the signal being sought, but not so large as to overwhelm it. A difficulty arises in real data because $-dQ/dt$ may drop by one or even several orders of magnitude during recession. What is an appropriate Δt at early times when $-dQ/dt$ is high may be too short at later times as ΔQ approaches the magnitude of the data noise. Conversely, what is an appropriate Δt at later times may be much too large to resolve the early part of the recession curve. The extent to which the standard numerical approximation to dQ/dt versus Q can affect data analysis has not been well-documented.

It is shown here that the use of a constant Δt leads to previously observed upper [*Mendoza, et al.*, 2003] and lower [*Brutsaert and Lopez*, 1998] boundaries to

real data graphed as log(-dQ/dt) versus log(Q). These are purely numerical artifacts, and can potentially lead to a misinterpretation of the recession data.

We present and apply a variation on the *Brutsaert and Nieber* [1977] method that explicitly takes into consideration data precision. We choose a time increment Δt that is shown to be properly scaled to the observed drop in discharge ΔQ. By using high temporal resolution data with the "scaled-Δt" method, the early part of the recession curve is preserved when the hydrograph is dropping most rapidly. Yet, by allowing Δt to increase as the recession progresses, the curve can be resolved for later times beyond the point at which precision effects or noise would cause the constant-Δt method to fail.

2. Analysis method with constant Δt

Brutsaert and Nieber [1977] proposed analyzing the time rate of change in discharge as a function of discharge:

$$dQ/dt = f(Q) \tag{1}$$

Operationally the data is analyzed using the approximation:

$$\frac{Q_{i+1} - Q_i}{\Delta t} = f\left(\frac{Q_{i+1} + Q_i}{2}\right) \tag{2}$$

where the subscript i refers to any time t and $i + 1$ to the time $t + \Delta t$ and where Δt is a suitable time increment [*Brutsaert and Nieber*, 1977]. *Brutsaert and Nieber* [1977] suggest fitting an analytical model of base flow generation to the data defined by the lower envelope of the data plotted as log(-dQ/dt) against log(Q) on the basis that data at the lower envelope are specifically those without contributions from overland flow, interflow, or channel storage. From this perspective understanding of any anomalies that might affect this lower envelope is important. We will show that the choice of Δt

alone defines an upper envelope, and that along with the precision of the discharge measurements, Δt also defines a lower envelope for the same graph.

2.1. Upper envelope to -dQ/dt vs. Q

An upper envelope is defined by the maximum possible observable rate of decline in discharge. Let Y_{max} be the bound on the decline dQ/dt estimable from (2), computed as a drop to zero flow in a single time step, and let X be the corresponding estimate of discharge Q:

$$Y_{max} = \frac{0 - Q_i}{\Delta t} \le \frac{Q_{i+1} - Q_i}{\Delta t} \tag{3}$$

$$X = \frac{0 + Q_i}{2} \le \frac{Q_{i+1} + Q_i}{2} \tag{4}$$

Combining (3) and (4), the equality in (2), or $Y_{max} = f(X)$, becomes

$$\frac{0 - Q_i}{\Delta t} = -\frac{2}{\Delta t}\left(\frac{0 + Q_i}{2}\right) \tag{5}$$

or simply

$$-Y_{max} = \frac{2}{\Delta t} X \tag{6}$$

Taking the logarithm of (6) yields

$$\log(-Y_{max}) = \log X + \log\left(\frac{2}{\Delta t}\right) \tag{7}$$

Thus, for constant Δt on a log-log graph of $-(Q_{i+1} - Q_i)/\Delta t$ versus $(Q_{i+1} + Q_i)/2$, (7) appears as a line of slope = 1 with y-intercept $\log(2/\Delta t)$. This would appear to explain the upper 1:1 envelope first reported by *Mendoza et al.* [2003] as appearing in many studies [*Brutsaert and Nieber*, 1977; *Troch, et al.*, 1993; *Brutsaert and Lopez*, 1998; *Parlange, et al.*, 2001; *Malvicini, et al.*, 2005] .

2.2. Lower envelope to *-dQ/dt* vs. *Q*

The lower envelope is a function of the precision of the discharge measurements and of Δt. We consider two types of precision in the discharge measurements. One is the precision at which Q is recorded (for example, to the nearest 0.01 $m^3 s^{-1}$), denoted as ω. However, discharge is rarely measured directly, but is usually determined as a function of stage height H. To stage height we assign another precision, ε.

In the case when Q is measured directly and the precision ω is constant for all Q, a minimum estimable non-zero rate of decline dQ/dt, denoted as Y_ω, is found when successive measurements differ by the precision:

$$Y_\omega = \frac{Q_{i+1} - Q_i}{\Delta t} = -\frac{\omega}{\Delta t} \qquad (8)$$

When graphed as $\log(-Y_\omega)$ against $\log(X)$, with Δt constant, this will plot as a line of slope = 0 and y-intercept $\log(\omega/\Delta t)$. Eq. (8) corresponds to the lower boundary in the graph of $\log[-(Q_{i+1} - Q_i)/\Delta t]$ versus $\log[(Q_{i+1} + Q_i)/2]$. However, successive measurements can also differ by integer multiplies of the precision, i.e. 2ω, 3ω, etc. Therefore, graphed points may also appear along horizontal lines with intercepts of $\log(2\omega/\Delta t)$, $\log(3\omega/\Delta t)$, etc., producing an apparent discretization of the data at low values of $\log(-dQ/dt)$ [*Brutsaert and Nieber*, 1977; *Brutsaert and Lopez*, 1998; *Parlange, et al.*, 2001; *Mendoza, et al.*, 2003].

The effect of the second type of precision, that of uncertainty in stage height H, is less obvious. In the case when $Q = Q(H)$ and stage precision ε is constant for all H, a minimum estimable non-zero rate of decline dQ/dt, denoted as Y_ε, may be calculated from (2) for any point X as

$$\frac{Q(H) - Q(H + \varepsilon)}{\Delta t} = f\left(\frac{Q(H) + Q(H + \varepsilon)}{2}\right) \tag{9}$$

The left side of (9) can be written as

$$\frac{Q(H) - Q(H + \varepsilon)}{\Delta t} = \frac{2}{\Delta t}\left[\frac{Q(H) + Q(H + \varepsilon)}{2} - Q(H + \varepsilon)\right] \tag{10}$$

or

$$Y_\varepsilon = \frac{2}{\Delta t}\left[X - Q(H + \varepsilon)\right] \tag{11}$$

Taking the logarithm of (11) yields

$$\log(-Y_\varepsilon) = \log[Q(H + \varepsilon) - X] + \log\left(\frac{2}{\Delta t}\right) \tag{12}$$

Eq. (12) shows how a lower envelope is defined by the stage height precision, the stage-discharge equation, and the time interval. However, (8) and (11) together form the effective lowest envelope.

In practice, this error-based lower envelope may be simplest to calculate numerically. Let Y_{min} be the minimum non-zero rate of decline dQ/dt estimable from (2) due to both ε and ω.

$$Y_{\min, j} = \frac{\hat{Q}(j\varepsilon) - \hat{Q}[(j+1)\varepsilon]}{\Delta t}$$

(13a)

and

$$X_j = \frac{\hat{Q}(j\varepsilon) + \hat{Q}[(j+1)\varepsilon]}{2}$$

(13b)

where $\hat{Q}$ refers to the stage-discharge function with discharge reported to a precision ω, and the subscript j is an integer greater than zero. Other curves parallel to but higher than the lower envelope defined by (13) may be appear in graphed data for integer multiples of ε as successive measurements differ by greater increments of the measurement precision.

Though stage height precision is considered as a constant above, there may be cases where precision changes over the range of measurements. In such cases, $\varepsilon(H)$ or $\varepsilon(j)$ would replace ε.

3. New recession analysis method

Because recession analyses that rely on the time derivative of Q amplify noise and inaccuracies in discharge data, it is important to select a time interval Δt suited to the quality of the data [*Tallaksen*, 1995]. Ideally, Δt would be chosen so that the data points lie well clear of the upper and lower envelopes described above. One approach, which we present here, is to choose a time increment Δt that is properly scaled to the observed drop in discharge ΔQ.

The time rate of change in discharge and the corresponding discharge are calculated, respectively, by

$$\frac{dQ}{dt} \approx \frac{Q_i - Q_{i-j}}{t_i - t_{i-j}}, \qquad i = 2, 3, \ldots, N; \ 0 < j < i \tag{14a}$$

and

$$Q \approx \frac{1}{(j+1)} \sum_{k=i-j}^{i} Q_k \tag{14b}$$

where i represents data points taken at discrete time increments (e.g., every 5 minutes), and j is the number of time increments over which dQ/dt is calculated. In previous studies, j would have been constant. Eq. (14b) is less biased than the approximation to Q given in the right-side of (2) when $j > 1$.

Here we let the time interval $t_i - t_{i-j}$ be a value such that the corresponding difference $Q_{i-j} - Q_i$ exceeds some threshold value that is a function of the measurement precision ε. Operationally, we step backwards in time from the ith observation a number of steps j until

$$Q_{i-j} - Q_i \geq C[Q(H_i + \varepsilon) - Q_i] \tag{15}$$

where C is a constant ≥ 1.

4. Data analysis

It is illuminating to see how the procedure described above can give widely different results than the use of a constant Δt when error is present in discharge data. Here we present two examples. The first is an analysis of a hypothetical recession curve derived from an analytical solution for aquifer discharge. The second is an analysis of two stream flow records of varying data quality.

4.1. Theoretical recession curve

The analysis of a synthetic recession curve permits us to see how the numerical approximations (2) and (14) differ from the "truth" when error is introduced into the data. For this example, recession data were generated from the analytical approximation to the Boussinesq equation derived by *Parlange et al.* [2001] (see Appendix A) with parameter values given for Basin 69013, Washita, Oklahoma, in *Brutsaert and Lopez* [1998]. The daily synthetic discharge was converted to a stage height H by inverting the stage-discharge relation, $Q = 6.72H^{2.5}$, with units of meters and seconds. The stage-discharge relation was derived by a fitting a power-law function to a portion of the discharge versus stage height data for Basin 69013 (Agricultural Research Service Water Database website, USDA). The actual stage-discharge equation appears to have changed many times during the lifetime of the station, but the one given here fits the later data very well. Measurement errors were introduced by rounding the values of H to the nearest 0.305 centimeter (0.01 ft), which is the precision of the data set for Basin 69013. Discharge Q was then recalculated from the same stage-discharge relation, reporting Q to the nearest 0.000283 m^3 s^{-1} (0.01 ft^3 s^{-1}), again as in the reported data. Lastly, we estimated dQ/dt versus Q using (14-15) with $C = 5$ and using (2) with a constant Δt of one day.

The use of a constant time increment generates an obvious discretization pattern in a plot of $\log(-dQ/dt)$ against $\log(Q)$ (Figure 1), which is similar to that seen in the recession curves of *Brutsaert and Lopez* [1998]. In contrast, the scaled-Δt method shows no strong discretization. The scaled-Δt method also retains the shape of the theoretical curve. This is not true for the constant-Δt method. Whereas the theoretical curve shows a transition in slope from 3 to 1.5, the constant-Δt curve begins with a slope of 3 that transitions to an entirely anomalous value of approximately 0.6. This value, not coincidentally, is the same as the slope of the lower envelope in Figure 1 of *Brutsaert and Lopez* [1998], which is clearly less than the theoretical predictions [*Michel*, 1999]. This lower envelope is an artifact of the estimation procedure and does not represent groundwater characteristics.
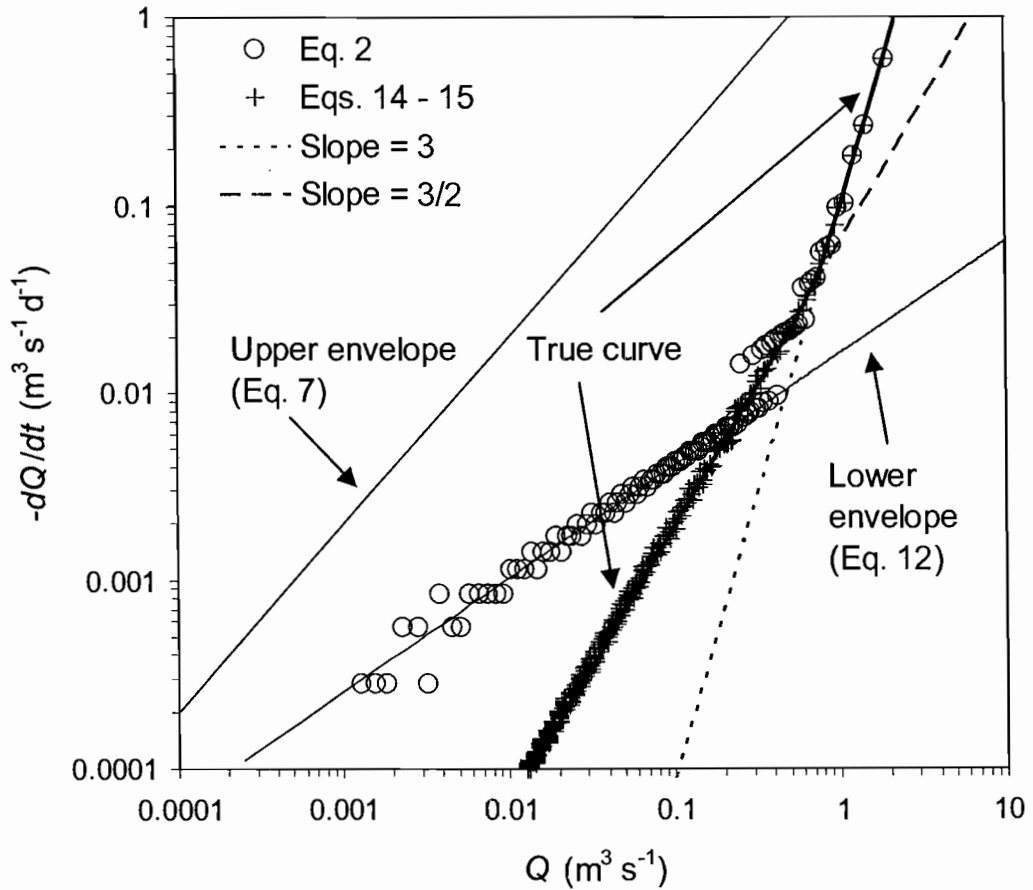
Figure 1. Effect of precision of stage height and discharge (Q) values and of time interval Δt on the estimation of dQ/dt. The heavy solid line, or true curve, is an analytical solution to the non-linear Boussinesq equation (see A1-A5). The symbols represent numerical approximations to dQ/dt. The open circles are obtained using a constant Δt over which dQ/dt is calculated (2), whereas the crosses are calculated with Δt that is scaled to the observed decrease in Q (14-15). Shown also are an upper envelope (7) with a slope = 1 and a lower envelope (12) with a slope ≈ 0.6 that arise when using a constant Δt of one day. Parameter values for the Boussinesq equation are for Basin 69013, Washita, Oklahoma [*Brutsaert and Lopez*, 1998].

It is clear from Figure 1 how stage height precision and use of a constant time increment bound the region that data can occupy. Interpreting data visually must be done with care as these upper and lower envelopes can attract the eye. Precaution should be taken even when regressing a line to data that fills this area, as the slope will reflect to some degree the lower and upper envelopes.

4.2. Observed recession curves

Two recession hydrographs of different quality, one from each of two gauging stations, were analyzed using both the constant-Δt and scaled-Δt methods. The stations are located on the leeward side of the coastal range of the 8th Region of Chile. The first station, Buenos Aires, gauges an area of 0.67 km^2. Water level was recorded inside a culvert every 5 minutes by a Troll 4000 pressure transducer (In-Situ, Inc.) that measures pressure relative to atmospheric through a vented cable. The instrument precision and reported factory error was 1 mm H_2O, and we found the high-frequency measurement noise to be about 2 mm H_2O. Discharge was calculated from stage height from Manning's equation [*Chow*, 1959]. The second station, San José, gauges an area of 7.25 km^2. Water level was recorded in a super-critical flume [*Smith, et al.*, 1981] every 5 minutes. Here a Diver pressure transducer (Van Essen Instruments) recorded absolute pressure at the flume, which was corrected for atmospheric pressure by second instrument located nearby. The Diver at the flume recorded to the nearest 5 mm H_2O and the Diver used to measure atmospheric pressure recorded to the nearest 1 mm H_2O. We observed a high-frequency noise in water level measurements of 10 to 15 mm. There was also a daily fluctuation of 20 mm to 25 mm that could be a response of the instruments to temperature, as these fluctuations were seen to be purely anomalous based on manual reading at the gauging stations.

The two recession events analyzed have noise to signal ratios that differ by nearly a factor of 25. The total change in stage height for the Buenos Aires event was 560 mm over about 6 days. The noise divided by range is about 0.004 for the event. For the 17-day San José event, the total change in stage height was 220 mm, which equates to a noise-to-range ratio of about 0.1.

For both recession hydrographs, the scaled-Δt method proved to be the better of the two procedures for resolving $dQ/dt = f(Q)$. For a constant Δt of 15 min, the Buenos Aires event is resolvable down to $-dQ/dt \approx 3 \times 10^{-6}$ m^3 s^{-2} before the signal is lost (Fig. 2a). Using a constant Δt of 12 hr extends the curve down to $\sim 8 \times 10^{-8}$ m^3 s^{-2}, but an accurate depiction of the early-part of the curve is lost above $\sim 3 \times 10^{-6}$ m^3 s^{-2} (Fig. 2b). However, use of the scaled-Δt method allows both early and late-time resolution of the curve (Fig. 2c).

In comparison, the San José event is essentially not resolvable using a constant Δt of 15 min (Fig 2d). Increasing Δt to a constant value of 12 hr produces only minor improvement (Fig 2e). Remarkably, however, the scaled-Δt method revealed not only the general trend of the curve but also an apparent break in slope (Fig. 2f).

With the scaled-Δt method, as $-dQ/dt$ decreases in time, the time over which $-dQ/dt$ is calculated, or $t_i - t_{i-j}$, tends to increase (Fig. 3). For the Buenos Aires event, for example, we achieved a good reduction in scatter yet were still able to extend the recession curve to low values of $-dQ/dt$ and Q by selecting a value for C such that, overall, $t_i - t_{i-j} \leq t_i/4$ (Fig 3a). Though increasing the value of C would further reduce scatter, it is desirable that C be large enough to resolve the signal but not so large as to overwhelm it. In the extreme case (very large C), for example, where $t_i - t_{i-j}$ approaches t_i, or $j \rightarrow i - 1$, the apparent slope break in the Buenos Aires curve is no longer visible (Fig. 4). In the case of San José, the large amount of noise relative to signal required that Δt on average encompass a much larger portion of the total recession curve (Fig 3b). The effect of the noise is evident in Fig. 3b as Δt varies greatly between successive values of t_i.
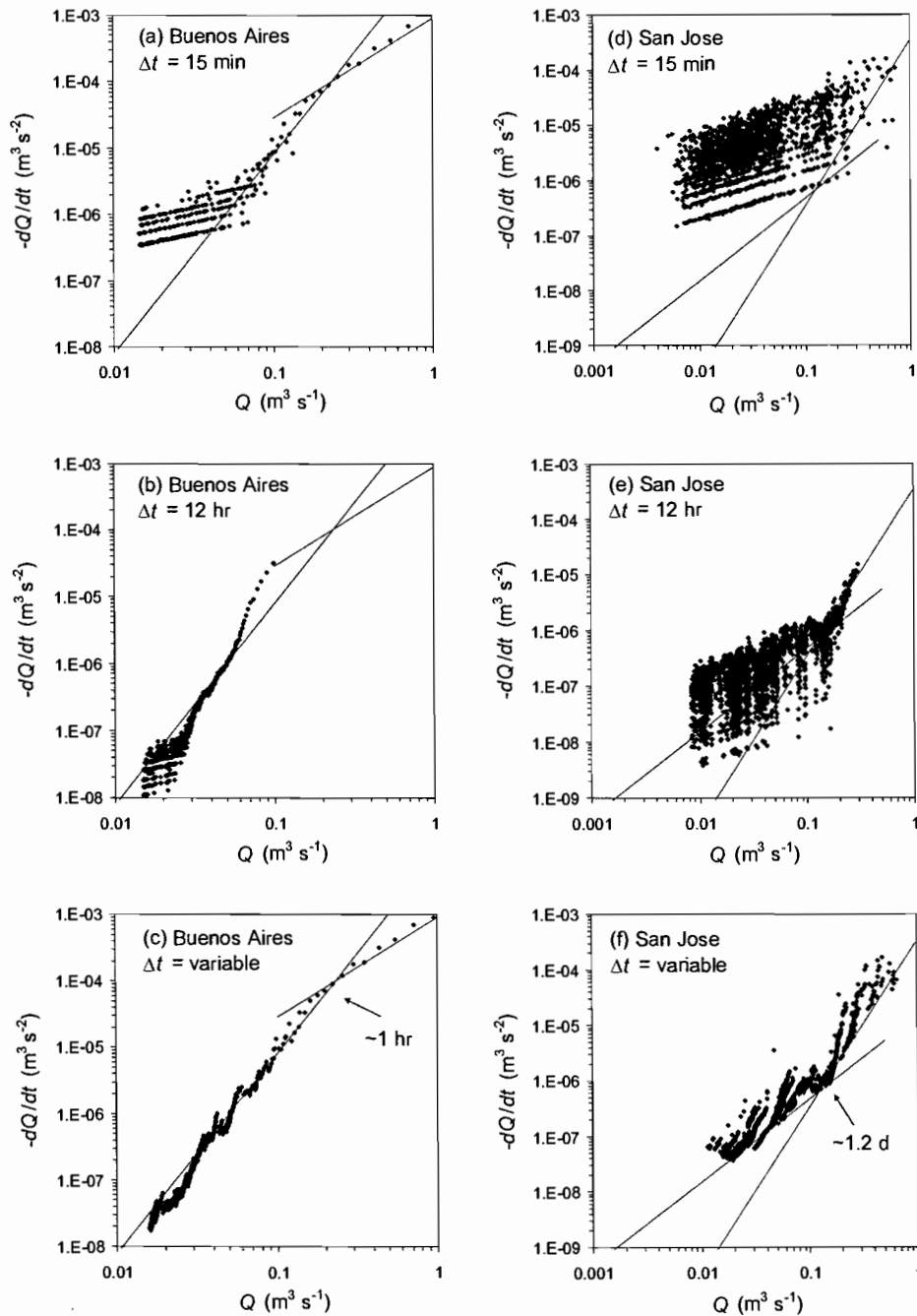
Figure 2. Example of effect of time increment Δt on calculation of $-dQ/dt$ versus Q for two recession hydrographs. The scaled-Δt method, which permits Δt to vary as $-dQ/dt$ decreases (c and f), can resolve much more of the relationship between dQ/dt and Q than can keeping Δt constant with either a short (a and d) or relatively long (b and e) Δt. The steeper lines shown have a slope of 3 and the shallower lines have a slope of 1.5.
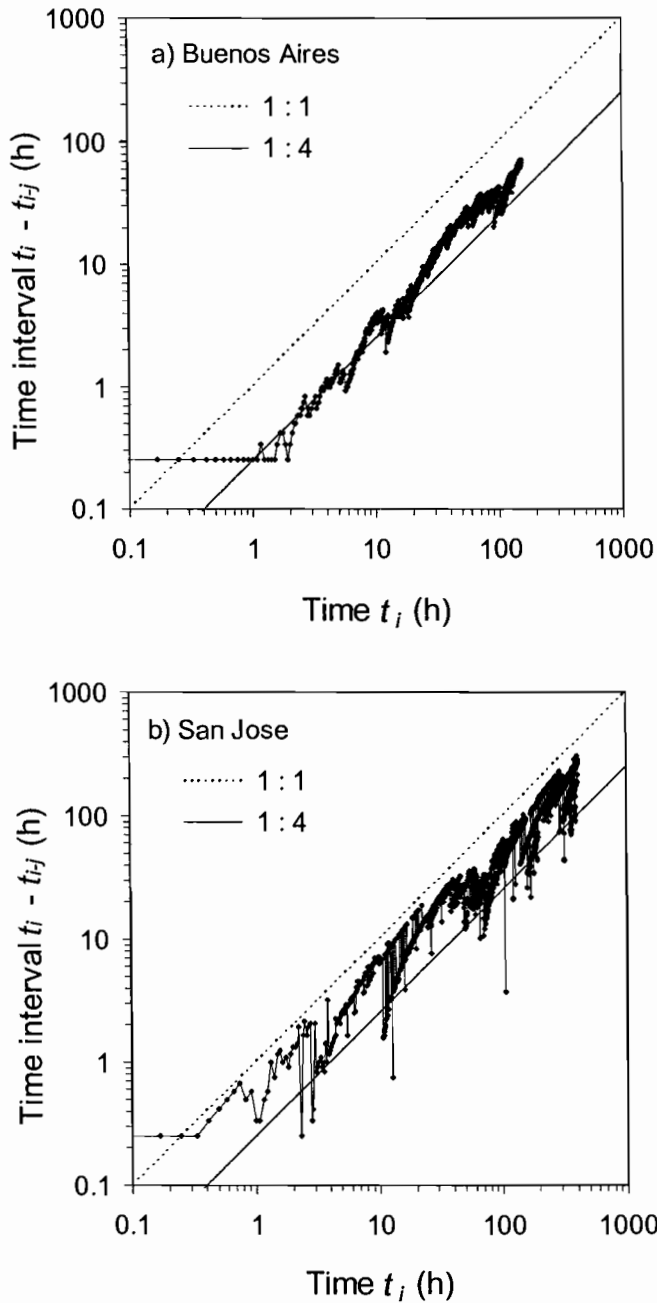
Figure 3. Time interval $t_i - t_{i-j}$ used to approximate $-dQ/dt$ plotted against time since the beginning of the recession period t_i for the events shown in Fig. 2c (a) and 2f (b). The time intervals were selected using (15). For (a), $\varepsilon = 0.001$ m, $C = 25$, and $j \geq 3$. For (b), $\varepsilon = 0.01$ m, $C = 7$, and $j \geq 3$. The observation frequency is 5 min.
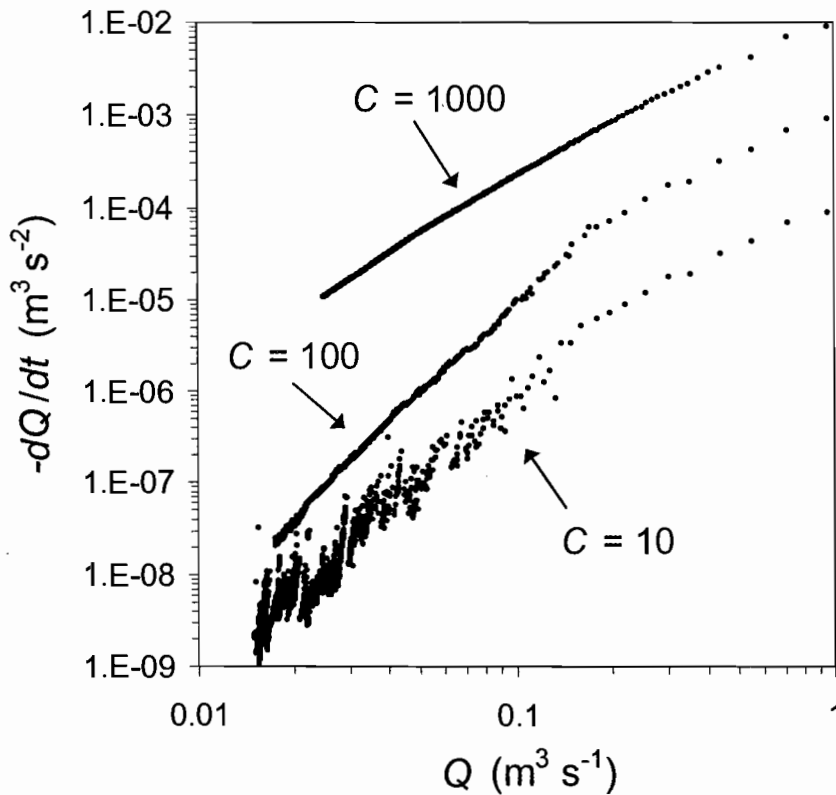
Figure 4. Example of effect of parameter *C* from (15) on the calculation of *-dQ/dt* versus *Q* for the Buenos Aires event. The curves are offset vertically by a factor of 10 to distinguish between them.

Though the scaled-Δt method can improve the analysis of recession data, it is still necessary that discharge data be taken at a sufficient resolution to meet to goals of the experiment. While a relationship between *dQ/dt* and *Q* seems apparent, for example, in Fig. 2f, there would still remain a large degree of uncertainty in fitting a curve through the data. It is clear for the basins of this size that millimeter precision is required for water level measurements.

5. Summary

A new method is presented for calculating dQ/dt as a function of Q for the recession limb of a hydrograph. The method differs from that of previous studies in that the time increment Δt over which dQ/dt is estimated is not held constant over the entire recession curve. Instead, Δt for each observation in time is properly scaled to the observed drop in discharge ΔQ. This avoids artifacts in data presented as log(-dQ/dt) versus log(Q) when using constant Δt that can lead to misinterpretations of the underlying relationships in the data. It also permits the analysis of data that may otherwise have been considered too noisy to interpret.

Acknowledgements

Appendix A. Time rate of change of discharge from *Parlange et al.* [2001].

The dimensionless discharge rate Q^* vs. dimensionless time t^* derived from the cumulative discharge Eq. 23 of *Parlange et al.* [2001], is

$$Q^* = \psi\left(1 - e^{(-1/t^*)}\right)t^{*-\frac{1}{2}} + \left[\frac{\sigma_1}{\sqrt{\pi}} - 2\psi + \frac{\sigma_2\mu}{\sqrt{\pi}}\left(\text{erfc}\,\frac{1}{\sqrt{t^*}}\right)^{\mu-1}\right]e^{(-1/t^*)}t^{*-\frac{3}{2}}$$

$$(A.1)$$

where erfc is the complementary error function, $\mu = \sqrt{7}$, $\sigma_1 = 5/4$, $\sigma_2 = -1/4$, and $\psi = (\sigma_1 + \mu\,\sigma_2)/\sqrt{\pi}$. Dimensional discharge Q and time t are, respectively,

$$Q = \frac{2kD^2L}{B}Q*$$

$$(A.2)$$

and

$$t = \frac{\varphi B^2}{kD}t*$$

$$(A.3)$$

where B is aquifer length from stream to basin divide, D is initial saturated thickness of the aquifer, L is length of stream network, k is saturated hydraulic conductivity, and φ is drainable porosity. The derivative of (A.1) with respect to time is:

$$-\frac{dQ*}{dt*} = \frac{\psi}{2}\left(1 - e^{(-1/t*)}\right)t*^{-3/2}$$
$$+\left[\frac{3\sigma_1}{2\sqrt{\pi}} - 2\psi + \frac{3\sigma_2\mu}{2\sqrt{\pi}}\left(\text{erfc}\,\frac{1}{\sqrt{t*}}\right)^{\mu-1}\right]e^{(-1/t*)}t*^{-5/2}$$
$$-\left[\frac{\sigma_1}{\sqrt{\pi}} - 2\psi + \frac{\sigma_2\mu}{\sqrt{\pi}}\left(\text{erfc}\,\frac{1}{\sqrt{t*}}\right)^{\mu-1}\right]e^{(-1/t*)}t*^{-7/2}$$
$$-\left[\frac{\sigma_2\mu(\mu-1)}{\pi}\left(\text{erfc}\,\frac{1}{\sqrt{t*}}\right)^{\mu-2}\right]e^{(-2/t*)}t*^{-3}$$

$$(A.4)$$

From (A.2) and (A.3), the dimensional rate of change of discharge in terms of the dimensionless rate of change is

$$\frac{dQ}{dt} = \frac{2k^2D^3L}{\varphi B^3}\frac{dQ*}{dt*}$$

$$(A.5)$$

References

Brutsaert, W., and J. P. Lopez (1998), Basin-scale geohydrologic drought flow features of riparian aquifers in the southern Great Plains, *Water Resour. Res.*, *34*, 233-240.

Brutsaert, W., and J. L. Nieber (1977), Regionalized drought flow hydrographs from a mature glaciated plateau, *Water Resour. Res.*, *13*, 637-643.

Chow, V. T. (1959), *Open-channel hydraulics*, McGraw-Hill, New York.

Malvicini, C. F., T. S. Steenhuis, M. T. Walter, J. Y. Parlange, and M. F. Walter (2005), Evaluation of spring flow in the uplands of Matalom, Leyte, Philippines, *Adv. Water Resour.*, *28*, 1083-1090.

Mendoza, G. F., T. S. Steenhuis, M. T. Walter, and J. Y. Parlange (2003), Estimating basin-wide hydraulic parameters of a semi-arid mountainous watershed by recession-flow analysis, *J. Hydrol.*, *279*, 57-69.

Michel, C. (1999), Comment on "Basin-scale geohydrologic drought flow features of riparian aquifers in the southern Great Plains" by Brutsaert and Lopez, *Water Resour. Res.*, *35*, 909-910.

Parlange, J. Y., M. B. Parlange, T. S. Steenhuis, W. L. Hogarth, D. A. Barry, L. Li, F. Stagnitti, A. Heilig, and J. Szilagyi (2001), Sudden drawdown and drainage of a horizontal aquifer, *Water Resour. Res.*, *37*, 2097-2101.

Rupp, D. E., J. M. Owens, K. L. Warren, and J. S. Selker (2004), Analytical methods for estimating saturated hydraulic conductivity in a tile-drained field, *J. Hydrol.*, *289*, 111-127.

Smith, R. E., D. L. Chery, K. G. Renard, and W. R. Gwinn (1981), Supercritical flow flumes for measuring sediment-laden flow, 72 pp, U.S. Department of Agriculture Bulletin No. 1665.

Szilagyi, J., and M. B. Parlange (1998), Baseflow separation based on analytical solutions of the Boussinesq equation, *J. Hydrol.*, *204*, 251-260.

Tallaksen, L. M. (1995), A review of baseflow recession analysis, *J. Hydrol.*, *165*, 349-370.

Troch, P. A., F. P. De Troch, and W. Brutsaert (1993), Effective water table depth to describe initial conditions prior to storm rainfall in humid regions, *Water Resour. Res.*, *29*, 427-434.

Zecharias, Y. B., and W. Brutsaert (1988), Recession characteristics of groundwater outflow and base flow from mountainous watersheds, *Water Resour. Res.*, *24*, 1651-1658.

Chapter 4 - Drainage of a Horizontal Boussinesq Aquifer with a Power-Law Hydraulic Conductivity Profile

David E. Rupp and John S. Selker

Department of Bioengineering, Oregon State University, Corvallis, OR

Abstract

Solutions to the Boussinesq equation describing drainage into a fully-penetrating channel have been used for aquifer characterization. Two analytical solutions exist for early- and late-time drainage from a saturated, homogeneous, and horizontal aquifer following instantaneous drawdown. The solutions for discharge Q can be expressed as $dQ/dt = -aQ^b$, where a is constant and b takes on the value 3 and 3/2 for early and late time, respectively. Though many factors can contribute to departures from the two predictions, we explore the effect of having permeability decrease with depth, as it is known that many natural soils exhibit this characteristic. We derive a new set of analytical solutions to the Boussinesq equation for $k \propto z^n$, where k is the saturated hydraulic conductivity, z is the height above an impermeable base, and n is a constant. The solutions reveal that in early time, b retains the value of 3 regardless of the value of n, while in late time, b ranges from 3/2 to 2 as n varies from 0 to ∞. Similar to discharge, water table height h in late time can be expressed as $dh/dt = -ch^d$, where $d = 2$ for constant k and $d \to \infty$ as $n \to \infty$. In theory, inclusion of a power-law k profile does not complicate aquifer parameter estimation because n can be solved for when fitting b to the late-time data, whereas previously b was assumed to be 3/2. However, if either early- or late-time data are missing, there is an additional unknown. Under appropriate conditions, water table height measurements can be used to solve for an unknown parameter.

1. Introduction

There are few tools available for deriving aquifer characteristics at the field or watershed scale. An important one which has received renewed attention, probably due to its apparent simplicity, is the method of recession analysis proposed by *Brutsaert and Nieber* [1977]. In the method, stream flow recession data, or discharge Q, is related to the time rate of change in discharge dQ/dt in order to eliminate time as the reference. *Brutsaert and Nieber* [1977] noted that several models for aquifer discharge can be expressed as

$$\frac{dQ}{dt} = -aQ^b \tag{1a}$$

where a and b are constants. A similar relationship may exist for the height of the water table h [e.g., *Rupp, et al.*, 2004]:

$$\frac{dh}{dt} = -ch^d \tag{1b}$$

where c and d are also constants.

The model used most often for interpreting the parameters in (1a) and (1b) is the Boussinesq equation for an unconfined, horizontal aquifer draining into a fully-penetrating channel (Figure 1) [*Brutsaert and Nieber*, 1977; *Brutsaert and Lopez*, 1998; *Parlange, et al.*, 2001; *Rupp, et al.*, 2004]. The Boussinesq equation is derived from Darcy's law and the Dupuit-Forchheimer assumption, and by neglecting capillarity above the water table. Given these assumptions, the flux q [$L^2 T^{-1}$] per unit aquifer width at any horizontal position x in an aquifer is

$$q = -kh(\partial h/\partial x) \tag{2}$$
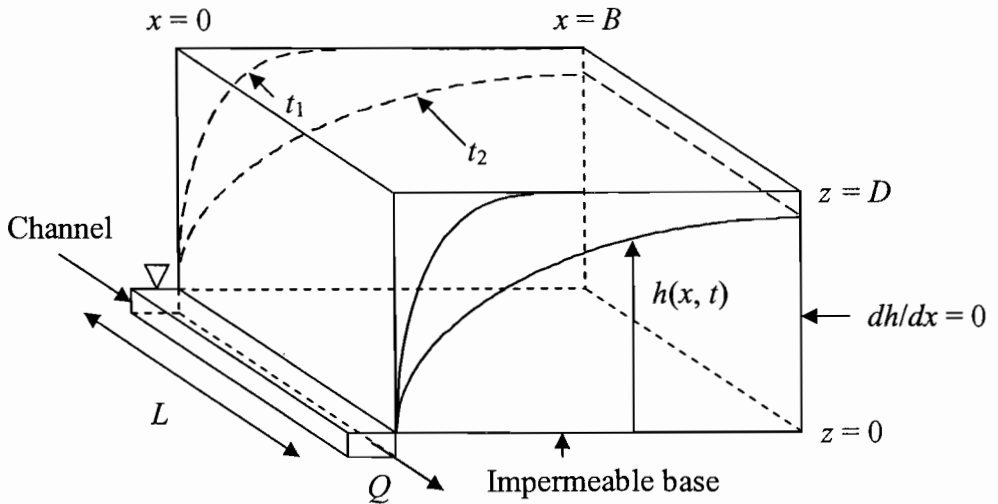
Figure 1. Diagram of the right-hand side of a symmetrical unconfined aquifer fully-incised by a channel. Water table profiles at t_1 and t_2 correspond to early and late times during sudden drawdown of an initially-saturated aquifer. The channel discharge Q is the sum of the discharge from both sides of the aquifer, or $2qL$. The vertical axis is exaggerated with respect to the horizontal axis, but in reality $B >> D$.

where k is hydraulic conductivity and $h = h(x, t)$ is the water table height. Applying the continuity equation in the presence of a recharge rate N leads to

$$\varphi \frac{\partial h}{\partial t} = \frac{\partial}{\partial x}\left(kh\frac{\partial h}{\partial x}\right) + N \tag{3}$$

where φ is the drainable porosity or specific yield. Typically, k is moved outside of the derivative as it is assumed spatially constant in the down-slope direction and the result is referred to as the Boussinesq equation.

Polubarinova-Kochina [1962, p. 507] presented an analytical solution for (3) given constant k following instantaneous drawdown of an initially-saturated aquifer where $h(0, t) = 0$. For this solution, $b = 3$ in (1a), and it is applicable in "early time" when the no-flux boundary at $x = B$ is not yet affecting drainage at $x = 0$. The solution was arrived at by using the Boltzmann transformation and further substitutions to express the Boussinesq equation in the form of the Blasius equation, for which there are known analytical solutions [see also *Heaslet and Alksne*, 1961; *Hogarth and Parlange*, 1999]. *Lockington* [1997] derived a similar early-time solution using a weighted residual method for the more general case where $h(0, t) \geq 0$ and is constant. For this latter solution, recast as (1a), $b = 3$ also.

For "late time", when the no-flux boundary affects flow, an analytical solution can also be derived for the boundary condition $h(0, t) = 0$ by noting that the solution $h(x, t)$ is separable into the product of a function of x and a function of t [*Boussinesq*, 1904; *Polubarinova-Kochina*, 1962, p. 516-517]. In this case, $b = 3/2$ in (1a). In the corresponding expression for water-table decline (1b), $d = 2$.

Parlange et al. [2001] provided an approximate analytical solution for discharge that unites the early- and late-time regimes.

In natural basins and aquifers, there are many factors that can lead to departures from the predictions of outflow by analytical solutions derived for the instantaneous drawdown of the idealized "lumped" aquifer depicted in Figure 1 [e.g., *Hall*, 1968; *Singh*, 1968]. Recent investigations have begun to quantify the effects of some of these factors by relaxing some of the previously-mentioned assumptions. *Szilagyi et al.* [1998] examined the robustness of the two analytical solutions discussed above by including horizontal heterogeneity in saturated hydraulic conductivity, complexity in watershed shape, and mild slope in a numerical model. Others have compared solutions of the one-dimensional Boussinesq equation to the more general two-dimensional Laplace equation for a horizontal aquifer. In particular, the assumptions of initial saturation and instantaneous drawdown [*van de Giesen, et al.*, 2005], full and partial penetration [*van de Giesen, et al.*, 1994; *Szilagyi*, 2003; *van de Giesen, et al.*, 2005], and no unsaturated flow [*Szilagyi*, 2003, 2004] were addressed.

One aspect that has not been well-studied within the context of the Boussinesq equation is the effect of saturated hydraulic conductivity that varies with depth. Vertically decreasing k has been observed in many soil types [e.g., *Beven*, 1984], particularly in forests [e.g., *Harr*, 1977; *Bonell, et al.*, 1981]. *Beven* [1982a] observed that the power-law function $k = k^* z^n$ fit well to existing data from five previous studies. Where z is the height above a relatively impermeable base and where k^* and n are fitting parameters, n ranged from 1.2 to 7.9, with correlation coefficients r between 0.85 and 0.97. In response, *Beven* [1982b] introduced a vertical k profile that is a power-law of h into the Boussinesq equation for a sloping aquifer [*Boussinesq*, 1877], but eliminated the second-order diffusive term to arrive at a linear kinematic wave equation.

We introduce a similar power-law conductivity profile into (3) and derive early- and late-time analytical transient solutions for an initially-saturated aquifer following instantaneous drawdown. We also present an analytical steady-state solution under constant recharge. For verification, the analytical solutions are compared to numerical solutions of the Boussinesq equation. Lastly, we discuss how k decreasing with depth may affect the derivation of aquifer characteristics using the recession slope analysis method of *Brutsaert and Nieber* [1977], or, in other words, how the power-law k profile affects the parameters in (1a) and (1b).

2. Analytical Solutions

Let the saturated hydraulic conductivity k at an elevation z above the impermeable base be described by

$$k(z) = \left(k_D - k_0\right)\left(\frac{z}{D}\right)^n + k_0 \qquad (4)$$

where D is the thickness of the aquifer, $k(D) = k_D$ and $k(0) = k_0$ are the constant values of k at the upper and lower contacts, respectively, and $n \geq 0$. The average

horizontal hydraulic conductivity corresponding to the entire saturated thickness of the aquifer h, or $k(h)$, is the vertical average of $k(z)$:

$$k(h) = \frac{1}{h} \int_0^h (\frac{k_D - k_0}{D^n} z^n + k_0) dz \tag{5}$$

or

$$k(h) = k^* h^n + k_0 \tag{6}$$

where

$$k^* = \frac{k_D - k_0}{(n+1)D^n} \tag{7}$$

2.1. Steady-State Case

We derive a steady-state solution to (3) given (6) because it serves both as a test here of the numerical model and as a plausible condition when considering extended wet periods. The steady-state solution of (3) requires that (2) be equal to a constant in time. Given a constant recharge rate N applied uniformly across the water table, the conservation of mass requires that the steady-state flux at x is equal to the recharge contributed up-gradient of x, or

$$q = -N(B - x) \tag{8}$$

where B is the distance from the channel to the no flow boundary (Figure 1). Substituting (6) and (8) into (2) gives

$$N(B - x) = (k^* h^n + k_0)h(\partial h/\partial x)\tag{9}$$

Integrating the left side of (9) from $x = 0$ to $x = x$ and the right side from $h(0) = h_0$ to $h(x) = h$ yields an exact implicit solution in x:

$$N(2Bx - x^2) = \frac{2k^*}{n+2}h^{n+2} + k_0 h^2 - \left(\frac{2k^*}{n+2}h_0^{n+2} + k_0 h_0^2\right)\tag{10}$$

where h_0 is the constant water level in the channel.

In the following sections, two transient solutions to the Boussinesq equation will be derived for the special case where $h_0 = 0$ and $k_0 = 0$. Given these two boundary conditions, the steady-state solution can be expressed for h explicitly:

$$h = \left[\frac{(n+2)}{2k^*}N(2Bx - x^2)\right]^{1/(n+2)}\tag{11}$$

2.2. Early-Time Transient Case

To arrive at analytical solutions for instantaneous drawdown and without recharge, we let $k_0 = 0$, so $k^* = k_D/[(1+n)D^n]$ and (2) and (3) become, respectively

$$q = -k^* h^{n+1}(\partial h/\partial x)\tag{12}$$

and

$$\frac{\partial h}{\partial t} = \frac{k^*}{\varphi}\frac{\partial}{\partial x}\left[h^{n+1}\frac{\partial h}{\partial x}\right]\tag{13}$$

A weighted residual method [*Lockington*, 1997] is used to solve (13) for early-time where the drawdown of the water table is not yet subject to the influence of the no-flux boundary at $x = B$ (see Figure 1, curve "t_1"). The aquifer can then be treated as being "semiinfinite" and the initial and boundary conditions are

$$h = 0 \qquad x = 0 \qquad t > 0 \tag{14}$$

$$h = D \qquad x \geq 0 \qquad t = 0 \tag{15}$$

$$h = D \qquad x \to \infty \qquad t > 0 \tag{16}$$

The substitutions $\phi = x / \sqrt{\tau}$, $H = h / D$, and $\tau = k^* t / \varphi$ reduce (13) to the two-variable problem

$$-\frac{\phi}{2} \frac{dH}{d\phi} = D^{n+1} \frac{d}{d\phi} \left(H^{n+1} \frac{dH}{d\phi} \right) \tag{17}$$

with boundary conditions

$$H = 0 \qquad \phi = 0 \tag{18}$$

$$H = 1 \qquad \phi \to \infty \tag{19}$$

Integrating (17) with respect to ϕ yields

$$2 D^{n+1} H^{n+1} = \int_H^1 \phi \, d\overline{H} \frac{d\phi}{dH} \tag{20}$$

because $dH/d\phi$ vanishes at $H = 1$. $\overline{H}$ is a dummy variable of integration.

The following approximate function ϕ^* used by *Lockington* [1997] for a homogeneous aquifer is proposed for ϕ:

$$\phi \approx \phi^* = \lambda\left[(1 - H^{-\mu}) - 1\right] \tag{21}$$

where λ and μ are constants with the same sign. As ϕ^* is not an exact solution to (20), a residual function $\varepsilon(H)$ is defined as

$$\varepsilon = 2D^{n+1}H^{n+1} - \int_H^1 \phi^*(\overline{H})d\overline{H}\,\frac{d\phi}{dH} \tag{22}$$

The residual is weighted with 1 and $(1-H)^m$ [*Lockington*, 1997] and integrated over the range of H to solve for λ and μ:

$$\int_0^1 \varepsilon \, dH = 0 \tag{23}$$

$$\int_0^1 (1 - H)^m \, \varepsilon \, dH = 0 \tag{24}$$

From (23)

$$\lambda^2 = \frac{(1-\mu)(1-2\mu)}{\mu^2}\frac{D^{n+1}}{n+2} \tag{25}$$

and from (24)

$$2D^{n+1}\mathrm{B}(n+2, m+1) = \frac{\lambda^2\mu^2(2 + m - 2\mu)}{(1 + m - \mu)(1 + m - 2\mu)} \tag{26}$$

where $\mathrm{B}(n+2, m+1)$ denotes the beta function evaluated for $n + 2$ and $m + 1$. Substituting (25) into (26) gives

$$A = \frac{(1-2\mu)(2+m-2\mu)}{(1+m-\mu)(1+m-2\mu)} \tag{27}$$

where

$$A = 2(n+2)B(n+2, m+1) \tag{28}$$

It can be shown by rearrangement that (27) is a quadratic equation. The useful root μ is that with real values of H (and thus h)

$$\mu = \frac{-\beta - \sqrt{\beta^2 - 4\alpha\gamma}}{2\alpha} \tag{29}$$

with

$$\alpha = 4 - 2A \tag{30}$$

$$\beta = 3A(m+1) - 2m - 6 \tag{31}$$

$$\gamma = 2 + m - A(m+1)^2 \tag{32}$$

The value $m = 1.251$ has been suggested for constant k [*Lockington*, 1997]. However, if $m = 1$, the effect of which is discussed later, (29) becomes

$$\mu = \frac{4 - 3A - \sqrt{A^2 - 2A + 4}}{4 - 2A} , \qquad m = 1 \tag{33}$$

Finally, substituting (25) into (21) and solving for H, and making the substitutions $H = h/D$ and $\phi^* = x/\sqrt{k^*t/\varphi}$, yield the approximate water table profile

$$h(x,t) = D\left[1 - \left(1 + \mu\frac{x}{\sqrt{t}}\sqrt{\frac{(n+2)(n+1)\varphi}{(1-\mu)(1-2\mu)k_D D}}\right)^{-1/\mu}\right] \tag{34}$$

The outflow from the aquifer is the flux at $x = 0$. Evaluating (12) at $\phi = 0$, or

$$q = -k^*\tau^{-1/2}D^{n+2}H^{n+1}\left(dH/d\phi\right)\big|_{\phi=0} \tag{35}$$

gives, from (22),

$$q = -\frac{k^*D}{2\tau^{1/2}}\int_0^1 \phi(H)dH \tag{36}$$

Substituting (21) and (25) into (36) and solving the integral yields the early-time outflow

$$q(t) = \frac{1}{2}\left[\frac{(1-2\mu)}{(1-\mu)(n+2)(n+1)}k_D\varphi D^3\right]^{1/2}t^{-1/2} \tag{37}$$

2.3. Late-Time Transient Case

A separation of variables is used to solve (13) for the late-time case where the drawdown of the water table is subject to the effect of the no-flux boundary at $x = B$ [*Boussinesq*, 1904; *Polubarinova-Kochina*, 1962] (see Figure 1, curve "t_2"). The boundary conditions are

$$h = 0 \qquad x = 0 \qquad t > 0 \tag{38}$$

$$dh/dx = 0 \qquad x = B \qquad t \geq 0 \tag{39}$$

$$h = D \qquad x = B \qquad t = 0 \tag{40}$$

We seek a solution for the free water surface h which is the product of two variables, one dependent solely on time and the other solely on the position:

$$h = X(x)T(t) \tag{41}$$

Substituting (41) into (13) and separating the variables yields

$$\frac{1}{T^{n+2}} \frac{dT}{dt} = \frac{k^*}{\varphi X} \frac{d^2}{dx^2} \left(\frac{X^{n+2}}{n+2} \right) = -C \tag{42}$$

where C is a constant. The boundary conditions are

$$X = 0 \qquad x = 0 \qquad t > 0 \tag{43}$$

$$X = D \qquad x = B \qquad t = 0 \tag{44}$$

$$T = 1 \qquad \qquad t = 0 \tag{45}$$

Integrating the left and right sides of (42) gives, respectively

$$T = \left[1 + (n+1)Ct \right]^{-1/(n+1)} \tag{46}$$

and

$$dx = \sqrt{\frac{k^*(n+3)}{2C\varphi}} \frac{X^{n+1} dX}{\sqrt{D^{n+3} - X^{n+3}}} \tag{47}$$

Integrating (47) again yields

$$x = \frac{B}{B_n} \int_0^v v^{-1/(n+3)} (1-v)^{-1/2} \, dv \, , \qquad\qquad v = (X/D)^{n+3} \qquad (48)$$

where B_n is a beta function

$$B_n = B\left(\frac{n+2}{n+3}, \frac{1}{2}\right) \qquad (49)$$

The integral in (48) is an incomplete beta function. A series expansion, for example, can be used to approximate the inverse of the incomplete beta function [see, e.g., equation 26.5.4, *Abramowitz and Stegun*, 1972].

The constant C subject to the boundary conditions is

$$C = \frac{k^* D^{n+1}}{2(n+3)\varphi B^2} B_n^2 \qquad (50)$$

From (41), (46), and (48), the water table height is

$$h(x,t) = \frac{D\Omega}{\left[1 + \dfrac{B_n^2}{2(n+3)} \dfrac{k_D D}{\varphi B^2} t\right]^{1/(n+1)}} \qquad (51)$$

where $\Omega(x/B) = X/D$. Examples of water table profiles for various values of n at $t = 0$ are shown in Figure 2.
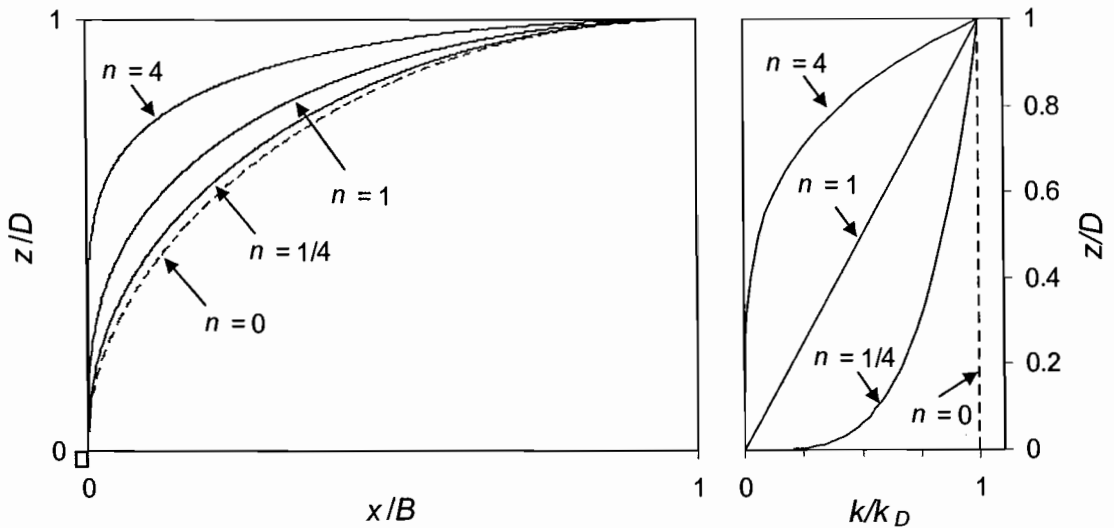
Figure 2. Dimensionless late-time transient water table profiles $h(x, 0)/D$ in an unconfined aquifer with a fully-penetrating channel at $x = 0$ (left figure). The water table heights shown are calculated from the late-time solution (51) for $t = 0$ and four vertical profiles of saturated hydraulic conductivity k corresponding to $n = 0$, 1/4, 1, and 4. Dimensionless hydraulic conductivity $k(z)/k_D$ versus dimensionless height z/D above the impermeable base is shown at right.

The outflow from the aquifer can be found from (12) evaluated at $x = 0$:

$$q = -k^* T^{n+2} X^{n+1} \left(dX/dx \right)\big|_{x=0} \tag{52}$$

Combining (47) with (52) and letting $X = 0$ gives

$$q(t) = \frac{B_n k_D D^2}{(n+3)(n+1)B\left[1 + \frac{B_n^2}{2(n+3)} \frac{k_D D}{\varphi B^2} t\right]^{\frac{n+2}{n+1}}}$$

(53)

3. Discussion

For permeability that varies as a power-function with depth, both the early-time (37) and late-time (53) solutions for discharge can be expressed in the form given by (1a). Taking the derivative of (37) with respect to time and recasting the result as a function of discharge instead of time, the recession constants a and b for the early-time solution are

$$a_1 = \Phi_1 \frac{(n+1)}{k_D \varphi D^3 L^2}$$

(54)

$$b_1 = 3$$

(55)

where

$$\Phi_1 = \frac{(1-\mu)(n+2)}{2(1-2\mu)}$$

(56)

Values of Φ_1 for various values of n are given in Table 1. Note also that the discharge Q in the channel is assumed to be the cumulative outflow from all upstream aquifers such that $Q = 2qL$ (see Figure 1).

Table 1. Recession coefficients for various vertical
hydraulic conductivity profiles, $k \propto z^n$

n	Early time ($b = 3$) Φ_1 (56) ($m = 1$)	Late time Φ_2 (59)	b_2 (58)
0	1.108	2.402	1.500
1/4	1.337	2.538	1.556
1/2	1.588	2.690	1.600
1	2.151	3.030	1.667
2	3.528	3.787	1.750
4	7.279	5.445	1.833
64	739.8	63.72	1.971
∞	∞	∞	2.000

Defining the width of the aquifer B as the characteristic distance from channel
to divide, the aquifer area A is given by $A = 2LB$. The recession parameters for the
late-time solution (53) can then be expressed as

$$a_2 = \Phi_2 \frac{4k_D D L^2}{(n+1)\varphi A^2} \left[\frac{(n+1)A}{4k_D D^2 L^2} \right]^{\frac{n+1}{n+2}} \tag{57}$$

$$b_2 = (2n+3)/(n+2) \tag{58}$$

where

$$\Phi_2 = \frac{n+2}{2(n+3)} B_n^2 \left[\frac{n+3}{B_n} \right]^{\frac{n+1}{n+2}} \tag{59}$$

See Table 1 for values of b_2 and Φ_2 for various values of n.

Unlike for discharge, the Boussinesq equation does not predict a power-law relationship between dh/dt and h in early time. However, the late time solution (51) can be expressed in the form of (1b) with constants

$$c = \frac{B_n^2}{2(n+3)(n+1)} \frac{k_D}{\varphi D^n B^2 \Omega^{n+1}} \tag{60}$$

$$d = n+2 \tag{61}$$

The analytical solutions derived above were compared to output from a numerical model of (23) using a fourth-order Runge-Kutta finite-difference method with 250 equally-spaced nodes in the x-direction. Numerical outflow hydrographs were generated for various values of n, k_D, and D. The data were plotted as log(-dQ/dt) versus log(Q), as proposed by *Brutsaert and Nieber* [1977] (see also *Rupp and Selker* [2005b] for discussion on the numerical approximation of log(-dQ/dt) versus log(Q) from discrete data). Plotted in log-log space, the analytical solutions appear as straight lines with slope b and intercept a. Three numerically-generated recession curves are given as examples in Figure 3.

The early-time slope b for discharge of the numerical simulations was not perceptibly different from 3 regardless of the value of n. It was observed, however, that the node spacing had to be decreased for large n, or else b appeared as less than 3 for very early times and gradually approached a value of 3 (data not shown). Therefore the node spacing was reduced by a factor of 10 to obtain just the early-time data for the largest values of n. The number of nodes was maintained at 250, as the early-time solution is not a function of the position of the no-flux boundary at $x = B$.

Following the sharp transition from the early- to late-time regime, the numerically-generated data show a slope b that is equal to that predicted by the late-time solution (58) (Figure 3). For late-time, the initial node spacing was adequate for all n.
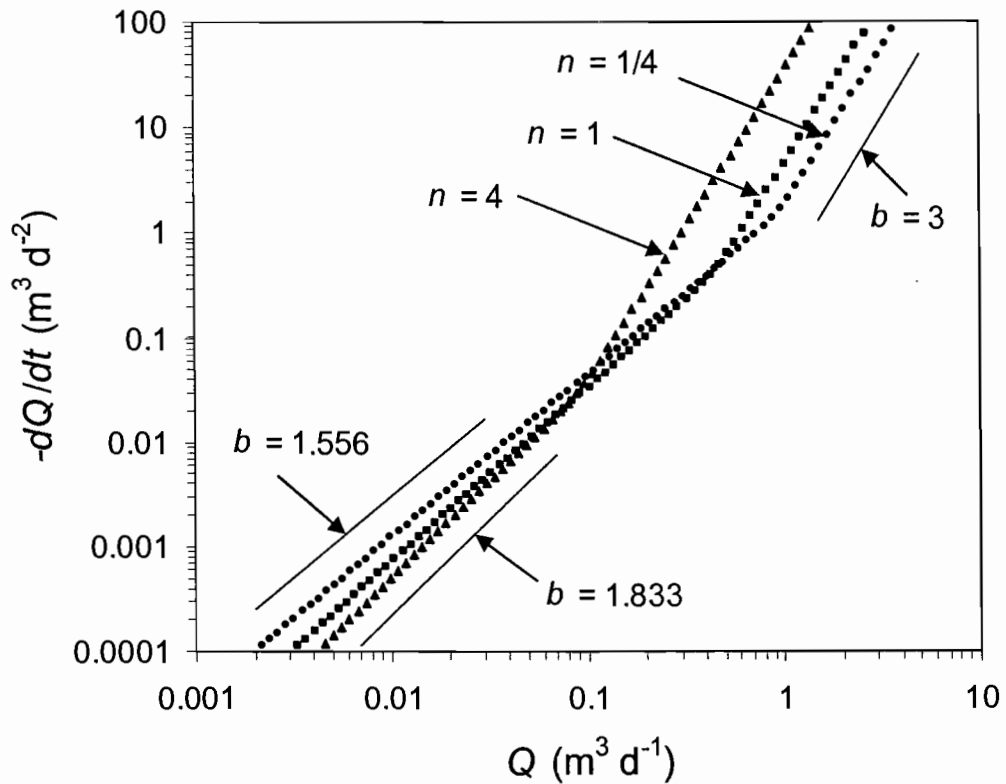
Figure 3. Recession curves from three numerical simulations using saturated hydraulic conductivities that decrease with depth from $k_D = 100$ m d^{-1} to $k_0 = 0$ m d^{-1} slowly ($n = 0.25$), linearly ($n = 1$) and rapidly ($n = 4$). In each case $D = 1$ m, $B = 100$ m, $\varphi = 0.01$, and $L = 1$ m. The analytically derived values of b are shown for $n = 0.25$ and $n = 4$.

In addition to the slope b, the analytically and numerically generated recession curves are nearly identically positioned in log-log space for late time (i.e., the values of the parameter a_2 are equal). There is a discrepancy, however, in early time. Using a value of $m = 1.251$ for (24) [*Lockington*, 1997] to calculate a_1 from (54), the numerical and analytical solutions diverge for increasing n (Figure 4). For small n (e.g., $n \leq 1$), this may not have practical consequence. However, for the example show in Figure 4a, the difference in a_1 between the solutions is about 15% for $n = 4$

and 40% for $n = 32$. The discrepancy does not appear to be due to numerical error, as changing the node-spacing or the time-step did not result in a convergence of predictions. On the other hand, if we let $m = 1$, the analytically and numerically derived values of a_1 show a much better match, with the difference being about 1% for all n (Figure 4).

Accurate estimates of Φ_1 in (54) are known for $n = 0$, so comparisons can be made to the value predicted by (56) for this specific case. The most accurate value of Φ_1, to the fourth decimal place, is 1.1337 [see *Parlange, et al.*, 2001]. In comparison, for $n = 0$, (57) gives $\Phi_1 = 1.1361$ for $m = 1.251$ and $\Phi_1 = 1.1076$ for $m = 1$. Thus, the value of m proposed by *Lockington* [1997] is superior to $m = 1$ for very small n, but performs poorly over all n. One might apply a correction factor to (56) for $m = 1$ to improve the prediction at $n = 0$, though this may not be justified for the purposes of recession slope analysis in log-log space.

It is remarkable that the recession parameter b retains the value of 3 in early time regardless of the shape of the k profile. The practical implication of this result for aquifer characterization is that the shape of the early-time outflow hydrograph alone gives no indication of vertical variability in k, thus adding at least one unknown variable to the parameterization problem. However, if late-time data is also available, the late-time value of b supplies information on the vertical variability in k (i.e., n), thus the problem of parameterization is in theory no more complicated than for the case of constant k with two equations and the same number of unknowns. (If, however, the vertical k profile were defined with an extra parameter, such as in (6), there would be another variable for which to solve).

a)

b)
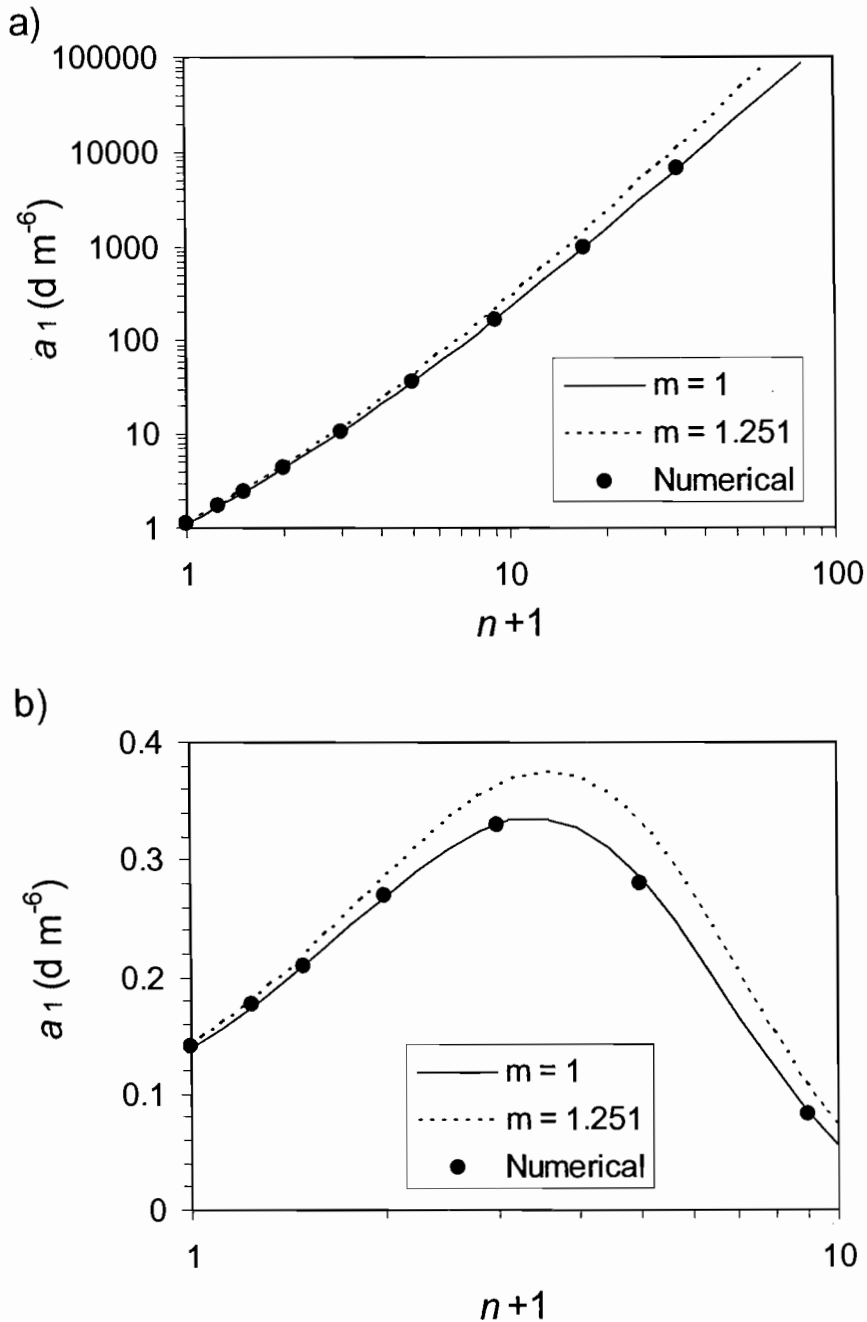
Figure 4. Early-time recession parameter a from (1a) as determined analytically (lines) from (55) with two values of m and numerically (circles) for various vertical profiles of saturated hydraulic conductivity. In (a), k_D/D was held constant as n was varied, with $k_D = 100$ m d^{-1}, $D = 1$ m, $B = 100$ m, $\varphi = 0.01$, and $L = 1$ m. In (b), k_D/D^n was held constant at 100 m^{1-n} d^{-1} as n was varied, with $D = 2$ m, and B, φ, and L as above.

Though the early- and late-time curves can be used together to solve for an unknown parameter by combining (54) and (57), it is likely that the predicted early-time response will not be evident in discharge data. This is because the assumption of sudden drawdown from an initially flat water table may be inappropriate for the data being analyzed [*van de Giesen, et al.*, 2005], or that observations during the early period of recession may still be reflecting processes other than merely aquifer outflow [*Brutsaert and Nieber*, 1977; *Brutsaert and Lopez*, 1998]. Furthermore, in the common case when only daily data is available, the temporal resolution may be too coarse to discern a relatively short-lived early-time regime.

From only the late-time data, estimating the characteristics of an aquifer with a power-law k profile requires solving for 6 variables, which is 2 more than for the case of a homogeneous aquifer (note that D falls out of (57) for $b = 3/2$ or $n = 0$). When available, representative transient water table data can constrain the parameter space through the combination of (57) and (60) [e.g., *Rupp, et al.*, 2004]. Water table observations may be especially useful for determining if there is important vertical variability in k, given that the parameter d in (61) corresponding to the transient water table height is much more sensitive to n than is the discharge parameter b_2 in (58).

It has been shown previously that three values of b arise out of three analytical solutions to the Boussinesq equation for a homogeneous aquifer [*Brutsaert and Nieber*, 1977]. As noted above, two of these values are $b = 3$ for early time and $b = 3/2$ for late time. The parameter b also takes on a third value of 1 for a solution resulting from a linearization in h in (3). Given that actual stream flow recession hydrographs show a range of values for b and are thus not limited to 1, 3/2, and 3, there is interest in finding theoretical solutions for basin discharge that give other values of b.

We have shown above how b may take on any value between 3/2 and 2 and may also take on a value of 3 when the saturated hydraulic conductivity decreases with depth as a power law. It is interesting to compare our results to those of *Michel* [1999], who used dimensional considerations to arrive at an expression for aquifer discharge for any arbitrary value of b.

Michel [1999] demonstrated that the three analytical solutions for a homogeneous aquifer can all be expressed in the form of (1a) through a single equation:

$$a = -\Psi(b)\frac{4kDL^2}{\varphi A^2}\left[\frac{A}{4kD^2L^2}\right]^{b-1} \tag{62}$$

$$b = 1, 3/2, \text{ or } 3 \tag{63}$$

Though there are only three known theoretical values of the coefficient Ψ, one each for $b = 1$, 3/2, and 3, *Michel* [1999] and *Brutsaert and Lopez* [1999] suggest functional forms for $\Psi(b)$, so that one might use (62) for any value of b. *Brutsaert and Lopez* [1999], for example, give

$$\Psi(b) = -10.513 + 15.030b^{1/2} - 3.662b \tag{64}$$

However, *Brutsaert and Lopez* [1999] recommend using caution when interpreting the recession parameter a through (62) and (64) for values of b different from 1, 3/2, and 3.

It is of interest to compare (62) and (64) to the new solutions for a non-constant k profile. Noting that $b - 1 = (n + 1)/(n + 2)$, it is clear that (62) and the late-time solution (57) for a power-law k profile are nearly identical in form. The late-time coefficient Φ_2 could also be expressed as function of b, as is Ψ. However, Φ_2 is functionally very distinct from Ψ (see also Table 1). In fact, $\Phi_2 \rightarrow \infty$ as $b \rightarrow 2$ (or as $n \rightarrow \infty$), whereas as Ψ in (64) has no such singularity. Moreover, though (62) for $b = 3$ is also similar in form to the early-time solution (54) for a power-law k profile, the early-time coefficient Φ_1 is not a function of b at all. Given that our results do not support the functional forms for the coefficient $\Psi(b)$ proposed by *Michel* [1999] and *Brutsaert and Lopez* [1999], it appears that the use of (62) with an "empirically-

derived" equation such as (64) without understanding why b takes on a certain value is not justified.

4. Conclusion

Recession hydrographs can differ in shape from those predicted by existing analytical solutions to the Boussinesq equation. In some cases, the initial and boundary conditions used to arrive at the analytical solutions may not be suited to the situation under analysis [e.g., *van de Giesen, et al.*, 2005]. In other cases, the assumptions of the Boussinesq equation may be inappropriate. In this study, we investigated the effect of deviating from the assumption of an aquifer with constant saturated hydraulic conductivity k.

It was found that for a power-law vertical conductivity profile, the recession discharge in early time can be expressed as $dQ/dt \propto Q^3$, which is the same as the case of a homogeneous aquifer. In late-time, however, the relation is $dQ/dt \propto Q^b$, where b is a function of the exponent n that defines the k profile ($k \propto z^n$). The value of b is 3/2 for a homogeneous aquifer ($n = 0$) and increases to 2 as n approaches ∞. Observed values of b exceeding 3/2 thus might be an indication of important decreases in k with depth within an aquifer.

The analytical solutions derived here for discharge allow for the derivation of aquifer characteristics much in the same way as that proposed by *Brutsaert and Nieber* [1977], with only slightly more complexity. The addition of transient water table data, analyzed in the same manner as that of discharge, can address some of the added complexity. It is acknowledged, however, that the analytical solutions assume that $k = 0$ at the base of the aquifer, thus may only be suitable for $k(D) \gg k(0)$.

Notation

a, b	general discharge recession constants.
a_1, b_1	early-time discharge recession constants.
a_2, b_2	late-time discharge recession constants.
A	horizontal aquifer area, equal to $2LB$.
B	length of impermeable base of aquifer.
c, d	late-time water-table recession constants.
C	constant of integration.
D	aquifer thickness.
h	water-table height.
h_0	water-table height at channel ($x = 0$).
H	dimensionless water-table height, equal to h/D.
$\overline{H}$	dummy variable of integration.
k	saturated hydraulic conductivity.
k_0	saturated hydraulic conductivity at bottom of aquifer.
k_D	saturated hydraulic conductivity at top of aquifer.
k^*	coefficient, equal to $(k_D - k_0)/[(n+1)D^n]$.
L	channel or stream length.
m	exponent in weight of residual, see (24).
n	exponent in expression for vertical profile of hydraulic conductivity.
N	rate of aquifer recharge.
q	aquifer discharge per unit width of aquifer.
Q	aquifer discharge.
t	time.
T	arbitrary function of t only.
v	transform, equal to $(X/D)^{n+3}$.
x	horizontal coordinate.
X	arbitrary function of x only.
z	elevation above aquifer base.
α, β, γ	coefficients in quadratic equation.
A	function of n, equal to $2(n+1)B(n+2, m+1)$.
$B(\,,)$	beta function.
B_n	beta function evaluated for $(n+1)/(n+2)$, $1/2$.
ε	residual function, defined in (22).
ϕ	Boltzmann transform, equal to $x/\sqrt{\tau}$.
ϕ^*	approximate function for ϕ, defined in (21).
Φ_1	early-time discharge recession coefficient, defined in (56)
Φ_2	late-time discharge recession coefficient, defined in (59)
λ, μ	coefficients in function ϕ^*.
φ	drainable porosity, or specific yield.
τ	transformed time, equal to $\tau = k^*t/\varphi$.

Ω inverse of the normalized incomplete beta function, equal to X/D.
Ψ discharge recession coefficient for homogeneous aquifer, see (62).

References

Abramowitz, M., and I. A. Stegun (Eds.) (1972), *Handbook of Mathematical Functions*, 1046 pp., Dover, New York.

Beven, K. (1982a), On subsurface stormflow: an analysis of response times, *Hydrol. Sci. J.*, *27*, 505-521.

Beven, K. (1982b), On subsurface stormflow: predictions with simple kinematic theory for saturated and unsaturated flows, *Water Resour. Res.*, *18*, 1627-1633.

Beven, K. (1984), Infiltration into a class of vertically non-uniform soils, *Hydrol. Sci. J.*, *29*, 425-434.

Bonell, M., D. A. Gilmour, and D. F. Sinclair (1981), Soil hydraulic properties and their effect on surface and subsurface water transfer in a tropical rainforest catchment, *Hydrol. Sci. Bull.*, *26*, 1-18.

Boussinesq, J. (1877), Essai sur la théorie des eaux courantes, *Mem. Acad. Sci. Inst. Fr.*, *23*, 252-260.

Boussinesq, J. (1904), Recherches théoriques sur l'écoulement des nappes d'eau infiltrées dans le sol et sur débit de sources, *J, Math. Pures Appl., 5me Ser.*, *5*, 5-78.

Brutsaert, W., and J. P. Lopez (1998), Basin-scale geohydrologic drought flow features of riparian aquifers in the southern Great Plains, *Water Resour. Res.*, *34*, 233-240.

Brutsaert, W., and J. P. Lopez (1999), Reply to comment on "Basin-scale geohydrologic drought flow features of riparian aquifers in the southern Great Plains", *Water Resour. Res.*, *35*, 911.

Brutsaert, W., and J. L. Nieber (1977), Regionalized drought flow hydrographs from a mature glaciated plateau, *Water Resour. Res.*, *13*, 637-643.

Hall, F. R. (1968), Base-flow recessions - a review, *Water Resour. Res.*, *4*, 973-983.

Harr, R. D. (1977), Water flux in soil and subsoil on a steep forested hillslope, *J. Hydrol.*, *33*, 37-58.

Heaslet, M. A., and A. Alksne (1961), Diffusion from a fixed surface with a concentration-dependent coefficient, *J. Soc. Ind. Appl. Math.*, *9*, 584-596.

Hogarth, W. L., and J. Y. Parlange (1999), Solving the Boussinesq equation using solutions of the Blasius equation, *Water Resour. Res.*, *35*, 885-887.

Lockington, D. A. (1997), Response of unconfined aquifer to sudden change in boundary head, *J. Irrig. Drain. Eng.*, *123*, 24-27.

Michel, C. (1999), Comment on "Basin-scale geohydrologic drought flow features of riparian aquifers in the southern Great Plains" by Brutsaert and Lopez, *Water Resour. Res.*, *35*, 909-910.

Parlange, J. Y., M. B. Parlange, T. S. Steenhuis, W. L. Hogarth, D. A. Barry, L. Li, F. Stagnitti, A. Heilig, and J. Szilagyi (2001), Sudden drawdown and drainage of a horizontal aquifer, *Water Resour. Res.*, *37*, 2097-2101.

Polubarinova-Kochina, P. Y. (1962), *Theory of Ground Water Movement*, 613 pp., Princeton University Press, Princeton, N. J.

Rupp, D. E., J. M. Owens, K. L. Warren, and J. S. Selker (2004), Analytical methods for estimating saturated hydraulic conductivity in a tile-drained field, *J. Hydrol.*, *289*, 111-127.

Rupp, D. E., and J. S. Selker (2005), Information, artifacts, and noise in dQ/dt-Q recession analysis, *Adv. Water Resour.*, *in press*.

Singh, K. P. (1968), Some factors affecting baseflow, *Water Resour. Res.*, *4*, 985-999.

Szilagyi, J. (2003), Sensitivity analysis of aquifer parameter estimations based on the Laplace equation with linearized boundary conditions, *Water Resour. Res.*, *39*, SBH81-SBH87.

Szilagyi, J. (2004), Vadose zone influences on aquifer parameter estimates of saturated-zone hydraulic theory, *J. Hydrol.*, *286*, 78-86.

Szilagyi, J., M. B. Parlange, and J. D. Albertson (1998), Recession flow analysis for aquifer parameter determination, *Water Resour. Res.*, *34*, 1851-1857.

van de Giesen, N., J. Y. Parlange, and T. S. Steenhuis (1994), Transient flow to open drains: comparison of linearized solutions with and without the Dupuit assumption, *Water Resour. Res.*, *30*, 3033-3039.

van de Giesen, N., T. S. Steenhuis, and J. Y. Parlange (2005), Short- and long-time behavior of aquifer drainage after slow and sudden recharge according to the linearized Laplace equation, *Adv. Water Resour.*, *28*, 1122-1132.

Chapter 5 - On the Use of the Boussinesq Equation and Recession Slope Analysis for Interpreting Hydrographs from Sloping Aquifers

David E. Rupp[1], Erin S. Brooks[2], Jan Boll[2], and John S. Selker[1]

1: Department of Bioengineering, Oregon State University, Corvallis, OR

2: Department of Biological and Agricultural Engineering, University of Idaho, Moscow, ID

Abstract

The method of recession analysis proposed by *Brutsaert and Nieber* [1977] remains one of the few analytical tools for estimating aquifer hydraulic parameters at the field-scale and greater. In the method, the recession hydrograph is examined as $-dQ/dt = f(Q)$, where Q is discharge and f is an arbitrary function. The parameters of the observed function f are related to analytical solutions to the 1-D Boussinesq equation for unconfined flow in a homogeneous, horizontal aquifer. While attractive in its simplicity, as originally presented it is not applicable to settings where slope is an important driver of flow and where hydraulic parameters vary greatly with depth. There exist, however, various analytical solutions to the 1-D Boussinesq equation for a sloping aquifer based on simplifying assumptions. These solutions are compared to numerical solutions of the full non-linear equation. Furthermore, an assessment is made of the behavior of the non-linear Boussinesq equation for a heterogeneous aquifer, where the heterogeneity is characterized by a lateral saturated hydraulic conductivity k that varies as a power-law with height z above the impermeable layer, i.e., $k \sim z^n$. It was found that all of the analytical solutions differ in key aspects from the non-linear solution when plotted as $-dQ/dt = f(Q)$, thus are inappropriate for a Brutsaert and Nieber-type analysis. However, a new analytical solution for the homogeneous aquifer is derived "empirically" from the numerical simulations that is applicable during the late period of recession. Moreover, the numerical solutions for the heterogeneous aquifer reveal that during the late period of recession, the shape of the recession curve is determined uniquely by the power n. Specifically, the recession curve converges to $-dQ/dt = aQ^b$, where $b = (2n+1)/(n+1)$. Therefore, while an interpretation of the parameter a remains elusive for the heterogeneous aquifer, the method of Brutsaert and Nieber can be used in theory to characterize the rate of change in k with depth. This is verified through discharge data from a hillslope where the k is known to decrease greatly with depth.

1. Introduction

Recession flow analysis for forecasting drought flows and investigating the ground water flow regime in basins has over a century-long history [*Hall*, 1968; *Tallaksen*, 1995]. *Brutsaert and Nieber* [1977] made a landmark contribution when they proposed plotting the observed recession slope of the drought flow hydrograph, or *dQ/dt*, against the discharge *Q*, such that

$$-\frac{dQ}{dt} = f(Q) \tag{1}$$

where *f* denotes an arbitrary function, and compared observations with analytical solutions to the Boussinesq equation for 1-dimensional flow in a rectangular horizontal aquifer. This method of analysis, referred to also hereafter as "recession slope analysis", has been used widely since for determining aquifer parameters [*Brutsaert and Nieber*, 1977; *Vogel and Kroll*, 1992; *Troch, et al.*, 1993; *Brutsaert and Lopez*, 1998; *Szilagyi, et al.*, 1998; *Eng and Brutsaert*, 1999; *Parlange, et al.*, 2001; *Mendoza, et al.*, 2003; *Rupp, et al.*, 2004; *Malvicini, et al.*, 2005] and for base flow separation [*Szilagyi and Parlange*, 1998]. Recession curves plotted as −*dQ/dt* versus *Q*, or similarly in log-log space, will be referred to as "recession slope curves" hereafter.

The primary function of presenting the recession curve as −*dQ/dt* versus *Q* is the elimination of time as the dependent variable, thus making it unnecessary to determine the precise beginning of the recession event (t_0) [*Brutsaert and Nieber*, 1977]. The ambiguity of t_0 in real discharge data leads to uncertainty when assigning values to parameters in functions that describe ground water outflow.

However, what has certainly made this method of analysis alluring is that three well-known analytical solutions to the Boussinesq equation for a unconfined horizontal aquifer (two exact solutions [*Boussinesq*, 1904; *Polubarinova-Kochina*,

1962] and one an approximation by linearization [*Boussinesq*, 1903]) can be expressed in the form

$$-\frac{dQ}{dt} = aQ^b \tag{2}$$

where a and b are constants [*Brutsaert and Nieber*, 1977]. Here geometric similarity of a unit-width representative rectangular aquifer (such as that shown in Fig. 1) distributed throughout a catchment is assumed, so that the total outflow Q is the integration of all flow q per unit width of aquifer entering a stream network of length L, i.e., $Q = 2qL$ [*Brutsaert and Nieber*, 1977]. Plotted as $\log(-dQ/dt)$ versus $\log(Q)$, (2) appears as a straight line with slope b and y-intercept a. Theoretically, one can fit a line of slope b to recession flow data graphed in this manner and determine aquifer characteristics from the resulting value of a.

In reality not all recession slope curves from a catchment will fall along a single curve. This is due in part to concurrent hydrological processes other than ground water flow, such as overland flow, quick subsurface flow (e.g., macropore flow), decline in channel or reservoir storage, and evapotranspiration [*Brutsaert and Nieber*, 1977]. The sum of these processes will result in a faster rate of decline in discharge for a given discharge than ground water flow alone. For this reason, it has been suggested that a curve be fit to the lower envelope of the data [*Brutsaert and Nieber*, 1977]. In addition to the above processes, variability in the spatial distribution of the hydraulic free surface (or water table) at the onset of recession events will also result in deviations in the recession slope curves.

In contrast to the number of studies cited above which compared data to the solutions for the horizontal Boussinesq aquifer, there has been only one attempt to interpret the parameters of basin recession slope curves based on a solution to the 1-dimensional Boussinesq equation for a sloping rectangular aquifer or hillslope [*Zecharias and Brutsaert*, 1988b], such as that shown in Fig. 1. While it is reasonable to assume that the drainage from a hillslope could be represented by the 1-dimensional

Boussinesq equation, it is not clear that the assumption of geometric similarity holds for basins.
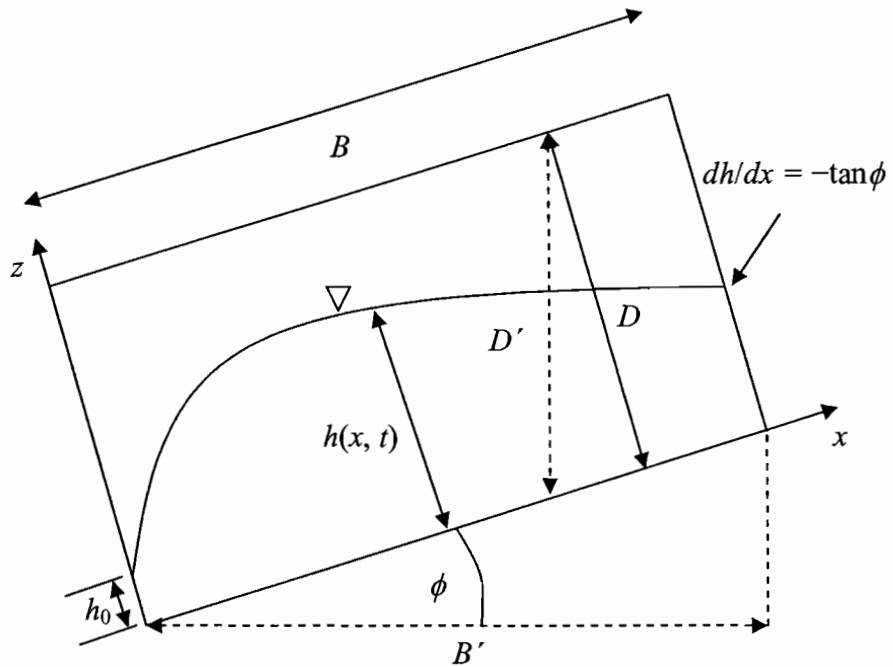
Fig. 1. Sketch of a transient water table profile $h(x, t)$ in an inclined aquifer fully-incised by a channel at the left-hand side boundary. The water level in the channel is h_0. There is no flux through the right-hand side and bottom boundaries.

In the case of a horizontal or very mildly sloping aquifer, *Szilagyi et al.* [1998] found the assumption of a representative single rectangular aquifer to be robust, based on numerical solutions of the 2-dimensional Boussinesq equation in a synthetic catchment. The general shape of the recession slope curves for catchment discharge was similar to that for discharge from a 1-dimensional rectangular aquifer, though

with a smoother transition between the late and early time domains. Furthermore, the basin-scale hydraulic and geometric aquifer parameters were reasonably estimated by recession slope analysis using (2), including cases where the saturated hydraulic conductivity varied across the catchment. A complication arises in hilly basins because the steeper and shorter hillslopes drain more rapidly and as time progresses the hydrograph will become dominated by the aquifer units with the shallowest slope and/or greatest lateral extent. This may explain in part while multi-catchment comparisons have not universally found slope to be an important factor in explaining drought flow variability among basins [*Zecharias and Brutsaert*, 1988a; *Vogel and Kroll*, 1992; *Lacey and Grayson*, 1998]. Additionally, recession slope data in some sites of moderate to high relief have been found to be consistent with a non-linear horizontal Boussinesq aquifer [*Brutsaert and Nieber*, 1977; *Mendoza, et al.*, 2003].

This paper is a partial assessment of the Brutsaert and Nieber method of recession analysis for sloping aquifers. There are three main objectives. The first is to review existing analytical solutions to the Boussinesq equation for a sloping aquifer, under their respective simplifying assumptions, and to compare them with numerical solutions of the full non-linear equation. In particular, we will examine how the solutions behave when plotted as $\log(-dQ/dt)$ versus $\log(Q)$.

The second objective is to examine how allowing the saturated hydraulic conductivity k to vary with depth affects the recession slope curves predicted by the Boussinesq equation for a sloping aquifer. This is of interest because studies have revealed large decreases in k with depth in many soils, particularly forest soil [*Harr*, 1977; *Bonell, et al.*, 1981; *Beven*, 1982a, 1984]. Specifically, a power-law function describing the change in k with height z above bedrock is incorporated into the Boussinesq equation (e.g., [*Beven*, 1982b; *Rupp and Selker*, 2005a]).

The third objective is to evaluate the ability of the 1-D Boussinesq equation to predict hillslope recession discharge under field conditions. In doing so, we analyze discharge data by means of the Brutsaert and Nieber method to assist in the calculation of hillslope-scale hydraulic parameters, namely k and drainable porosity. The data

was collected from a previously-studied hillslope where k is believed to decrease considerably with depth.

2. Review of Analytical Solutions

For flow in an unconfined aquifer overlaying an impermeable base of slope ϕ, *Boussinesq* [1877] made use of the Dupuit-Forchheimer approximation to derive

$$q = -kh\left[\cos\phi(\partial h/\partial x) + \sin\phi\right] \tag{3}$$

where q is the flow rate per unit width of aquifer in the x direction, k is the saturated hydraulic conductivity in the down-slope direction, and $h = h(x, t)$ is the thickness of the water layer perpendicular to the impermeable layer (see Fig. 1). Inserting (3) into the continuity equation yields, in the absence of recharge or evaporation,

$$\varphi\frac{\partial h}{\partial t} = \left[\cos\phi\frac{\partial}{\partial x}\left(kh\frac{\partial h}{\partial x}\right) + \sin\phi\frac{\partial}{\partial x}(kh)\right] \tag{4}$$

where φ is the drainable porosity, and ϕ is assumed to be constant [see also, *Childs*, 1971]. Eq. (4) is often expressed for constant k, in which case k is brought outside of the derivative.

Existing analytical solutions to (4) for a horizontal and a sloping aquifer are reviewed below. All the solutions either take the form of (2) exactly, or when b is a function of time, they converge to (2) as t goes to infinity and, in most cases, as t goes to zero. The definitions of the recession parameters a and b in (2) for each solution are listed in Tables 1 and 2. While the following information for a horizontal aquifer is available elsewhere in the published literature, it is useful to have it compiled. More importantly, to our knowledge this is the first time that the most of these analytical solutions for a sloping aquifer have been presented in the form of (2).

2.1. Horizontal Aquifer

For the case of a horizontal aquifer ($\phi = 0$), several analytical solutions to (4) can be presented exactly in the form given by the power law in (2) [*Brutsaert and Nieber*, 1977]. Beginning with an initially saturated aquifer subjected to instantaneous drawdown, *Polubarinova-Kochina* [1962] derived an exact solution to (4) for a homogeneous and infinitely wide aquifer, which is applicable for early time when the zero-flux boundary at $x = B$ has no effect on the discharge rate. The parameters a and b for this solution, when expressed in the form of (2) are given in Table 1 (see parameter set (i)). In this case, the head h_0 at the discharge boundary or channel is assumed to be zero. *Lockington* [1997] arrived at a more general early-time solution for any constant value of h_0 between 0 and the initial horizontal water table height D (see (ii) in Table 1). Most recently, *Rupp and Selker* [2005a] solved (4) for the early-time domain for an aquifer in which k increases with height z as a power law (Fig. 2), i.e.,

$$k(z) = k_D (z/D)^n \tag{5}$$

where k_D is the saturated hydraulic conductivity at height $z = D$, and n is a constant greater than or equal to 0 (see parameter set (iii) in Table 1). Note from Table 1 that the recession slope parameter b equals 3 for each of these three early-time solutions regardless of the head at the aquifer outlet or the vertical distribution of k.
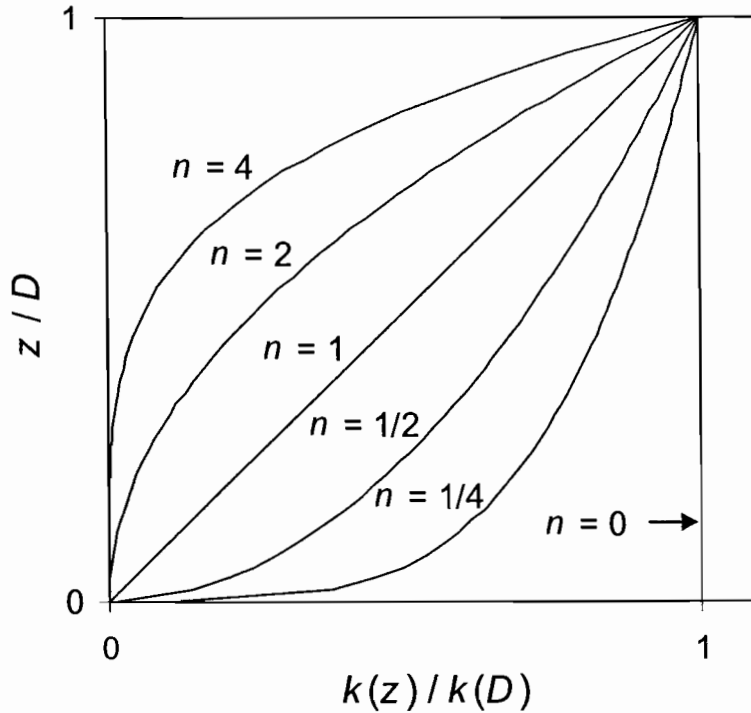
Fig. 2. Examples of saturated hydraulic conductivity (k) profiles in an aquifer of thickness D where k is proportional to the height z to a power n.

For late times, defined to be when the up-slope zero-flux boundary is influencing the discharge at the drainage boundary, *Boussinesq* [1904] provided an exact solution for a homogeneous aquifer (see parameter set (iv) in Table 1). *Rupp and Selker* [2005a] later generalized the solution to include the power-law k-profile in (5) (see parameter set (v) in Table 1). For both solutions, $h_0 = 0$. Note that the recession slope parameter b equals 3/2 for the power $n = 0$ (a homogeneous aquifer) and approaches the value of 2 as n goes to infinity (see Table 1).

Parlange et al. [2001] derived an approximate solution to (4) that unites both the early and late-time solutions for a homogeneous aquifer with $h_0 = 0$.

The early- ($b = 3$) and late-time ($b = 3/2$) behavior predicted by the Boussinesq equation for a homogeneous aquifer where $h_0 \approx 0$ have been corroborated by

laboratory tank experiments (i.e., Hele Shaw models) [*Ibrahim and Brutsaert*, 1965; *Hammad, et al.*, 1966; *Ibrahim and Brutsaert*, 1966; *Mizumura*, 2002, 2005].

An approximate solution given by *Boussinesq* [1903] for the homogeneous aquifer, also limited to late times, can be obtained by linearization of (4) (see parameter set (vi) in Table 1). In this case, the variable h outside of the brackets in (3) is set equal to a constant pD, where $0 < p \leq 1$. Note, however, that the linearization yields a value of 1 for b, which is inconsistent with the laboratory findings cited in the previous paragraph. The linearization is more appropriate when the drop in head at the outflow boundary is much less than the initial saturated thickness of the aquifer, i.e., $D - h_0 << D$. This condition has been shown to yield $b = 1$ in late time (e.g., [*Szilagyi*, 2004; *van de Giesen, et al.*, 2005]).

This method of linearization is used to arrive at many of the solutions for a sloping aquifer reviewed in the following section. The significance of the linearization parameter p is also discussed in the following section.

2.2. Sloping Aquifer

Numerous transient analytical solutions exist to the Boussinesq equation based on the kinematic wave approximation [*Henderson and Wooding*, 1964; *Beven*, 1981, 1982b] and various approaches to linearization [*Zecharias and Brutsaert*, 1988b; *Sanford, et al.*, 1993; *Brutsaert*, 1994; *Steenhuis, et al.*, 1999].

The kinematic wave equation arises from assuming that in (3) the hydraulic gradient in at any point x is equal to the bed slope, or $dh/dx = 0$, thus $q = -kh \sin \phi$. This results in the loss of the second-order diffusive term in (4), making it applicable only for steep slopes and/or highly conductive aquifers relative to the recharge rate [*Henderson and Wooding*, 1964]. As there is no diffusion, the entire recession slope curve is defined by the initial shape of the water table. For an initially saturated aquifer with the power-law k profile in (7), it can be shown that the kinematic wave equation predicts a recession discharge that is constant in time [*Beven*, 1982b]:

$$Q = 2k_D DL \sin \phi /(n + 1) \tag{6}$$

Thus, $dQ/dt = 0$ for all Q and the recession constants a and b both equal 0 (see (vii) in Table 2). On the other hand, beginning with a steady-state water table profile following a period of constant and spatially uniform recharge N, the recession constant b equals 0 for a homogeneous aquifer and approaches 1 as n approaches infinity (see (viii) in Table 2).

Another approach to making (4) more tractable is to use the quasi-steady state assumption that the shape of the moving water table is the same as that calculated for steady flow [e.g., *Zecharias and Brutsaert*, 1988b]. *Zecharias and Brutsaert* [1988b] made this assumption along with the linearization discussed above to obtain a solution for a sloping homogeneous aquifer (see parameter set (ix) in Table 2). Note that in Table 2 the recession parameter a is expressed as the nearly equivalent value of a for a linearized horizontal aquifer (see (vi) in Table 1) multiplied by a "slope factor" which contains the dimensionless term η:

$$\eta = \frac{B}{D}\tan\phi \tag{7}$$

This is also done, when appropriate, for several other solutions reviewed below. Though it does not generally result in the simplest expression for the parameter a, it facilities the comparison of the various solutions.

The parameter η is similar to the term introduced by *Brutsaert* [1994]: $\eta^* = B\tan\phi/2pD$, where η^* "represents the relative magnitude of the slope term, i.e., gravity, versus the diffusion term" [*Brutsaert*, 1994]. We write the reviewed solutions here in terms of η instead of η^* because not all solutions make use of the parameter p, though it is admitted that η^* is the more meaningful term because pD represents the effective water table height (see discussion below).

Using a similar quasi-steady state approach, *Sanford et al.* [1993] presented three solutions for cumulative discharge, each based on a different method for approximated h. We refer the reader to *Sanford et al.* [1993] for a description of the

three approximations used. The three solutions are presented in the form of (2) for the case where $h_0 = 0$ for comparison with the other solutions presented herein. The first two solutions yield a constant value of the recession constant b (1 and 1.5, respectively) (see (x) and (xi) in Table 2). The third solution differs in that the value of b transitions in time from 1.5 to 1 (see (xii) and (xiii) in Table 2).

Steenhuis et al. [1999] addressed the conditions of the steep hillslope experiments at the Coweeta Hydrological Laboratory. For their solution, $h_0 = D$ and the initial water table is a straight line with boundaries $h(0, 0) = D$ and $h(B, 0) = 0$. The solution can be expressed as

$$\frac{dQ}{dt} = -\frac{2Q(Q - kDL\sin\phi)^2}{\varphi\, kD^3 L^2 \cos\phi} \tag{8}$$

It can be shown that as t goes to infinity, (8) converges to the form of (2) with the recession parameter b equal to 1 (see (xiv) in Table 2).

Brutsaert [1994] used a linearization in h to arrive at an infinite series summation solution for an instantaneous drawdown to $h(0,t) = 0$ in an initially saturated homogeneous aquifer. It can be shown [*Brutsaert and Lopez*, 1998] that as t goes to zero the early-time value of b goes to 3 (see (xv) in Table 2). For late time, the solution can also be expressed as (2) by neglecting all but the first term in the summation in Eq. 17 in [*Brutsaert*, 1994] (see (xvi) in Table 2).

Others have used the same linearization approach as *Brutsaert* [1994], but included variable recharge rates and non-zero stream water levels [*Verhoest and Troch*, 2000; *Pauwels, et al.*, 2002]. *Chapman* [1995] also addressed a pulse of recharge, but rewrote (4) for h^2 and used a linearization in h^2 to arrive at a solution. Though these solutions differ from *Brutsaert* [1994] in early time due to different initial conditions, it can be shown that they are essentially equal in the late time domain ($b = 1$ and a is a given by (xvi) in Table 2).

One can see from Table 2 that $b = 1$ for all but one of the late-time solutions for a homogeneous aquifer. In experiments using an inclined Hele Shaw model,

Mizumura [2005] observed that at late time the discharge declined exponentially with time, which is equivalent to $b = 1$.

It is worth briefly discussing the parameter p that arises from the linearization method employed by *Brutsaert* [1994] and others [*Zecharias and Brutsaert*, 1988b; *Chapman*, 1995; *Verhoest and Troch*, 2000; *Pauwels, et al.*, 2002]. The assumption of the linearization is that changes in the water table height are small such that a constant "effective" water table of height equal to pD can be assumed. Though this method has yielded analytical solutions to the Boussinesq equation, it leads to one more parameter for which to solve. It has been suggested that p be treated as a calibration parameter [*Brutsaert*, 1994], but this not desirable if the goal is to identify the value of other unknowns, such a k and φ.

For an initially-saturated aquifer, *Brutsaert* [1994] points out that previous analytical solutions for a horizontal aquifer suggest a relatively narrow range of values for p between 1/3 and 1/2. However, an initially-saturated unconfined aquifer will often not occur in natural conditions [*van de Giesen, et al.*, 2005], so the determination of p is not straightforward. Where the aquifer is sloping, *Koussis* [1992] proposed the following implicit equation for pD for the special case of a steady-state water table profile due to a constant recharge rate N and a channel head $h_0 = 0$:

$$\frac{B \tan \phi}{2pD} = \frac{k \sin^2 \phi}{N} + \frac{pD}{B \tan \phi} - \left(\frac{pD}{B \tan \phi} + 1 \right) \exp \left(-\frac{B \tan \phi}{pD} \right) \tag{9}$$

Though (9) is slightly cumbersome, explicit approximations can be derived that are applicable for given ranges of η^* [*Koussis*, 1992].

Table 1

Definitions of parameters a and b in $-\dfrac{dQ}{dt} = aQ^b$ for a horizontal aquifer

Form of Boussinesq Equation[†]	Time Domain	b	a[‡]	Parameter Set	Source
Non-linear	Early	3	$\dfrac{1.133}{k\varphi D^3 L^2}$	(i)	[*Polubarinova-Kochina*, 1962]
Non-linear	Early	3	$\dfrac{f_{Lo}}{k\varphi (h_0 - D)^2 (h_0 + D) L^2}$	(ii)	[*Lockington*, 1997]
Non-linear; $k(z) = k_D (z/D)^n$	Early	3	$\dfrac{f_{R1}}{k_D \varphi D^3 L^2}$	(iii)	[*Rupp and Selker*, 2005a]
Non-linear	Late	3/2	$\dfrac{4.804 k^{1/2} L}{\varphi A^{3/2}}$	(iv)	[*Boussinesq*, 1904]
Non-linear; $k(z) = k_D (z/D)^n$	Late	$\dfrac{2n+3}{n+2}$	$f_{R2} \dfrac{k_D D L^2}{\varphi A^2} \left(\dfrac{A}{k_D D^2 L^2} \right)^{\frac{n+1}{n+2}}$	(v)	[*Rupp and Selker*, 2005a]
Linearized	Late	1	$\dfrac{\pi^2 p k D L^2}{\varphi A^2}$	(vi)	[*Boussinesq*, 1903]

[†]Unless specified, k = constant.

[‡]See Appendix for definitions of f_{Lo}, f_{R1} and f_{R2}

Table 2

Definitions of parameters a and b in $-\dfrac{dQ}{dt} = aQ^b$ for a sloping aquifer

Form of Boussinesq Equation[†]	Time Domain	b	a	Parameter Set	Source
Kinematic wave; initially saturated; $k(z) = k_D(z/D)^n$	All	0	0	(vii)	[*Beven*, 1982b]
Kinematic wave; initially steady-state; $k(z) = k_D(z/D)^n$	All	$\dfrac{n}{n+1}$	$(n+1)^{n/(n+1)} \dfrac{N}{\varphi} \left(\dfrac{2k_D L \sin\phi}{D^n} \right)^{1/(n+1)}$	(viii)	[*Beven*, 1982b]
Linearized	Late	1	$\dfrac{8pkDL^2}{\varphi A^2} \left(1 + \dfrac{\eta}{p} \right)$	(ix)	[*Zecharias and Brutsaert*, 1988b]
Linearized	Late	1	$\dfrac{8kDL^2}{\varphi A^2} \cos\phi$	(x)	[*Sanford, et al.*, 1993]
Linearized	Late	3/2	$\dfrac{6.928\,k^{1/2}L}{\varphi A^{3/2}} \left(1 + \dfrac{3}{4}\eta \right)^{-1/2}$	(xi)	[*Sanford, et al.*, 1993]
Linearized	Early	3/2	$\dfrac{6.928\,k^{1/2}L}{\varphi A^{3/2}} \cos^{1/2}\phi \left\{ \dfrac{1 + \eta/4}{[1 + (\eta/2)]^{-1/2}} \right\}$	(xii)	[*Sanford, et al.*, 1993]

Table 2 cont.

Linearized	Late	1	$\dfrac{6kDL^2}{\varphi A^2}\eta\cos\phi$	(xiii)	[*Sanford, et al.,* 1993]
Linearized	Late	1	$\dfrac{8kDL^2}{\varphi A^2}\eta^2\cos\phi$	(xiv)	[*Steenhuis, et al.,* 1999]
Linearized	Early	3	$\dfrac{1.133}{k\varphi D^3 L^2\cos\phi}$	(xv)	[*Brutsaert*, 1994]
Linearized	Late	1	$\dfrac{\pi^2 pkDL^2}{\varphi A^2}\cos\phi\left[1+\left(\dfrac{\eta}{\pi p}\right)^2\right]$	(xvi)	[*Brutsaert*, 1994]
Non-linear; $k(z)=k_D(z/D)^n$	Late	$\dfrac{2n+1}{n+1}$	Unknown	(xvii)	‡
Non-linear	Late	1	$\dfrac{432kDL^2}{\varphi A^2}\eta\cos^2\phi$	(xviii)	‡

†Unless specified, k = constant.

‡This article.

$$\eta=\dfrac{B}{D}\tan\phi\,;\ \ A=2BL$$

3. Methods

3.1. Numerical Solution of the Boussinesq Equation

The subsurface flow in a sloping aquifer with a power-law k profile can be expressed as

$$q = -\frac{k_D D}{n+1}(h/D)^{n+1}\left[\cos\phi(\partial h/\partial x) + \sin\phi\right] \tag{10}$$

Note that k has been replaced by $k(h)$ in (4) where

$$k(h) = \frac{k_D}{(n+1)}(h/D)^n \tag{11}$$

The corresponding transient water table height is

$$\frac{\partial h}{\partial t} = \frac{k_D}{\varphi(n+1)D^n}\left[\cos\phi\frac{\partial}{\partial x}\left(h^{n+1}\frac{\partial h}{\partial x}\right) + \sin\phi\frac{\partial}{\partial x}\left(h^{n+1}\right)\right] + \frac{N}{\varphi} \tag{12}$$

for a recharge rate N. Eq. (12) was solved numerically using a fourth-order Runge-Kutta finite-difference method. A zero-flux condition was maintained on the upslope boundary.

Three sets of model runs were done. The first two sets served to evaluate the analytical solutions reviewed above. The first set simulated the drawdown of an initially saturated aquifer, and the second set simulated drawdown following steady-state recharge conditions. For the steady-state cases, a nearly steady-state water table profile was generated by applying a constant recharge rate of $N = 0.1$ m d^{-1} to an initially dry aquifer until the discharge rate reached approximately 99.99% of the

recharge rate. Only the model parameters $\tan\phi$ and h_0 were varied for these two set of runs. The aquifer slope $\tan\phi$ was set at 0.005, 0.02, 0.08, and 0.32. For the initially saturated cases, the head at the discharge boundary was set at $h_0 = 0$, 0.5, and 1 m, while for the steady-state cases $h_0 = 0$ only. The remaining parameters were kept constant as follows: $n = 0$, $k_D = 50$ m d^{-1}, $\varphi = 0.1$, $D = 1$ m, and $B = 50$ m.

The third set of simulations was done to assess the effect of having k decrease with depth as power law. The power n was set at 0, 0.25, 0.5, 1, 2, and 4 (see Fig. 2). To see how slope might affect the result in conjunction with n, $\tan\phi$ was also set at 0.003, 0.03, and 0.3. The remaining parameters were kept constant as follows: $k_D = 10$ m d^{-1}, $\varphi = 0.1$, $h_0 = 0$, $D = 1$ m, and $B = 50$ m.

3.2. Generation of Recession Slope Curves

Because the instantaneous slope of the recession curve at any time t is not a measured variable, it needs to be approximated by calculating the change in discharge over some time interval Δt. Typically, a constant value of Δt is used throughout the recession period, though it has been shown that this can lead to artifacts in graphs of $\log(-dQ/dt)$ versus $\log(Q)$ than can hinder analysis [*Rupp and Selker*, 2005b]. Here we use a variation on an improved method of estimating $-dQ/dt = f(Q)$ proposed by *Rupp and Selker* [2005b].

Before calculating dQ/dt, the recession time series is "smoothed" by selecting a subset of discharge observations Q in the following manner. Beginning with the first recession discharge measurement Q_i, $i = 1$, we step forward in time until reaching the first measurement Q_i, $i = k_j$, at which the cumulative discharge volume V equals or exceeds a constant cumulative discharge threshold V_{min}. The discharge Q_i associated with this point in time is selected and placed in a new time series as Q_j, $j = 1$. The integer j is increment by 1 and the process is repeated:

$$V_j = \sum_{i=k_{j-1}+1}^{k_j} Q_i(t_i - t_{i-1}), \qquad V_{min} \le V_j < V_{min} + Q_{k_j}(t_i - t_{i-1}) \qquad (13a)$$

$$Q_j = Q_{k_j}, \qquad t_j = t_{k_j} \tag{13b}$$

where $k_0 = 0$. This procedure will tend to retain all the data from the early part of the recession curve while providing longer time intervals between discharge observations during the later part of the curve. The appropriate choice of V_{min} is specific to the data set and will depend upon the precision and the degree of noise of the data.

The time rate of change in discharge and the corresponding discharge are calculated, respectively, by

$$\frac{dQ}{dt} \approx \frac{Q_j - Q_{j-1}}{t_j - t_{j-1}}, \qquad j = 2, 3, 4\ldots \tag{14}$$

and

$$Q \approx \frac{Q_j + Q_{j-1}}{2} \tag{15}$$

3.3. Site and Data Description

We analyzed discharge data for an instrumented hillslope near Troy, ID. The hillslope is a 35 x 18 m plot with an average slope of 20%. The plot is lined on all sides with plastic and sheet metal which extend downward to a fragipan layer, such that the lining creates well-defined zero-flux vertical boundaries. The soil profile consists of a moderately well-drained loam to silt-loam with an average depth of 0.65 m underlain by a relatively impermeable fragipan layer. A tile drain installed at the fragipan layer at the downslope boundary intercepts subsurface flow and diverts it to an automated tipping bucket. Three automated observations wells were also installed at distances of 2.3, 17.8, and 34.4 m upslope from the tile drain, See *Brooks, et al.* [2004] for more information on the site and the data.

To determine the lateral hillslope-scale $k(h)$, *Brooks et al.* [2004] solved (3) for $k(h)$ and used simultaneous measurements of q and dh/dx. The hydraulic gradient dh/dx was calculated using water table heights recorded at the well located 2.3 m upslope from the tile drain.

4. Results and Discussion

4.1. Comparison of Analytical and Numerical Solutions

The analytical solutions reviewed in Section 2.2 are not consistent among themselves, particularly as the slope ϕ or as η increases. Figs. 3 and 4 show the recession slope curves for several of the solutions given equivalent values for the parameters B, D, k and φ. For mild slopes ($\eta < 1$), many of the solutions are similar, and differences can largely be accounted for by the constant in the recession parameter a: for example, the value of 8 in (ix) versus the value of π^2 in (xvi) in Table 2. An exception is the second equation of *Sanford et al.* [1993] (see parameter set (xi), which does a better job of reproducing the intermediate part of the recession slope curve as it has the same value for b as the solution for a horizontal aquifer (i.e., $b = 3/2$). As the slope ϕ or η increases, the analytical solutions diverge greatly (see Fig. 4). The solution of *Steenhuis et al.* [1999] is also shown in Fig. 4, though it is understood that it was derived for different boundary conditions.

A look at the numerical solutions to the non-linear Boussinesq equation for a sloping aquifer reveals some interesting features. First, however, we review the case of a horizontal aquifer. The solution for an initially level water table subjected to an instantaneous drop in head at the outflow boundary can be separated into two very distinct temporal domains separated by a sharp transition when plotted as $\log(-dQ/dt)$ versus $\log(Q)$ (e.g., [*Parlange, et al.*, 2001]). The early-time domain corresponds to the period during which the water table height h at the no-flux boundary at $x = B$ remains at its initial height, i.e., $h(B,t) = D$. During the late-time domain, the water table is moving downward at the no-flux boundary. For other initial water table

profiles, the early-time domain may not be so distinct and the transition to the late-time domain may appear gradual [*van de Giesen, et al.*, 2005].
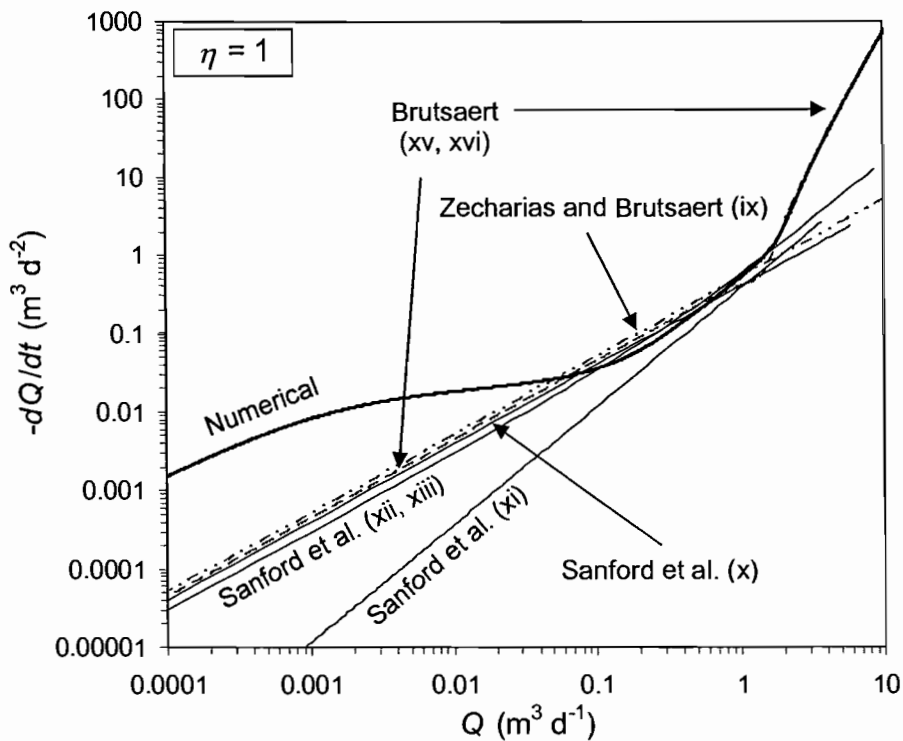
Fig. 3. Recession slope curves predicted by several analytical solutions to the Boussinesq equation for a mildly sloping homogeneous aquifer. Also shown is the numerical solution of an initially saturated aquifer subjected to an instantaneous drop to 0 in channel head h_0. For all solutions, $\tan\phi = 0.02$, $D = 1$ m, $B = 50$ m, $L = 1$ m, and $k = 50$ m d^{-1}. The roman numerals correspond to the recession parameters for each curve given in Table 2.
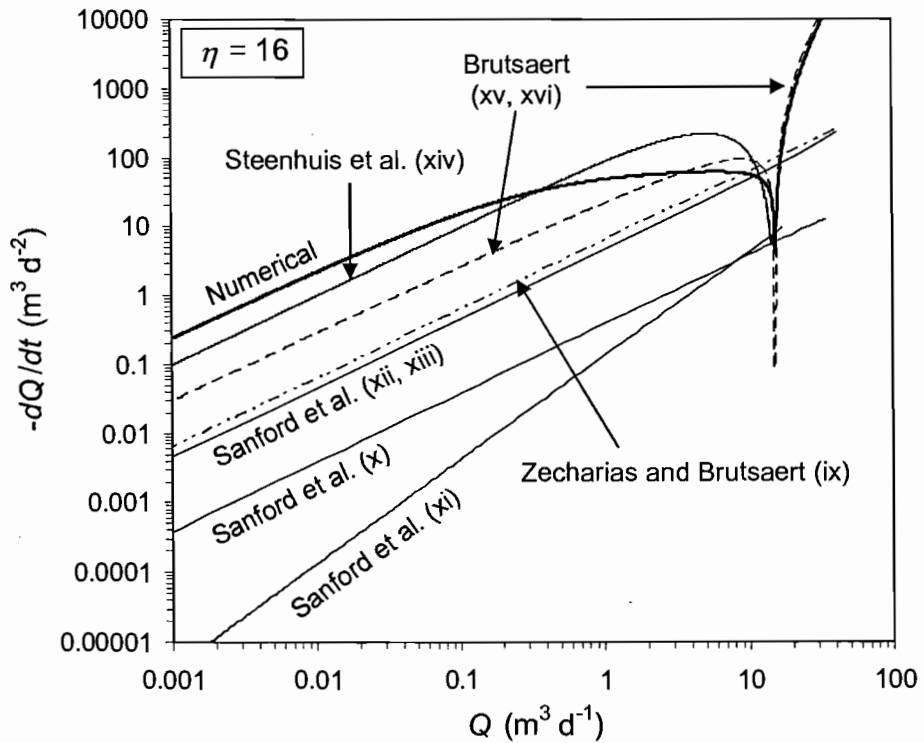
Fig. 4. Recession slope curves predicted by several analytical solutions to the Boussinesq equation for a moderately sloping homogeneous aquifer. Also shown is the numerical solution of an initially saturated aquifer subjected to an instantaneous drop to 0 in channel head h_0. For all solutions, $\tan\phi = 0.02$, $D = 1$ m, $B = 50$ m, $L = 1$ m, and $k = 50$ m d^{-1}. The roman numerals correspond to the recession parameters for each curve given in Table 2.

For the case of a sloping aquifer, the transition between the early- and late-time domains for an initially saturated aquifer is not so brief. This is because the water table at both the channel and the ridge line begins to drop immediately forming a "mound" and the mound progresses downslope. In recession slope plots, this results in three distinct temporal domains (see the numerical solutions in Figs. 3, 4, and 5a), which are referred to here as early, intermediate, and late. During early time, the slope b of the recession curve equals 3 initially and then increases towards infinity. The degree to which b increases depends on the slope. For steep slopes (e.g., $\eta > 16$), the period when b reaches a maximum is when the entire body of water is essentially sliding downslope with little change in the shape. During this period the kinematic wave assumption holds. Following this period, b undergoes a sign reversal and the curve enters the intermediate-time domain. In contrast, for mildly sloping aquifers the transition from the early- to the intermediate-time domain is similar to the transition from early to late time in a horizontal aquifer.

For steep aquifers, the intermediate-time domain is characterized by a change in b from a large negative value to 0. This is followed by a gradual increase in slope which converges to 1 during the late-time domain. For mild slopes, the intermediate-time domain roughly mimics the late-time domain for a horizontal aquifer, but then undergoes a transition where b decreases to some value less than 1 and then converges gradually to a value of 1 in late-time. For intermediate slopes, the behavior falls somewhere in between (Fig. 5a).

When the water table is initially at steady-state due to a constant recharge rate, the early-time domain all but disappears (Fig. 6). For steep aquifers, b transitions quickly from ∞ to 0. The range of Q over which b remains 0 corresponds to the kinematic wave behavior and falls within the intermediate-time domain. In late-time, b converges to a value of 1. For mildly sloping aquifers, b transitions quickly from ∞ to near 3/2. The following intermediate period during which b remains generally constant can range over multiple orders of magnitude in Q. Eventually, b decreases to less than 1 and then converges to 1 at late time.
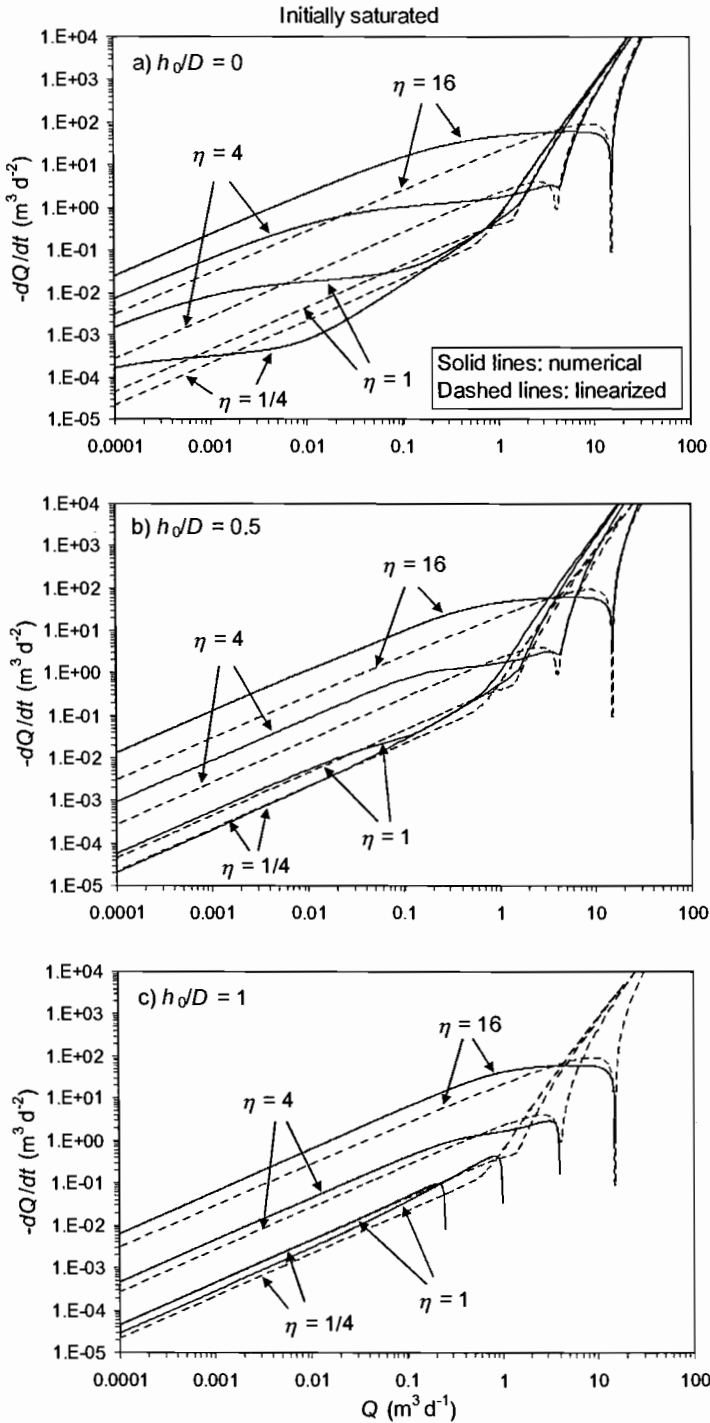
Fig. 5. Comparison of analytical solutions (dashed lines) of the linearized Boussinesq equation following *Brutsaert* [1994] and numerical solutions (solid lines) of the non-linear Boussinesq equation. The simulations are for a homogeneous aquifer initially

saturated to a height D subjected to an instantaneous drop in channel head to a height h_0. Each graph corresponds to a different head h_0 in the channel: a) $h_0 = 0$, b) $h_0 = 0.5$, and c) $h_0 = 1$. For each value of h_0, recession curves were generated for $\tan\phi = 0.005$, 0.02, 0.08, and 0.32. For all solutions, $D = 1$ m, $B = 50$ m, $L = 1$ m, and $k = 50$ m d^{-1}.

Fig. 6. Comparison of analytical solutions (dashed lines) of the linearized Boussinesq equation following *Verhoest and Troch* [2000] and numerical solutions (solid lines) of the non-linear Boussinesq equation. The simulations are for a homogeneous aquifer initially at steady state due to a constant recharge N of 0.1 m d^{-1}. Recession curves were generated for $\tan\phi = 0.005$, 0.02, 0.08, and 0.32. For all solutions, $h_0 = 0$, $D = 1$ m, $B = 50$ m, $L = 1$ m, $k = 50$ m d^{-1}.

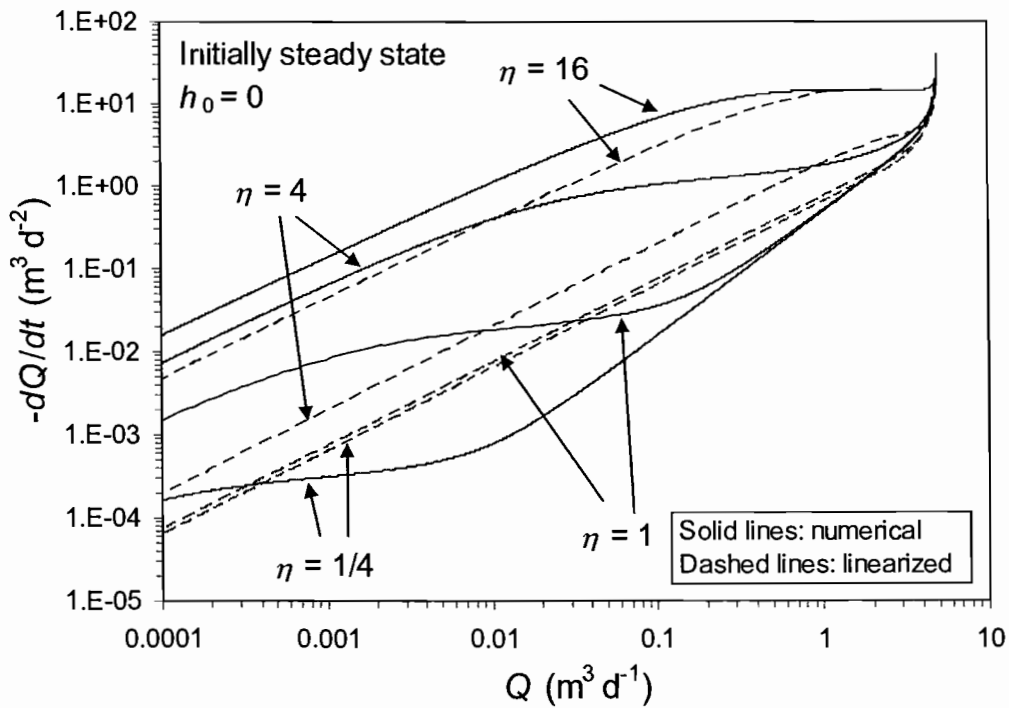The linearized solution of *Brutsaert* [1994] was found to respond most appropriately to changes in η, thus it was examined most closely in comparisons with the numerical solutions. It also shows some, but not all, of the features of the non-linear solution. The related analytical solution of *Verhoest and Troch* [2000] given a water table initially at steady-state was also assessed. For the remainder of this section, references to the "linearized solution" refer only to those solutions following Brutsaert's technique [*Brutsaert*, 1994; *Verhoest and Troch*, 2000; *Pauwels, et al.*, 2002]. For comparison with the numerical solutions, the linearized solution was solved with nearly the identical parameterization. An exception is that the linearized solutions do not explicitly account for cases where $h_0 \neq 0$. Interestingly, though h_0 is a parameter in the linearized equation for the transient water table height in [*Pauwels, et al.*, 2002], it is absent from the equation for discharge. On is left then to account for a non-zero value of h_0 through the parameter p. Because there is not yet a theory for determining p a priori, we let $p = 0.3465$ [*Brutsaert and Nieber*, 1977] for all solutions for an initially-saturated aquifer. For the initially-steady state cases, pD was estimated by (9).

For steeply and moderately sloped aquifers, the linearized solution generates the three temporal domains described previously (Figs. 5 and 6). The early time domain in the initially saturated case is well-reproduced by the linearized solution. An important difference, however, is that the intermediate-time domain extends over a narrower range of discharge values, and the convergence toward a value of $b = 1$ is more rapid, than in the numerical result. The significance for aquifer characterization is that the value of parameter a is not the same for the solutions to the non-linear and linearized equation; in some cases, the value of a differs by an order of magnitude. For mildly sloping aquifers, the linearized solution clearly does not match the numerical solution at intermediate and late times.

As h_0/D approaches 1, the linearized solutions move closer to the numerical solutions at late time. This is not surprising because, as mentioned earlier, linearization is more suited to conditions where $D - h_0 << D$. A more appropriate choice of p for $h_0 > 0$ may bring the solutions even closer together. Curiously, the

linearized solution of the initially-saturated aquifer retains the early-time domain even when $h_0 = D$, in contrast with the numerical solution (Fig. 5c).

4.2. Effect of the Power-Law Conductivity Profile

The value of the power n determines the shape of the recession slope curve (see Fig. 7). As n is increases, the intermediate time domain occupies a progressively smaller range of discharges. At late time the curves converge to a power-law function of the form of (2) with

$$b = (2n + 1)/(n + 1) \tag{16}$$

In contrast, in the early-time domain the curves retain their general shape irrespective of the value of n. This similarity in early time is consistent with the analytical solution for a horizontal aquifer [*Rupp and Selker*, 2005a].

It is of interest to compare the late-time result (16) to the analytical solution for drought flow derived for TOPMODEL given a power-law transmissivity profile [*Ambroise, et al.*, 1996; *Duan and Miller*, 1997; *Iorgulescu and Musy*, 1997]. Subsurface flow per unit contour length in TOPMODEL is assumed to be equal to the local topographic gradient $\tan\beta$ multiplied by the transmissivity T, which is itself a function of the soil moisture deficit δ [*Beven and Kirkby*, 1979]. Following [*Duan and Miller*, 1997], the subsurface flow given as function of the soil moisture deficit δ taken to a power m is

$$q = T \tan \beta = T_0 (\tan \beta)(1 - \delta / m)^m \tag{17}$$

where T_0 is the transmissivity at saturation, or at $\delta = 0$ [*Duan and Miller*, 1997]. Defining a degree of storage S, where $S = 1 - \delta/m$, (17) can be rewritten as

$$q = T_0 (\tan \beta) S^m \tag{18}$$
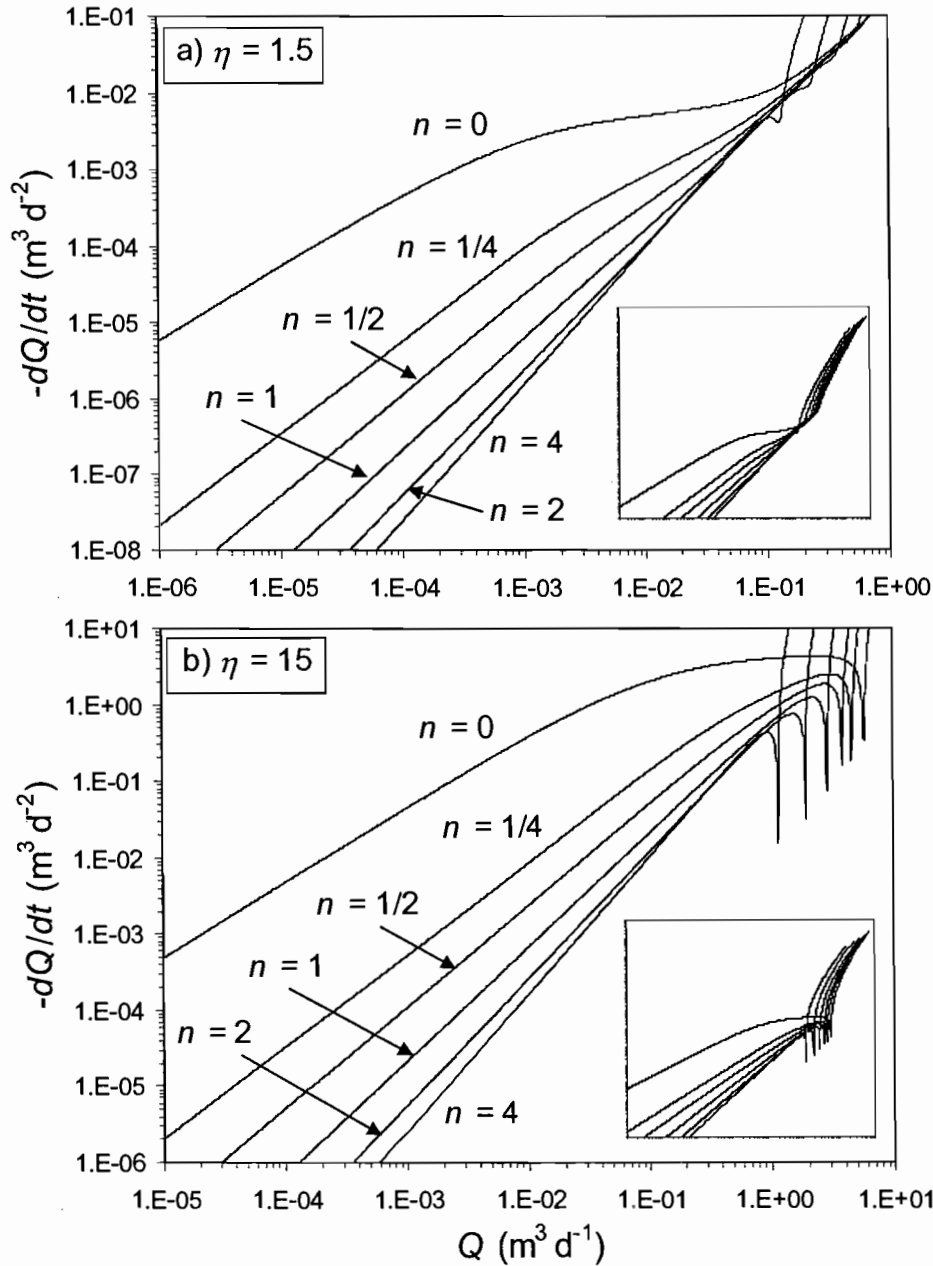
Fig. 7. Numerically generated recession slope curves for a mildly (a; $\tan\phi = 0.03$) and moderately (b; $\tan\phi = 0.3$) sloping aquifer where the saturated hydraulic conductivity profile is a power function of the height above the impermeable base. Shown are curves for various values of the power n. The curves are for an initially saturated aquifer subjected to an instantaneous drop to 0 in channel head h_0. For all curves, $D = 1$ m, $B = 50$ m, $L = 1$ m, and $k_D = 10$ m d^{-1}. The inset figures include the early time domain.

Note that (18) resembles the non-linear reservoir discharge equation: $Q = \alpha S^m$, where α is a constant of proportionality. Given in terms of the Boussinesq aquifer discussed in this paper, (18) becomes

$$q = T_D \tan\phi (h/D)^{n+1} \tag{19}$$

where $T_D = k_D D/(n+1)$ and $m = n + 1$. Eq. (19) is nearly identical to the flux term in the kinematic wave approximation [*Beven*, 1982b], except that $\tan\phi$ has replaced $\sin\phi$.

When m and T_0, or similarly n and T_D, are uniformly distributed throughout a catchment, it has been shown [*Duan and Miller*, 1997; *Iorgulescu and Musy*, 1997] that the subsurface discharge to the channel under drought conditions can be expressed in the form of (2) with $b = (2m - 1)/m$. The lumped non-linear reservoir equation also results in $b = (2m - 1)/m$ [*Brutsaert and Nieber*, 1977], which is expected as it is identical in form to (18). Expressed in terms of n, $b = (2n + 1)/(n + 1)$, which is equivalent to (16).

For the Boussinesq equation, obtaining a late-time definition for the parameter a in (2) without an analytical solution is not straightforward. Dimensional considerations [*Brutsaert and Lopez*, 1999; *Michel*, 1999; *Rupp and Selker*, 2005a] hint at a function of the form

$$a = f(n,\phi,\eta)\frac{1}{\varphi}\left[\frac{k_D D^{1-n} L^2}{(n+1)(2LB)^{n+2}}\right]^{\frac{1}{n+1}} \tag{20}$$

The parameter η has been included in the function $f(n,\phi,\eta)$ after inspection of the analytical solutions to the linearized Boussinesq equation. In particular, see the definitions for the parameter a in (ix), (xiii), (xiv) and (xvi) in Table 2.

The function $f(n,\phi,\eta)$ remains unknown and is certain to be complicated, given, as a clue, the exact function $f_{R2}(n)$ in the late-time analytical solution for the simpler case of the horizontal aquifer [*Rupp and Selker*, 2005a] (see (A5)). One could begin

to arrive at approximate expressions for $f(n,\phi,\eta)$ through numerous numerical simulations. While such a extensive analysis is beyond the scope of this paper, the numerical simulations already done here provide an opportunity to investigate the function in (20) for the simplest case of a homogeneous aquifer with $h_0 = 0$.

Letting $n = 0$, (20) reduces to

$$a = f(\phi,\eta)\frac{kD}{4\varphi B^2} \tag{21}$$

Using the definitions of a in Table 2 as a guide, various functions for $f(\phi,\eta)$ were substituted into (21). Comparisons were made between (21) and the late-time values of a derived by fitting the power function (2) to the numerically generated recession slope curves for the initially-saturated Boussinesq aquifer. Of the functions tested, the best is

$$f(\phi,\eta) = 432\eta\cos^2\phi \tag{22}$$

Substituting (22) into (21) yields the expression for a given in Table 2 (see parameter set (xviii). However, that expression reduces to the following simpler form:

$$a = \frac{108k}{\varphi B}\sin\phi\cos\phi \tag{23}$$

Given the simplicity of (23), there is a surprisingly good 1:1 match with the numerically derived values of a (see Fig. 8).

It is worth noting that D, the depth of the aquifer, is absent from (23). Of the analytical solutions reviewed above, the final solution of *Sanford et al.* [1993] most resembles (23) (see parameter set (xviii) in Table 2), though (23) has an extra "$\cos\phi$" term and the constant multiplier of "108" is much larger than that in the *Sanford et al.* [1993] equation.

This is a useful result with regards to hydraulic parameter estimation as it eliminates the problem of uncertainty in knowing D in the field.
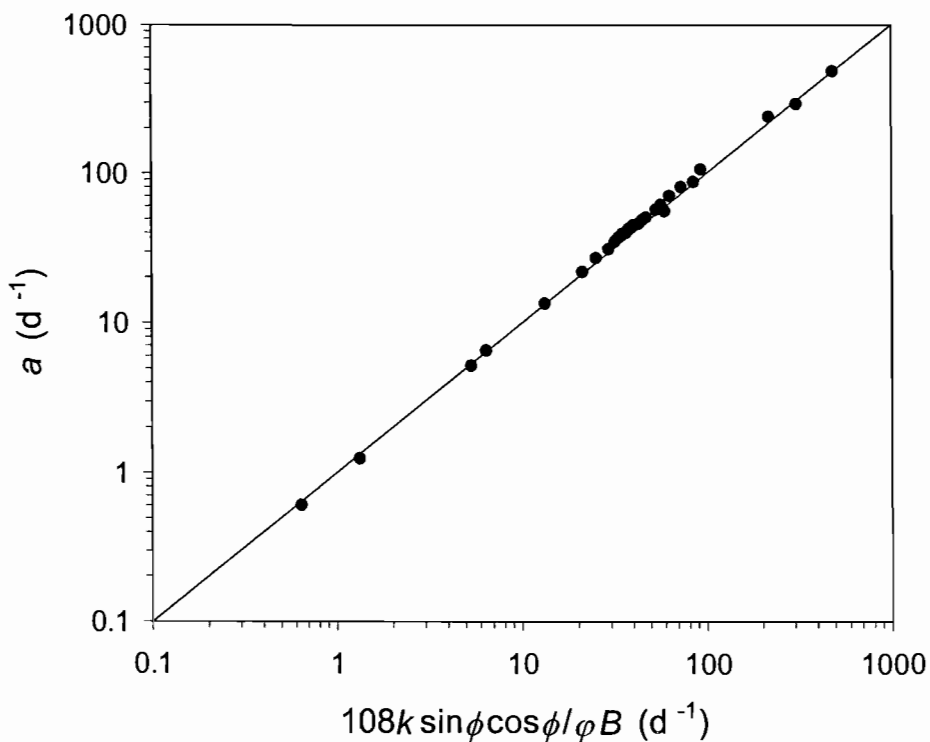
Fig. 8. Late-time recession parameter a determined from numerically-derived recession slope curves versus $2k\sin\phi\cos\phi/\varphi D$, where k is the saturated hydraulic conductivity, ϕ is the aquifer slope, φ is the drainable porosity, and D is the depth of the initially saturated aquifer. Each point corresponds to a drainage simulation of a homogeneous aquifer with varying values of ϕ, k, φ, B and D. Also shown is the 1:1 line.

4.3. Recession Slope Analysis of Field Data

The five recession events covering the greatest range in discharge at the Troy hillslope from the winter of 2002 – 03 were selected for analysis. They are the events beginning on 31 Jan., 16 Mar., 22 Mar., 26 Mar., and 27 Apr. The composite recession slope plot for the six events with discharge given as outflow per unit length of drainage channel (q) is given in Fig. 9. The data appear linear in a log-log space, and clearly show a slope b greater than 1. By visual inspection a line with a slope of 1.6 fits reasonably well. From (16), this corresponds to a power-law k profile with $n = 1.5$.
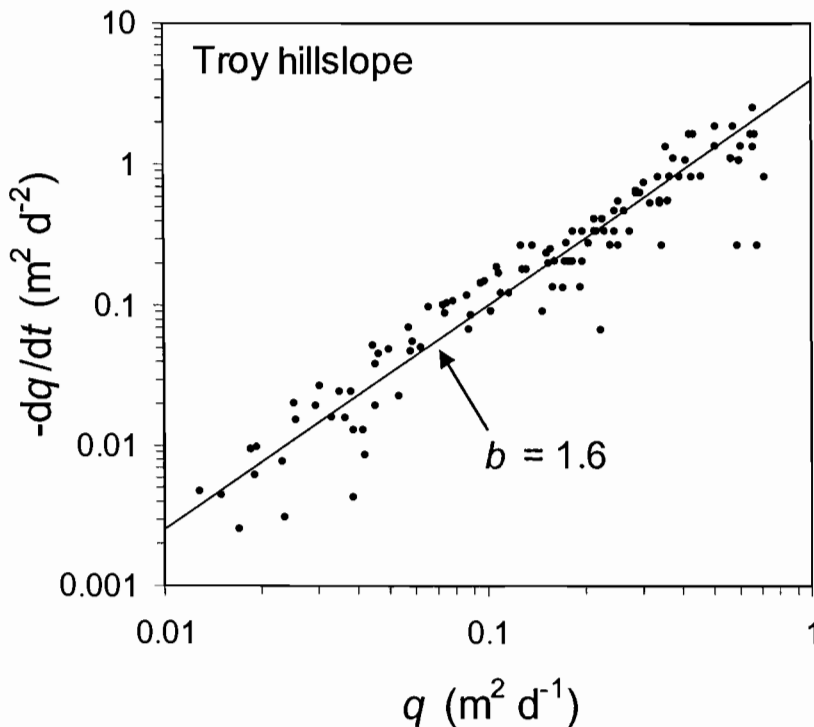
Fig. 9. Composite recession slope plot of the 5 largest and longest recession events from Jan – May 2003 at the Troy, ID, hillslope. The line drawn through the data points has a slope of 1.6.

Though *Brooks et al.* [2004] fit a double exponential function fit through the data of $k(h)$ versus h, one could arguably fit the single power law in (11) through their data for all but the uppermost $10 - 15$ cm of soil (see Fig. 8 in *Brooks et al.* [2004]). The recession slope analysis along with the calculations in *Brooks et al.* [2004] suggest that the data can be modeled by (11) with $k_D = 5$ m d^{-1}, $D = 0.65$ m, and $n = 1.5$, at least for $0 < h < 0.55$.

As a test of the ability of the 1-D Boussinesq equation to reproduce the observed hillslope discharge, the entire hydrograph for the rainfall event beginning on 21 Mar. 2003 was simulated numerically using the parameterization above. An hourly net recharge rate was calculated as the sum of the observed rainfall rate and modeled snowmelt and evapotranspiration rate [*Brooks, et al.*, 2004]. The initial water table profile $h(x,0)$ was generated by linear interpolation of the observed water table height at the 3 observation wells and by assuming $h = 0$ at the tile drain. The only remaining unknown parameter was the drainable porosity φ, which was varied by trial and error until the peak discharges for the observed and simulated hydrographs were similar, which occurred at approximately $\varphi = 0.023$.

The simulated recession curve fits well to the observed data, though there is a large time lag (Fig. 10). The initial rise in the simulated hydrograph also lags behind the observations. The simulated rising limb could certainly be improved by not assuming an initially dry aquifer. The rapid decrease in observed discharge during the early part of the falling limb of the hydrograph is more problematic. The model may require adjustments to adequately account for this behavior. The model, for example, does not incorporate the sharp change in k in the upper $10 - 15$ cm of soil, nor does it include macropore flow, both of which would cause the aquifer to drain more quickly during the first portion of the recession phase.
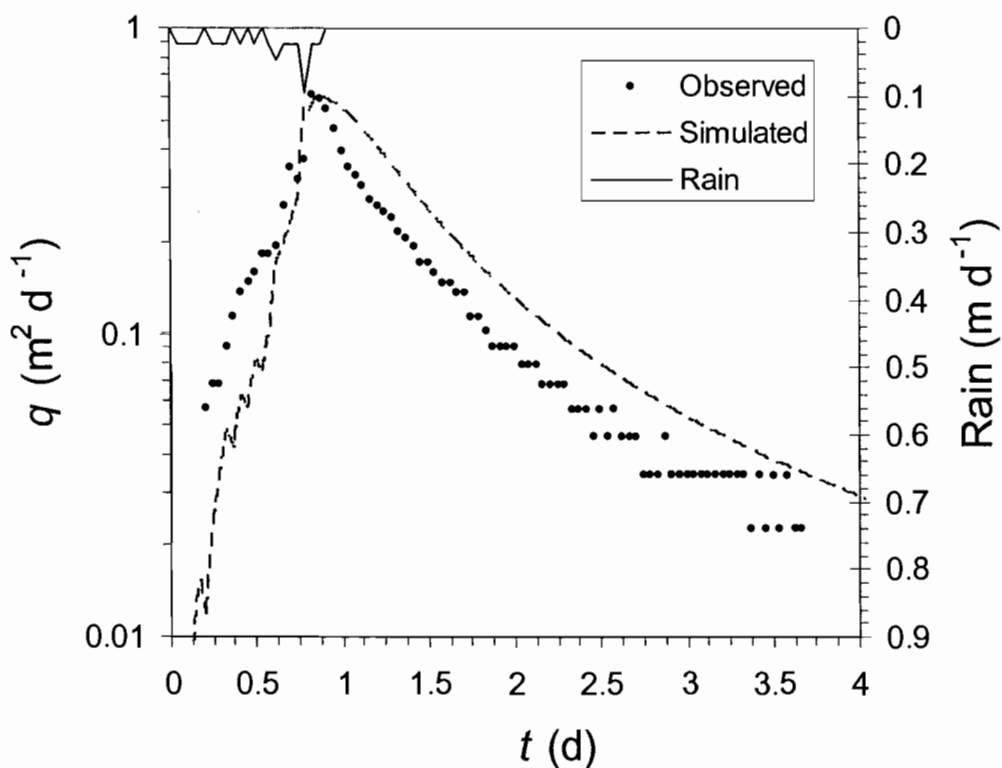
Fig. 10. Simulated and measured hydrographs for the rainfall event beginning on 21 Mar. 2003, at the Troy, ID, hillslope. The simulated hydrograph was generated numerically from the non-linear Boussinesq equation with saturated hydraulic conductivity varying as a power function of depth.

5. Conclusions

This study has addressed two topics in the theory of groundwater discharge to streams from unconfined aquifers. The first topic is the affect on discharge predictions arising from the linearization methods used to derive analytical solutions to the 1-D Boussinesq equation for a sloping aquifer. Particular attention was placed on how the analytical solutions appeared when plotted as $\log(-dQ/dt)$ versus $\log(Q)$. This plotting technique has been used previously to compare recession data with analytical solutions to the Boussinesq equation for a horizontal aquifer. Known also

as the method of *Brutseart and Nieber* [1977], it may be the only analytical tool available for estimating basin-scale hydraulic properties [*Szilagyi*, 2004].

It was shown by comparison with numerically-generated recession curves of the non-linear Boussinesq equation, that the existing analytical solutions for the sloping aquifer are generally inappropriate for this type of analysis. An exception may be for when the water height in the stream does not differ greatly from the height of the water table relative to the total depth of the aquifer. Even in this case however, a better theory is needed for what the effective water table height should be in the linearized equation, i.e., what is the value of pD?

The second topic of this paper is on the use of the non-linear 1-D Boussinesq equation for characterizing the subsurface of a hillslope with shallow soils. The Boussinesq equation in its basic form assumes a homogeneous aquifer. However, soil hydraulic properties, and particularly saturated hydraulic conductivity k, often vary with depth. We allowed lateral k to vary continuously with height h as a power law and solved the modified Boussinesq equation numerically. It was found that the recession parameter b in (2) converges to $(2n+1)/(n+1)$, where n is the power in the k function. Discharge data from a hillslope where lateral $k(h)$ with depth was determined by an independent method showed similar behavior. These results back the notion the recession slope analysis can be used to aid in characterizing the hydraulic properties of sloping aquifers. However, appropriate analytical functions for the parameter a in (2) are still unknown, though we hint at a functional form for a.

An important issue not addressed here is how well the Brutsaert and Nieber method holds up under more complex terrain, in particular in catchments composed of a variety of hillslopes in which flow may also be convergent or divergent. While a 1-D Boussinesq equation-based model has been developed for divergent and convergent hillslopes [*Troch, et al.*, 2003] (including an analytical solution for a special case [*Troch, et al.*, 2004]), it is not yet clear if the composite discharge from various hillslopes could be simulated by a single "representative" Boussinesq aquifer with catchment-scale effective parameters, as required by the Brutsaert and Nieber method.

Acknowledgements

Appendix

Table 1 lists the functions f_{Lo}, f_{R1}, and f_{R2} that are part of the definitions for the recession parameter a for three solutions to the Boussinesq equation for a horizontal aquifer. The definitions of these three functions are given below.

For the early-time solution with a non-zero head h_0 in the channel, f_{Lo} is a rather complex function of h_0 and D [*Lockington*, 1997]. However, f_{Lo} takes on a narrow range of values between 1.136 and 0.785 and can be approximated by a polynomial function. The following third-order polynomial can be used for f_{Lo} with little loss in accuracy:

$$f_{Lo} = -0.4604(h_0/D)^3 + 1.0734(h_0/D)^2 - 0.9673(h_0/D) + 1.1361 \tag{A1}$$

For the early-time solution for the power-law saturated hydraulic conductivity profile [*Rupp and Selker*, 2005a], f_{R1} is

$$f_{R1} = \frac{(1-\mu)(n+1)(n+2)}{2(1-2\mu)} \tag{A2}$$

where

$$\mu = \frac{4 - 3\gamma - \sqrt{\gamma^2 - 2\gamma + 4}}{4(1-2\gamma)} \tag{A3}$$

and

$$\gamma = 2(n+2)B_{R1} \tag{A4}$$

The parameter B_{R1} is the beta function evaluated at $n+2$ and 2, i.e., $B(n+2,2)$.

For the late-time solution with the power-law saturated hydraulic conductivity profile [*Rupp and Selker*, 2005a], f_{R2} is

$$f_{R2} = \frac{n+2}{2(n+1)(n+3)} B_{R2} \left[\frac{(n+1)(n+3)}{B_{R2}} \right]^{\frac{n+1}{n+2}} \tag{A5}$$

Where B_{R2} is the beta function evaluated at $(n+2)/(n+3)$ and $1/2$.

References

Ambroise, B., K. Beven, and J. Freer (1996), Toward a generalization of the TOPMODEL concepts: topographic indices of hydrological similarity, *Water Resour. Res.*, *32*, 2135-2145.

Beven, K. (1981), Kinematic subsurface stormflow, *Water Resour. Res.*, *17*, 1419-1424.

Beven, K. (1982a), On subsurface stormflow: an analysis of response times, *Hydrol. Sci. J.*, *27*, 505-521.

Beven, K. (1982b), On subsurface stormflow: predictions with simple kinematic theory for saturated and unsaturated flows, *Water Resour. Res.*, *18*, 1627-1633.

Beven, K. (1984), Infiltration into a class of vertically non-uniform soils, *Hydrol. Sci. J.*, *29*, 425-434.

Beven, K., and M. J. Kirkby (1979), A physically-based variable contributing-area model of catchment hydrology, *Hydrol. Sci. Bull.*, *24*, 43-69.

Bonell, M., D. A. Gilmour, and D. F. Sinclair (1981), Soil hydraulic properties and their effect on surface and subsurface water transfer in a tropical rainforest catchment, *Hydrol. Sci. Bull.*, *26*, 1-18.

Boussinesq, J. (1877), Essai sur la théorie des eaux courantes, *Mem. Acad. Sci. Inst. Fr.*, *23*, 252-260.

Boussinesq, J. (1903), Sur le débit, en temps de sécheresse, d'une source alimentée par une nappe d'eaux d'infiltration, *C. R. Hebd. Seances Acad. Sci.*, *136*, 1511-1517.

Boussinesq, J. (1904), Recherches théoriques sur l'écoulement des nappes d'eau infiltrées dans le sol et sur débit de sources, *J. Math. Pures Appl., 5me Ser.*, *10*, 5-78.

Brooks, E. S., J. Boll, and P. A. McDaniel (2004), A hillslope-scale experiment to measure lateral saturated hydraulic conductivity, *Water Resour. Res.*, *40*, W042081-W0420810.

Brutsaert, W. (1994), The unit response of groundwater outflow from a hillslope, *Water Resour. Res.*, *30*, 2759-2763.

Brutsaert, W., and J. P. Lopez (1998), Basin-scale geohydrologic drought flow features of riparian aquifers in the southern Great Plains, *Water Resour. Res.*, *34*, 233-240.

Brutsaert, W., and J. P. Lopez (1999), Reply to comment on "Basin-scale geohydrologic drought flow features of riparian aquifers in the southern Great Plains", *Water Resour. Res.*, *35*, 911.

Brutsaert, W., and J. L. Nieber (1977), Regionalized drought flow hydrographs from a mature glaciated plateau, *Water Resour. Res.*, *13*, 637-643.

Chapman, T. (1995), Comment on "The unit response of groundwater outflow from a hillslope" by Wilfried Brutsaert, *Water Resour. Res.*, *31*, 2377-2378.

Childs, E. C. (1971), Drainage of groundwater resting on a sloping bed, *Water Resour. Res.*, *7*, 1256-1263.

Duan, J., and N. L. Miller (1997), A generalized power function for the subsurface transmissivity profile in TOPMODEL, *Water Resour. Res.*, *33*, 2559-2562.

Eng, K., and W. Brutsaert (1999), Generality of drought flow characteristics within the Arkansas River basin, *J. Geophys. Res.-Atmos.*, *104*, 19,435-419,441.

Hall, F. R. (1968), Base-flow recessions - a review, *Water Resour. Res.*, *4*, 973-983.

Hammad, H. Y., R. Carravetta, and J. Y. Ding (1966), Discussions of "Inflow hydrographs from large unconfined aquifers", *J. Irrig. Drain. Eng. - ASCE*, *92*, 101-107.

Harr, R. D. (1977), Water flux in soil and subsoil on a steep forested hillslope, *J. Hydrol.*, *33*, 37-58.

Henderson, F. M., and R. A. Wooding (1964), Overland flow and groundwater flow from a steady rainfall of finite duration, *J. Geophys. Res.*, *69*, 1531-1540.

Ibrahim, H. A., and W. Brutsaert (1965), Inflow hydrographs from large unconfined aquifers, *J. Irrig. Drain. Eng. - ASCE*, *91*, 21-38.

Ibrahim, H. A., and W. Brutsaert (1966), Closure to "Inflow hydrographs from large unconfined aquifers", *J. Irrig. Drain. Eng. - ASCE*, *92*, 68-69.

Iorgulescu, I., and A. Musy (1997), A generalization of TOPMODEL for a power law transmissivity profile, *Hydrol. Processes*, *11*, 1353-1355.

Koussis, A. D. (1992), A linear conceptual subsurface storm flow model, *Water Resour. Res.*, *28*, 1047-1052.

Lacey, G. C., and R. B. Grayson (1998), Relating baseflow to catchment properties in south-eastern Australia, *J. Hydrol.*, *204*, 231-250.

Lockington, D. A. (1997), Response of unconfined aquifer to sudden change in boundary head, *J. Irrig. Drain. Eng. - ASCE*, *123*, 24-27.

Malvicini, C. F., T. S. Steenhuis, M. T. Walter, J.-Y. Parlange, and M. F. Walter (2005), Evaluation of spring flow in the uplands of Matalom, Leyte, Philippines, *Adv. Water Resour.*, *28*, 1083-1090.

Mendoza, G. F., T. S. Steenhuis, M. T. Walter, and J. Y. Parlange (2003), Estimating basin-wide hydraulic parameters of a semi-arid mountainous watershed by recession-flow analysis, *J. Hydrol.*, *279*, 57-69.

Michel, C. (1999), Comment on "Basin-scale geohydrologic drought flow features of riparian aquifers in the southern Great Plains" by Brutsaert and Lopez, *Water Resour. Res.*, *35*, 909-910.

Mizumura, K. (2002), Drought flow from hillslope, *J. Hydrologic. Eng.*, *7*, 109-115.

Mizumura, K. (2005), Recession analysis of drought flow using Hele Shaw model, *J. Hydrologic. Eng.*, *10*, 125-132.

Parlange, J.-Y., M. B. Parlange, T. S. Steenhuis, W. L. Hogarth, D. A. Barry, L. Li, F. Stagnitti, A. Heilig, and J. Szilagyi (2001), Sudden drawdown and drainage of a horizontal aquifer, *Water Resour. Res.*, *37*, 2097-2101.

Pauwels, V. R. N., N. E. C. Verhoest, and F. P. De Troch (2002), A metahillslope model based on an analytical solution to a linearized Boussinesq equation for temporally variable recharge rates, *Water Resour. Res.*, *38*, 331-3311.

Polubarinova-Kochina, P. Y. (1962), *Theory of Ground Water Movement*, 613 pp., Princeton University Press, Princeton, N. J.

Rupp, D. E., J. M. Owens, K. L. Warren, and J. S. Selker (2004), Analytical methods for estimating saturated hydraulic conductivity in a tile-drained field, *J. Hydrol.*, *289*, 111-127.

Rupp, D. E., and J. S. Selker (2005a), Drainage of a horizontal Boussinesq aquifer with a power-law hydraulic conductivity profile, *Water Resour. Res.*, *41*, in press.

Rupp, D. E., and J. S. Selker (2005b), Information, artifacts, and noise in dQ/dt-Q recession analysis, *Adv. Water Resour.*, in press.

Sanford, W. E., J. Y. Parlange, and T. S. Steenhuis (1993), Hillslope drainage with sudden drawdown: closed form solution and laboratory experiments, *Water Resour. Res.*, *29*, 2313-2321.

Steenhuis, T. S., F. Stagnitti, M. F. Walter, J. Y. Parlange, W. E. Sanford, and A. Heilig (1999), Can we distinguish Richards' and Boussinesq's equations for hillslopes? The Coweeta experiment revisited, *Water Resour. Res.*, *35*, 589-595.

Szilagyi, J. (2004), Vadose zone influences on aquifer parameter estimates of saturated-zone hydraulic theory, *J. Hydrol.*, *286*, 78-86.

Szilagyi, J., and M. B. Parlange (1998), Baseflow separation based on analytical solutions of the Boussinesq equation, *J. Hydrol.*, *204*, 251-260.

Szilagyi, J., M. B. Parlange, and J. D. Albertson (1998), Recession flow analysis for aquifer parameter determination, *Water Resour. Res.*, *34*, 1851-1857.

Tallaksen, L. M. (1995), A review of baseflow recession analysis, *J. Hydrol.*, *165*, 349-370.

Troch, P. A., F. P. De Troch, and W. Brutsaert (1993), Effective water table depth to describe initial conditions prior to storm rainfall in humid regions, *Water Resour. Res.*, *29*, 427-434.

Troch, P. A., C. Paniconi, and E. E. Van Loon (2003), Hillslope-storage Boussinesq model for subsurface flow and variable source areas along complex hillslopes: 1. Formulation and characteristic response, *Water Resour. Res.*, *39*, SBH31-SBH312.

Troch, P. A., A. H. Van Loon, and A. G. J. Hilberts (2004), Analytical solution of the linearized hillslope-storage Boussinesq equation for exponential hillslope width functions, *Water Resour. Res.*, *40*, W086011-W086016.

van de Giesen, N. C., T. S. Steenhuis, and J.-Y. Parlange (2005), Short- and long-time behavior of aquifer dainage after slow and sudden recharge according to the linearized Laplace equation, *Adv. Water Resour.*, *28*, 1122-1132.

Verhoest, N. E. C., and P. A. Troch (2000), Some analytical solutions of the linearized Boussinesq equation with recharge for a sloping aquifer, *Water Resour. Res.*, *36*, 793-800.

Vogel, R. M., and C. N. Kroll (1992), Regional geohydrologic-geomorphic relationships for the estimation of low-flow statistics, *Water Resour. Res.*, *28*, 2451-2458.

Zecharias, Y. B., and W. Brutsaert (1988a), The influence of basin morphology on groundwater outflow, *Water Resour. Res.*, *24*, 1645-1650.

Zecharias, Y. B., and W. Brutsaert (1988b), Recession characteristics of groundwater outflow and base flow from mountainous watersheds, *Water Resour. Res.*, *24*, 1651-1658.

Chapter 6 - Conclusions

The general goal of this investigation has been to further the understanding of the physics of groundwater flow. The means has been through an assessment of existing analytical solutions, and the derivation of new analytical solutions, to the differential equations describing flow in unconfined aquifers. These analytical solutions were arrived at by making several restrictive assumptions to the full non-linear equations describing single-phase flow in porous media. The primary assumptions are that the three-dimensional flow field can be reduced to a single dimension, that the spatial domain of the aquifer can be represented by a rectangle in which the hydraulic parameters are uniform laterally in space, and that flow in the unsaturated zone can be neglected.

Analytical solutions are desirable because they can permit both the theoretical analysis of physical processes and the interpretation of real data in a relatively simple manner. For example, estimation of field- or catchment-scale hydraulic properties can be made from discharge data using a simple graphical method that relates properties of the graphed data to properties of the analytical solutions to the 1-dimensional Boussinesq equation. This method, proposed by *Brutsaert and Nieber* [1977], has been the subject of much of the research presented here.

Chapter 2 provides evidence showing how well such a simplified representation of groundwater flow can predict the recession discharge and water table decline rate in a tile-drained field. It also shows how both the Brutsaert and Nieber method yields an estimate of field-scale saturated hydraulic conductivity k that is near the geometric mean of soil cores collected at various locations throughout the field and tested in the laboratory. This runs counter to the widely-held notion that k should increase with volume sampled.

Chapter 3 discusses a practical shortcoming of the Brutsaert and Nieber method. Specifically, it reveals how the typical method of estimating the slope of the recession curve can lead to artifacts in the graphical representation of the data,

artifacts that had either been previously misinterpreted or identified but left unexplained. An alternative method for estimating the slope of the recession curve is proposed which does not generate the artifacts.

Chapter 4 provides new analytical solutions to the non-linear 1-dimensional Boussinesq equation for a horizontal aquifer in which k is allowed to vary with depth as power law. This is probably the first advance in this research direction since *Beven* [1982b] arrived at an analytical solution for a power-law k profile by simplifying the Boussinesq equation for a sloping aquifer to a linear kinematic wave equation. This is of interest because previous analytical solutions had been limited to a homogeneous aquifer, yet many soils are known to show reductions in k with depth.

Chapter 5 gives an assessment of the Brutsaert and Nieber method for use with sloping aquifers. While previous studies have all made use of the analytical solutions to the Boussinesq equation for a horizontal aquifer, various analytical solutions do exist for the sloping case. However, these solutions, all of which are based on some technique for linearizing the equation, were found to be inappropriate for a Brutsaert and Nieber-type analysis. This conclusion was reached by comparing the analytical solutions to numerical solutions of the non-linear equation. However, an examination of the numerical solutions did reveal relationships between aquifer parameters and recession slope curves. Thus, some analytical expressions linking aquifer parameters to properties of the graphed solutions could be "empirically-derived", permitting at least partial characterization of the aquifer.

In summary, the 1-dimensional Boussinesq equation was found to be applicable in field and hillslope settings where the boundary conditions were relatively well-defined and the assumption of 1-dimensional flow was valid. Consequently, the Brutsaert and Nieber method was also useful in these settings where an analytical relationship was available that linked the recession curve parameters to the hydraulic/geometric properties of the aquifer. Uncertainty remains as to whether it is valid to extend the Brutsaert and Nieber method to hilly basins, though it has been done so in the past. Further investigation is required into recession discharge patterns

resulting from a composite of divergent and convergent flows as would be expected in a real basin.

Bibliography

Abramowitz, M., and I. A. Stegun (Eds.) (1972), *Handbook of Mathematical Functions*, 1046 pp., Dover, New York.

Ambroise, B., K. Beven, and J. Freer (1996), Toward a generalization of the TOPMODEL concepts: topographic indices of hydrological similarity, *Water Resour. Res.*, *32*, 2135-2145.

Beven, K. (1981), Kinematic subsurface stormflow, *Water Resour. Res.*, *17*, 1419-1424.

Beven, K. (1982a), On subsurface stormflow: an analysis of response times, *Hydrol. Sci. J.*, *27*, 505-521.

Beven, K. (1982b), On subsurface stormflow: predictions with simple kinematic theory for saturated and unsaturated flows, *Water Resour. Res.*, *18*, 1627-1633.

Beven, K. (1984), Infiltration into a class of vertically non-uniform soils, *Hydrol. Sci. J.*, *29*, 425-434.

Beven, K., and M. J. Kirkby (1979), A physically-based variable contributing-area model of catchment hydrology, *Hydrol. Sci. Bull.*, *24*, 43-69.

Bonell, M., D. A. Gilmour, and D. F. Sinclair (1981), Soil hydraulic properties and their effect on surface and subsurface water transfer in a tropical rainforest catchment, *Hydrol. Sci. Bull.*, *26*, 1-18.

Boussinesq, J. (1877), Essai sur la théorie des eaux courantes, *Mem. Acad. Sci. Inst. Fr.*, *23*, 252-260.

Boussinesq, J. (1903), Sur le débit, en temps de sécheresse, d'une source alimentée par une nappe d'eaux d'infiltration, *C. R. Hebd. Seances Acad. Sci.*, *136*, 1511-1517.

Boussinesq, J. (1904), Recherches théoriques sur l'écoulement des nappes d'eau infiltrées dans le sol et sur débit de sources, *J. Math. Pures Appl., 5me Ser.*, *10*, 5-78.

Brooks, E. S., J. Boll, and P. A. McDaniel (2004), A hillslope-scale experiment to measure lateral saturated hydraulic conductivity, *Water Resources Research*, *40*, W042081-W0420810.

Brutsaert, W. (1994), The unit response of groundwater outflow from a hillslope, *Water Resour. Res.*, *30*, 2759-2763.

129

Brutsaert, W., and J. P. Lopez (1998), Basin-scale geohydrologic drought flow features of riparian aquifers in the southern Great Plains, *Water Resour. Res.*, *34*, 233-240.

Brutsaert, W., and J. P. Lopez (1999), Reply to comment on "Basin-scale geohydrologic drought flow features of riparian aquifers in the southern Great Plains", *Water Resour. Res.*, *35*, 911.

Brutsaert, W., and J. L. Nieber (1977), Regionalized drought flow hydrographs from a mature glaciated plateau, *Water Resour. Res.*, *13*, 637-643.

Chapman, T. (1995), Comment on "The unit response of groundwater outflow from a hillslope" by Wilfried Brutsaert, *Water Resour. Res.*, *31*, 2377-2378.

Childs, E. C. (1971), Drainage of groundwater resting on a sloping bed, *Water Resour. Res.*, *7*, 1256-1263.

Chow, V. T. (1959), *Open-channel hydraulics*, McGraw-Hill, New York.

Duan, J., and N. L. Miller (1997), A generalized power function for the subsurface transmissivity profile in TOPMODEL, *Water Resour. Res.*, *33*, 2559-2562.

Dumm, L. D. (1954), New formula for determining depth and spacing of subsurface drains in irrigated lands, *Agric. Engng.*, *35*, 726-730.

Dumm, L. D. (1964), Transient-flow concept in subsurface drainage: its validity and use, *Trans. ASAE*, *7*, 142-151.

El-Mowelhi, N. M., and J. Van Schilfgaarde (1982), Computation of soil hydrological constants from field drainage experiments in some soils of Egypt, *Trans. ASAE*, *25*, 984-986.

Eng, K., and W. Brutsaert (1999), Generality of drought flow characteristics within the Arkansas River basin, *J. Geophys. Res.-Atmos.*, *104*, 19,435-419,441.

Hall, F. R. (1968), Base-flow recessions - a review, *Water Resour. Res.*, *4*, 973-983.

Hammad, H. Y., R. Carravetta, and J. Y. Ding (1966), Discussions of "Inflow hydrographs from large unconfined aquifers", *J. Irrig. Drain. Eng. - ASCE*, *92*, 101-107.

Harr, R. D. (1977), Water flux in soil and subsoil on a steep forested hillslope, *J. Hydrol.*, *33*, 37-58.

Heaslet, M. A., and A. Alksne (1961), Diffusion from a fixed surface with a concentration-dependent coefficient, *J. Soc. Ind. Appl. Math.*, *9*, 584-596.

Henderson, F. M., and R. A. Wooding (1964), Overland flow and groundwater flow from a steady rainfall of finite duration, *J. Geophys. Res.*, *69*, 1531-1540.

Hoffman, G. J., and G. O. Schwab (1964), Tile spacing prediction based on drain outflow, *Trans. ASAE*, *13*, 444-447.

Hogarth, W. L., and J. Y. Parlange (1999), Solving the Boussinesq equation using solutions of the Blasius equation, *Water Resour. Res.*, *35*, 885-887.

Hooghoudt, S. B. (1940), Bijdragon tot de Kennis van Eenige Natuurkundige Groothen van den Grond, 7. Algemeene Beschouwing van het Probleem van de Detail Ontwatering en de Infiltratie door middle van Parallel Loopende Drains, Greppels, Slooten en Kanalen, *Verslag. Landbouwk. Onderzoek.*, *46*, 515-707.

Ibrahim, H. A., and W. Brutsaert (1965), Inflow hydrographs from large unconfined aquifers, *J. Irrig. Drain. Eng. - ASCE*, *91*, 21-38.

Ibrahim, H. A., and W. Brutsaert (1966), Closure to "Inflow hydrographs from large unconfined aquifers", *J. Irrig. Drain. Eng. - ASCE*, *92*, 68-69.

Iorgulescu, I., and A. Musy (1997), A generalization of TOPMODEL for a power law transmissivity profile, *Hydrol. Processes*, *11*, 1353-1355.

Klute, A. (1986), Water Retention: Laboratory Methods, in *Methods of Soil Analysis. Part 1, second ed, Agronomy Monograph No. 9*, edited, pp. 635-662.

Klute, A., and C. Dirksen (1986), Hydraulic Conductivity and Diffusivity: Laboratory Methods, in *Methods of Soil Analysis. Part 1, second ed, Agronomy Monograph No. 9*, edited, pp. 687-734.

Koussis, A. D. (1992), A linear conceptual subsurface storm flow model, *Water Resour. Res.*, *28*, 1047-1052.

Lacey, G. C., and R. B. Grayson (1998), Relating baseflow to catchment properties in south-eastern Australia, *J. Hydrol.*, *204*, 231-250.

Lockington, D. A. (1997), Response of unconfined aquifer to sudden change in boundary head, *J. Irrig. Drain. Eng.*, *123*, 24-27.

Luthin, J. N. (1959), The falling water table in tile drainage. II. Proposed criteria for spacing tile drains, *Trans. ASAE*, 44-45.

Luthin, J. N., and R. V. Worstell (1959), The falling water table in tile drainage. III. Factors affecting the rate of fall, *Trans. ASAE*, 45-51.

Malvicini, C. F., T. S. Steenhuis, M. T. Walter, J. Y. Parlange, and M. F. Walter (2005), Evaluation of spring flow in the uplands of Matalom, Leyte, Philippines, *Adv. Water Resour.*, *28*, 1083-1090.

Manning (1891), On the flow of water in open channels and pipes., *Trans. Institute of Civil Engineers of Ireland.*

Mendoza, G. F., T. S. Steenhuis, M. T. Walter, and J. Y. Parlange (2003), Estimating basin-wide hydraulic parameters of a semi-arid mountainous watershed by recession-flow analysis, *J. Hydrol.*, *279*, 57-69.

Michel, C. (1999), Comment on "Basin-scale geohydrologic drought flow features of riparian aquifers in the southern Great Plains" by Brutsaert and Lopez, *Water Resour. Res.*, *35*, 909-910.

Mizumura, K. (2002), Drought flow from hillslope, *J. Hydrologic. Eng.*, *7*, 109-115.

Mizumura, K. (2005), Recession analysis of drought flow using Hele Shaw model, *J. Hydrologic. Eng.*, *10*, 125-132.

Neale, L. C., and R. E. Price (1964), Flow characteristics of PVC sewer pipe, *J. Sanitary Engng Div., Div. Proc. 90SA3, ASCE*, 109-129.

Otte, G. E., D. K. Setness, W. A. Anderson, F. J. Herbert, and C. A. Knezevich (1974), Soil Survey of the Yamhill Area, 138 pp, USDA, Soil Conservation Service; in Cooperation with the Oregon Agriculture Experiment Station.

Parlange, J.-Y., M. B. Parlange, T. S. Steenhuis, W. L. Hogarth, D. A. Barry, L. Li, F. Stagnitti, A. Heilig, and J. Szilagyi (2001), Sudden drawdown and drainage of a horizontal aquifer, *Water Resour. Res.*, *37*, 2097-2101.

Pauwels, V. R. N., N. E. C. Verhoest, and F. P. De Troch (2002), A metahillslope model based on an analytical solution to a linearized Boussinesq equation for temporally variable recharge rates, *Water Resour. Res.*, *38*, 331-3311.

Polubarinova-Kochina, P. Y. (1962), *Theory of Ground Water Movement*, 613 pp., Princeton University Press, Princeton, N. J.

Rupp, D. E., J. M. Owens, K. L. Warren, and J. S. Selker (2004), Analytical methods for estimating saturated hydraulic conductivity in a tile-drained field, *J. Hydrol.*, *289*, 111-127.

Rupp, D. E., and J. S. Selker (2005a), Drainage of a horizontal Boussinesq aquifer with a power-law hydraulic conductivity profile, *Water Resour. Res.*, *41*, in press.

Rupp, D. E., and J. S. Selker (2005b), Information, artifacts, and noise in dQ/dt-Q recession analysis, *Adv. Water Resour.*, in press.

Sanford, W. E., J. Y. Parlange, and T. S. Steenhuis (1993), Hillslope drainage with sudden drawdown: closed form solution and laboratory experiments, *Water Resour. Res.*, *29*, 2313-2321.

Singh, K. P. (1968), Some factors affecting baseflow, *Water Resour. Res.*, *4*, 985-999.

Smith, R. E., D. L. Chery, K. G. Renard, and W. R. Gwinn (1981), Supercritical flow flumes for measuring sediment-laden flow, 72 pp, U.S. Department of Agriculture Bulletin No. 1665.

Steenhuis, T. S., F. Stagnitti, M. F. Walter, J. Y. Parlange, W. E. Sanford, and A. Heilig (1999), Can we distinguish Richards' and Boussinesq's equations for hillslopes? The Coweeta experiment revisited, *Water Resour. Res.*, *35*, 589-595.

Szilagyi, J. (2003), Sensitivity analysis of aquifer parameter estimations based on the Laplace equation with linearized boundary conditions, *Water Resour. Res.*, *39*, SBH81-SBH87.

Szilagyi, J. (2004), Vadose zone influences on aquifer parameter estimates of saturated-zone hydraulic theory, *J. Hydrol.*, *286*, 78-86.

Szilagyi, J., and M. B. Parlange (1998), Baseflow separation based on analytical solutions of the Boussinesq equation, *J. Hydrol.*, *204*, 251-260.

Szilagyi, J., M. B. Parlange, and J. D. Albertson (1998), Recession flow analysis for aquifer parameter determination, *Water Resour. Res.*, *34*, 1851-1857.

Tallaksen, L. M. (1995), A review of baseflow recession analysis, *J. Hydrol.*, *165*, 349-370.

Talsma, T., and H. C. Haskew (1959), Investigation of water-table response to tile drains in comparison with theory, *J. Geophys. Res.*, *64*, 1933-1944.

Troch, P. A., F. P. De Troch, and W. Brutsaert (1993), Effective water table depth to describe initial conditions prior to storm rainfall in humid regions, *Water Resour. Res.*, *29*, 427-434.

Troch, P. A., C. Paniconi, and E. E. Van Loon (2003), Hillslope-storage Boussinesq model for subsurface flow and variable source areas along complex hillslopes: 1. Formulation and characteristic response, *Water Resour. Res.*, *39*, SBH31-SBH312.

Troch, P. A., A. H. Van Loon, and A. G. J. Hilberts (2004), Analytical solution of the linearized hillslope-storage Boussinesq equation for exponential hillslope width functions, *Water Resour. Res.*, *40*, W086011-W086016.

van de Giesen, N., J. Y. Parlange, and T. S. Steenhuis (1994), Transient flow to open drains: comparison of linearized solutions with and without the Dupuit assumption, *Water Resour. Res.*, *30*, 3033-3039.

van de Giesen, N., T. S. Steenhuis, and J. Y. Parlange (2005), Short- and long-time behavior of aquifer drainage after slow and sudden recharge according to the linearized Laplace equation, *Adv. Water Resour.*, *28*, 1122-1132.

van Schilfgaarde, J. (1963), Design of tile drainage for falling water tables, *J. Irrigation Drainage Div., Proc. ASCE IR*, 1-10.

Verhoest, N. E. C., and P. A. Troch (2000), Some analytical solutions of the linearized Boussinesq equation with recharge for a sloping aquifer, *Water Resour. Res.*, *36*, 793-800.

Vogel, R. M., and C. N. Kroll (1992), Regional geohydrologic-geomorphic relationships for the estimation of low-flow statistics, *Water Resour. Res.*, *28*, 2451-2458.

Zecharias, Y. B., and W. Brutsaert (1988a), The influence of basin morphology on groundwater outflow, *Water Resour. Res.*, *24*, 1645-1650.

Zecharias, Y. B., and W. Brutsaert (1988b), Recession characteristics of groundwater outflow and base flow from mountainous watersheds, *Water Resour. Res.*, *24*, 1651-1658.